



FACULTY OF SCIENCE AND TECHNOLOGY

## MASTER THESIS

Study programme / specialisation:

Marine and Offshore Technology

The spring semester, 2022

Author:

**Marina Simplicio da Silva**

Open / Confidential

*Marina Silva*  
.....  
(signature author)

Course coordinator:

**Professor Yihan Xing, Ph.D.**

Supervisor(s):

**Professor Daniel Karunakaran, Ph.D.**

Thesis title: **Free Hanging Catenary Riser with Steel and Titanium**

Credits (ECTS): 30

Keywords:

SCR, SCRT, Titanium, Deepwater, Harsh  
Environment, Extreme Response  
Analysis, Fatigue Performance

Pages: 103

+ appendix: 06

Stavanger, June 15, 2022  
date/year

## Abstract

Deepwater developments are becoming increasingly common in several parts of the world. Although the technological advances have grown exponentially since the first development in such great depth, challenges are still faced regarding the harsh environmental conditions. Considering that, the riser system is a critical part of the subsea architecture.

The Steel Catenary Riser (SCR) is usually the preferred option for deep and ultra-deep waters when its feasibility is ensured. However, this type of riser is very sensitive to the host platform's large motions due to the harsh environment. The large motion has the downward velocity at the hang-off point as a critical component, which can induce high levels of fatigue in that location and at the touchdown point (TDP). Thus, risers are usually designed with a flex joint on their top end, reducing or eliminating the fatigue issues in this area. For the TDP, other alternatives have been studied.

An alternative that has been considered is the implementation of a titanium section on the touchdown area (TDA) of an SCR, which feasibility in a deepwater and harsh environment is the focus of this work. A comparison with a conventional SCR is made in order to evaluate how the titanium affects the response on the TDA.

Results of the strength analyses showed that the SCR is unsuitable when the downward velocity is 3.8 m/s. By implementing the titanium section, which material has higher yield strength, the riser can cope with that downward velocity. The fatigue performance of the risers is checked considering the wave-induced fatigue. The conventional SCR demonstrates to have high fatigue damage, resulting in only 3.5 years on the TDP, which can be explained by its results on the strength analysis. On the other hand, the SCR with a titanium section has a fatigue life of over 20,000 years at the TDP, demonstrating it can improve the results significantly. Sensitivity studies are presented and explain how the riser with titanium is affected by changes in the section length, wall and coating thicknesses, and hang-off angle.

Overall, this thesis shows the feasibility of an SCR with a titanium section on the TDA when applied on a spread moored FPSO in deepwater and harsh environmental conditions.

**Keywords:** Deep water, SCR, SCR with titanium section, Extreme Response Analysis

## Acknowledgments

All glory to God and the spiritual guides that accompany me in my life.

All my love and gratitude to my parents and sister, which raised me with the freedom to follow my dreams and have always supported me in my decisions. Being away from home is not always an easy decision, but knowing that I have your support on my journey makes the distance just a detail that can be easily overcome.

I sincerely appreciate Professor Dr. Daniel Karunakaran for accepting being my supervisor and for all the guidance, input, and comments on the evaluation of my thesis. Also, I would like to express my gratitude to Andre Ramiro for all the explanations and help with my simulations and analysis.

To my fellow colleagues that stayed together on this journey, sharing the easy moments and bringing joy to the hard ones. Also, a big thank you to my Brazilian friends, who welcomed me and became family.

To my beloved boyfriend, Jonatan Byman, for being so supportive and patient and reminding me of the important things in life. Your love helped me to go through the bad days and was a highlight of the good ones.

To the Norwegian government for giving the opportunity of high-quality and free education.

---

## Table of Contents

Chapter 1. Introduction .....	1
1.1 Objective.....	3
1.2 Scope .....	3
Chapter 2. Riser System.....	5
2.1 Riser.....	5
2.2 Riser Technology.....	5
2.2.1 Top Tensioned Risers (TTRs) .....	6
2.2.2 Compliant Riser.....	7
2.2.3 Hybrid Riser .....	8
2.3 Riser Material .....	9
2.3.1 Flexible Riser.....	9
2.3.1 Rigid riser .....	10
2.3.1.1 Carbon Steel Pipe .....	10
2.3.1.2 Titanium risers.....	10
2.4 Riser components .....	12
2.4.1 Flex joint.....	12
2.4.2 Tapered stress joint.....	12
2.4.3 Bend Stiffener and Bell Mouths .....	13
2.4.4 Bend restrictor .....	14
2.4.5 Buoyancy modules .....	14
2.5 Riser design loads.....	15
2.5.1 Pressure loads .....	15
2.5.2 Functional loads.....	15
2.5.3 Environmental loads .....	16
2.5.3.1 Waves .....	16
2.5.3.2 Current.....	16

---

2.5.3.3	Floater motions.....	17
2.5.4	Accidental loads .....	17
2.6	Deep-water challenges.....	17
2.6.1	Sizing .....	17
2.6.2	Dynamic response .....	18
2.6.3	Riser/vessel interaction.....	18
2.6.4	Material selection .....	18
Chapter 3.	Steel Catenary Riser .....	19
3.1	Conventional SCR.....	19
3.2	Weight distributed SCR (WDSCR).....	20
3.3	Steel Lazy Wave Riser (SLWR).....	22
Chapter 4.	Design Codes and Standards .....	24
4.1	Introduction .....	24
4.2	Dynamic Riser Design.....	25
4.2.1	WSD Code – API-RP-2RD .....	25
4.2.1.1	Allowable stresses .....	26
4.2.1.2	Allowable deflections.....	27
4.2.1.3	Collapse pressure.....	27
4.2.1.4	Collapse propagation.....	28
4.2.1.5	Overall Column Buckling .....	28
4.2.1.6	Fatigue/service life .....	28
4.2.2	LRFD Code – DNV-ST-F201 .....	29
4.2.2.1	Design loads .....	30
4.2.2.2	Ultimate Limit States .....	31
4.2.2.2.1	Bursting.....	32
4.2.2.2.2	System Hoop Buckling (Collapse) .....	33
4.2.2.2.3	Propagating buckling .....	34

---

---

4.2.2.2.4	Combined load criteria.....	35
4.2.2.3	Accidental Limit State.....	36
4.2.2.4	Serviceability Limit State.....	36
4.2.2.4.1	Fatigue Limit State.....	37
Chapter 5.	Design Basis and Methodology.....	39
5.1	Introduction .....	39
5.2	Description .....	39
5.3	Design standards.....	40
5.4	Design data .....	40
5.4.1	FPSO data.....	40
5.4.2	FPSO motions.....	41
5.4.2.1	Wave frequency motions (WF).....	41
5.4.2.2	Low-frequency motions (LF).....	41
5.4.2.3	FPSO static offsets .....	41
5.4.3	Environmental data.....	42
5.4.4	Operational and accidental design conditions .....	44
5.4.5	Riser properties.....	45
5.4.5.1	Titanium section.....	45
5.4.5.2	Internal fluid.....	46
5.4.6	Design life .....	46
5.4.7	Hydrodynamic data and Marine Growth.....	47
5.4.8	Riser–soil interaction.....	47
5.5	Wall thickness .....	48
5.6	Design cases .....	49
5.7	Extreme response methodology .....	49
5.8	Acceptance criteria .....	50
Chapter 6.	Extreme Response Analysis .....	52

---

---

6.1	Introduction .....	52
6.2	Static analysis .....	52
6.3	Dynamic Analysis .....	55
6.3.1	Dynamic analysis of conventional SCR .....	55
6.3.2	Dynamic analysis of SCRT .....	58
Chapter 7.	Fatigue Analysis .....	61
7.1	Fatigue design conditions .....	61
7.1.1	Riser structural modeling .....	61
7.1.2	S-N curve .....	62
7.1.3	Stress concentration factor .....	65
7.1.4	Wave-induced fatigue damage .....	66
7.2	Fatigue analysis results .....	68
7.2.1	Conventional SCR .....	68
7.2.2	SCRT .....	69
Chapter 8.	Sensitivity Analysis .....	70
8.1	Introduction .....	70
8.2	Titanium length sensitivity study .....	70
8.2.1	Dynamic analysis (ULS) – Titanium length sensitivity .....	71
8.2.2	Dynamic analysis (ALS) – Titanium length sensitivity .....	75
8.3	Wall and coating thicknesses sensitivity .....	75
8.3.1	Dynamic analysis (ULS) - Wall and coating thicknesses sensitivity .....	76
8.4	Hang-off angle sensitivity .....	79
8.4.1	Dynamic analysis (ULS) – Hang-off angle sensitivity .....	79
8.4.2	Dynamic analysis (ALS) – Hang-off angle sensitivity .....	83
Chapter 9.	Conclusion and Recommendations .....	84
9.1	Conclusion .....	84
9.2	Recommendations .....	87

---

References ..... 88

Appendix ..... 1

    Appendix A - Description of OrcaFlex Software ..... 1



## List of Figures

Figure 1-1. World record on offshore petroleum production - 1979-2012 (Morais, 2013). .....	1
Figure 2-1. Top Tensioned Risers on TLP and Spar. (Bai and Bai, 2010).....	6
Figure 2-2. Compliant Riser configurations (Bai and Bai, 2005). ....	7
Figure 2-3. Hybrid riser configuration (Bai and Bai, 2010).....	8
Figure 2-4. Unbonded flexible pipe (Zhang et al., 2003).....	10
Figure 2-5. Flex-joint (DNV, 2001). ....	12
Figure 2-6. Tapered Stress Joint (API, 2006).....	13
Figure 2-7. Bend stiffener and Bell mouth (Bai and Bai, 2014). ....	13
Figure 2-8. Bend restrictor (API, 2002). ....	14
Figure 2-9. Riser with buoyancy modules (Fergestad and Løtveit, 2014). ....	14
Figure 3-1. SCR schematic (Sen, 2006). ....	19
Figure 3-2. Weight distributed SCR for harsh environments (Karunakaran et al., 2013). .....	21
Figure 3-3. SLWR schematic (Lal et al., 2019).....	23
Figure 5-1. Brazilian south and southeast basins (Souza and Sgarbi, 2019).....	39
Figure 5-2. SCR configuration. ....	40
Figure 5-3. SCR near, mean, and far position. ....	42
Figure 5-4. Distribution of maximum vertical velocity versus wave direction.....	43
Figure 5-5. Vessel orientation. ....	44
Figure 5-6. SCR with titanium section. ....	46
Figure 6-1. Time history: Bending moment - SCR Near - ULS. ....	56
Figure 6-2. Point of the maximum bending moment for the far offset position in a) ULS and b) ALS. ....	57
Figure 6-3. Time history: Max Von Mises stress - SCR Near - ULS. ....	57
Figure 6-4. Time history: Bending moment - SCRT Near - ULS. ....	59
Figure 6-5. Time history: Max Von Mises stress - SCRT Near - ULS. ....	59
Figure 7-1. S-N curves in seawater with cathodic protection (DNV, 2016). ....	63
Figure 7-2. S-N curves in air (DNV, 2016).....	64
Figure 7-3. 5G and 1G curves (Systems, 2005). ....	65
Figure 7-4. Example of a block sub-division on a scatter diagram. ....	66
Figure 7-5. Total fatigue damage of SCR.....	68

---

Figure 7-6. Total fatigue damage of SCRT. ....	69
Figure 8-1. Location of the highest bending moment for far offset position when the length of titanium section is: a) 400 m, b) 500 m, c) 550 m, d) 575 m, and e) 600 m. ...	73
Figure 8-2. Maximum Von Mises stress for the titanium section. ....	73
Figure 8-3. Maximum Von Mises stress for the steel section after titanium.....	74
Figure 8-4. SCRT with 450-meter length titanium section. ....	74
Figure 8-5. Maximum Von Mises stress for titanium section. ....	78
Figure 8-6. Maximum Von Mises stress for steel section after titanium. ....	78
Figure 8-7. Highest bending moment for near offset position with a hang-off angle of a) 8°, b) 9°, c) 10°, and d) 11°. ....	81
Figure 8-8. Highest bending moment for the far offset position with a hang-off angle of a) 8°, b) 9°, c) 10°, and d) 11°. ....	81
Figure 8-9. Maximum Von Mises stress for titanium section in near offset position - ULS. ....	82
Figure 8-10. Maximum Von Mises stress for steel section after titanium in far offset position - ULS. ....	82
Figure A-1. OrcaFlex main window (Orcina, 2022). ....	1
Figure A-2. Model states of OrcaFlex (Orcina, 2022). ....	3
Figure A-3. Coordinate System (Orcina, 2022). ....	4
Figure A-4. Headings and directions (Orcina, 2022). ....	4
Figure A-5. Time and simulation stages (Orcina, 2022). ....	5
Figure A-6. OrcaFlex line model (Orcina, 2022). ....	6

---

## List of Tables

Table 4-1. Design matrix for rigid risers (API, 2006).....	27
Table 4-2. Simplified design check for accidental loads (DNV, 2018). .....	36
Table 4-3. Design fatigue factors. ....	38
Table 5-1. FPSO dimensions.....	41
Table 5-2. Project wave.....	44
Table 5-3. SCR hang-off position.....	44
Table 5-4. FPSO offsets. ....	45
Table 5-5. Riser properties. ....	45
Table 5-6. Titanium properties. ....	46
Table 5-7. Hydrodynamic coefficients. ....	47
Table 5-8. Soil properties. ....	48
Table 5-9. Load case matrix. ....	49
Table 5-10. Maximum allowable stresses. ....	51
Table 6-1. Static results - SCR. ....	53
Table 6-2. Static Results - SCRT.....	54
Table 6-3. Dynamic response for SCR.....	55
Table 6-4. Dynamic response of SCRT.....	58
Table 7-1. D-curve in seawater with cathodic protection.....	63
Table 7-2. F1-curve in air.....	63
Table 7-3. Parameters for 5G and 1G curves (Systems, 2005). ....	64
Table 7-4. Fatigue life of SCR at the critical location.....	68
Table 7-5. Fatigue life of SCRT at critical location. ....	69
Table 8-1. Cases for titanium length sensitivity study. ....	71
Table 8-2. Titanium length sensitivity in near offset position.....	71
Table 8-3. Titanium length sensitivity in far offset position. ....	71
Table 8-4. 600-meter length titanium section for ALS condition. ....	75
Table 8-5. Parameters for steel section.....	76
Table 8-6. Parameters for titanium section.....	76
Table 8-7. Wall thickness and coating thickness sensitivity in near offset position. ....	77
Table 8-8. Wall thickness and coating thickness sensitivity in far offset position.....	79
Table 8-9. Cases for hang-off angle sensitivity study. ....	79
Table 8-10. Hang-off angle sensitivity in near offset position.....	80

Table 8-11. Hang-off angle sensitivity in far offset position. .... 80

Table 8-12. Hang-off angles for ALS conditions. .... 83

Table A-1. OrcaFlex toolbar (Orcina, 2022). .... 2

## Abbreviations

ALS	Accidental Limit State
API	American Petroleum Institute
ASTM	American Society for Testing and Materials
DNV	Det Norske Veritas
FLS	Fatigue Limit State
FPS	Floating Production System
FPSO	Floating Production, Storage and Offloading
HPHT	High Pressure High Temperature
JONSWAP	Joint North Sea Wave Project
LF	Low Frequency
LRFD	Load and Resistance Load Factor
LSD	Limit State Design
NACE	National Association of Corrosion Engineers
NORSOK	Norsk Søkkel Konkurransesjjon
RAO	Response Amplitude Operator
SCF	Stress Concentration Factor
SCR	Steel Catenary Riser
SCRT	Steel Catenary Riser with Titanium Section
SMYS	Specified Minimum Yield Stress
SMTS	Specified Minimum Tensile Stress
SLOR	Single Line Offset Riser
SLS	Serviceability Limit State
SLWR	Steel Lazy Wave Riser
TDA	Touchdown Area
TDP	Touchdown Point
TLP	Tension Leg Platform
TTR	Top Tension Riser
ULS	Ultimate Limit State
VIV	Vortex Induced Vibration
WDSCR	Weight Distributed Steel Catenary Riser
WF	Wave Frequency
WSD	Working Stress Design

## Chapter 1. Introduction

Petroleum is one of the most important sources of energy in the world. Even with advances in sustainable energy sources such as wind and solar power, the oil and gas industry still occupies a fundamental position in several economies. With the high demand of growing industries, this sector has to continuously invest in new technologies that can enhance and increase production at a lower price.

Oil production started many years ago and moved from land prospectations (onshore) to offshore. After that, production has moved considerably fast from shallow waters to deep and ultra-deep-water depths, in which the latter is above 1,500 meters. However, offshore exploration is much more challenging than onshore because of the sea environment. Due to the different geology and environmental conditions encountered worldwide, countries with petroleum resources started developing different technologies to overcome the challenges and make them successful in exploration and production.

Areas such as Brazil, the Gulf of Mexico, West Africa, and the Norwegian Continental Shelf (NCS) have been investing heavily in research, development, and innovation due to their resources located in ultra-deep water.

The world records of oil and gas production from 1979 to 2012 in deep and ultra-deep waters depicted in Figure 1-1 show that production has increased with the water depth. This was only possible given the new technological advances that made it feasible to explore the latest discoveries, which are being found at greater water depths over the years.

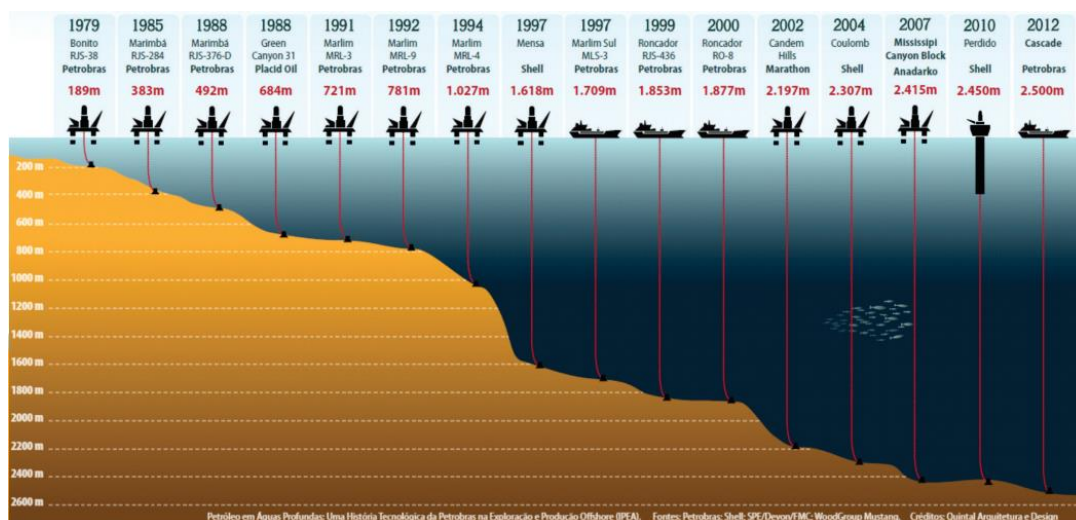


Figure 1-1. World record on offshore petroleum production - 1979-2012 (Morais, 2013).

With the increase in water depth, new platform hosts had to be developed in order to cope with the environmental conditions for the field of operation. Semi-submersibles, spar, and FPSO can be cited as feasible examples for this condition. After having the host selected, a significant challenge during the production phase is the selection of a reliable riser that is able to handle the host's motion, especially the ones derived from the heave and pitch motions in harsh environmental conditions. Thus, for a successful operation, it is essential to design a robust riser concept that is also safe and economical.

Three types of riser configurations have been installed in oil and gas exploration: Steel Catenary Risers (SCR), flexible risers, and hybrid risers. SCR is the most attractive choice for deep and ultra-deepwater applications. The advantages of this concept are that, for greater water depths, it is a simple and cost-effective alternative when compared to the flexible riser (Orimolade, 2014). Also, possible problems due to higher hydrostatic pressure and higher temperature rates in deep water can be overcome with increased wall thickness. This concept includes a conventional SCR, a Weight Distributed SCR (WDSCR), and a Steel Lazy Wave Riser (SLWR).

However, the SCR is very sensitive to the platform motions; thus, its integrity is affected by the cyclic loading. Taking this into account, a challenge faced with applying the SCR to the floating units in deep and ultra-deep water is the high fatigue damage estimated in offshore and onshore welds at the touchdown area (TDA) (Aggarwal et al., 2007).

A feasibility study was performed by Gemilang (2015), where it was stated that different configurations of SCR can cope with distinct downward velocity. While a conventional SCR with coating is restricted to a downward velocity on the hang-off point below 2.33 m/s, the WDSCR is restricted below 3.2 m/s. The SLWR showed more promising, coping with 6 m/s on the hang-off point. Those results showed that innovative solutions could be applied to extend its feasibility in harsh environments.

Considering this, an alternative approach that the industry has evaluated is a variation on the catenary riser design by changing its material type. In this context, implementing a titanium section on the TDA is an alternate solution that may significantly increase the fatigue performance of the riser (Systems, 2005).

The titanium material has a lower elastic modulus (114GPa) compared to steel (207GPa), which lowers the amplitude of fatigue stresses. This, in combination with superior fatigue properties, can eliminate the fatigue issues faced with the use of steel only. Therefore, in

the design, it is important that the titanium section covers the TDA for the host's mean offset position and its maximum displacements when in near and far offset positions. Also, in addition to the fatigue benefit, the grades suitable for offshore risers are highly resistant to seawater, production fluids, and most injected/workover and completion fluids (System, 2005).

Although implementing a titanium section on the TDA is advantageous, more qualifying works on its applicability need to be carried out. This need comes from the fact that the exploration and production of oil and gas are being developed in deeper, remote, and harsh environments, which demand new solutions to the issues faced nowadays.

## 1.1 Objective

The main objectives of this study are the establishment of an SCR configuration with a titanium section on the TDA, and an assessment of the dynamic responses and fatigue performance of this riser configuration in extreme sea states. A comparison with a conventional SCR will also be covered to analyze how titanium's use affects the riser response and its feasibility.

A typical deep-water and harsh environmental design data and conditions will be considered for the design basis, which will supply the necessary input for modeling. The location of the study is the Brazilian offshore coast. Thus, its wave and current data will be used for the extreme response behavior and fatigue performance.

The main parameter considered for the feasibility of the configurations is the stress experienced by the riser. A sensitivity analysis will be performed at the end of the work to establish how different configuration parameters affect the behavior of the riser. This will drive the initial base case and the sensitivity studies performed. All strength and fatigue performance simulations will be carried out using the OrcaFlex software.

## 1.2 Scope

A brief scope of this thesis is presented as follows:

- Chapter 2 presents a general description of riser systems regarding technology, material, components, design loads, and deep-water challenges.
- Chapter 3 discusses the types of Steel Catenary Riser (SCR).
- Chapter 4 presents some main information about the design codes and standards considered for riser system design.



- Chapter 5 provides the design basis of the riser configuration used in this study. Design data, analysis methodology, and the design acceptance criteria are also included.
- Chapter 6 presents the extreme response analysis of the conventional SCR and the SCR with titanium section. Static and dynamic responses are discussed.
- Chapter 7 presents the fatigue analyses check of both risers discussed in the previous chapter.
- Chapter 8 presents the sensitivity study carried out on the SCR with titanium section to find an optimum configuration.
- Chapter 9 discusses the conclusions of the work and recommendations for future study.

## Chapter 2. Riser System

Some of the main concepts discussed in this work will be presented in the chapter. The reason is to have a better overview and understanding of the proposed topic.

### 2.1 Riser

Subsea risers transport products from the seafloor to production and drilling facilities and from the facilities to the seafloor. They can be classified based on their function, which can be one of the following:

#### Drilling riser

This type of riser is typically a Top Tensioned Riser (TTRs) and is composed of a section of vertical pipe supported by top tension force at the vessel and connected to the subsea wellhead via a tieback connector (Padepolous and Thethi, 2012).

#### Production riser

This riser transports hydrocarbons from the subsea well to the facility. The shape assumed for this riser will be according to the compliant system used to absorb the vessel motion in the environment it is being used (Gemilang, 2015).

#### Injection riser

This riser is used to inject circulating fluids from the facility to the subsea well. Like the production riser, it will have its concept according to the complaint system (API, 2006).

#### Import/Export riser

The function of this type of riser is to transport processed fluids (oil, gas, water, or a combination of these) from the floating production system to another facility (API, 2006).

### 2.2 Riser Technology

When designing a riser, some drivers are considered to define the best technology to be applied. Factors such as floater type, floater motion, water depth, environmental conditions, and design pressure/temperature are utilized and categorize the risers in the following three types.

### 2.2.1 Top Tensioned Risers (TTRs)

This concept is based on an entirely vertical riser system supported by a tensioner located at the facility. The behavior of this type of riser should satisfy the condition that, even with the floater motion, the applied top tension should maintain a constant target in order to prevent an undesirable bending on the bottom of the riser. The capacity of the riser motion relative to the floater motion in a vertical direction is called a stroke. In addition to the applied top tension, this factor is an essential design parameter governing mechanical behavior (DNV, 2017).

These risers are mainly used on Tension-leg-platforms (TLPs) and Spars, as represented in Figure 2-1 below.

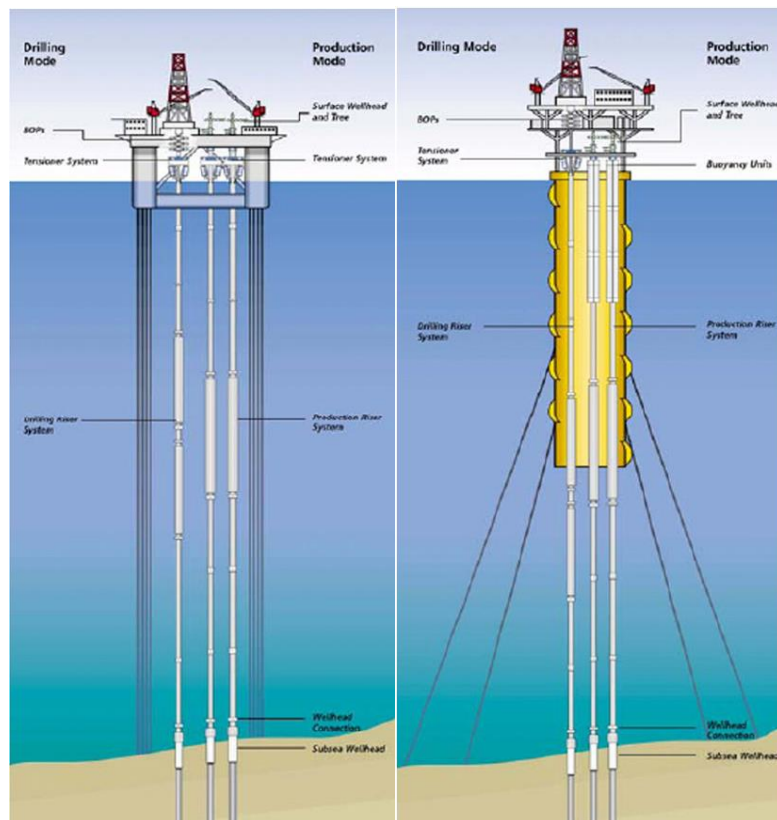


Figure 2-1. Top Tensioned Risers on TLP and Spar. (Bai and Bai, 2010)

In both cases, the platforms are moored, but this does not prevent them from moving laterally when subjected to wind and waves. Because of that, and considering that the rigid risers are also fixed to the seafloor, vertical displacement can occur between the top of the riser and its connection point on the facility. This undesirable issue can be prevented with a motion compensator that allows constant tension on the riser (Rigzone, 2021).

They are applicable for TLP and Spar due to their small heave motion, which has a small stroke capacity requirement with small offsets (Gemilang, 2015). Considering this, harsh environments that can cause significant motions on the floater make TTRs unsuitable.

### 2.2.2 Compliant Riser

DNV (2001) states that compliant riser configurations do not use any heave compensation systems and are designed to absorb floater motions by geometry change. This makes them feasible to be applied in deep water and harsh environments instead of TTRs. The material of a compliant riser is either flexible or rigid pipe, and they are mainly used as production, export, and injection risers.

The configuration in the design of this type of riser can assume many different shapes according to the environmental conditions they must cope with. The most straightforward layout commonly addressed with a rigid pipe is the free-hanging which, as the name says, free hangs of the floater and assume a bending shape when close to the seabed. Its material is usually steel, which gives it the name of Steel Catenary Riser.

Due to key factors such as water depth, environmental conditions, floater motion, and floater type and costs, it can be installed in different configurations, as shown in Figure 2-2 below.

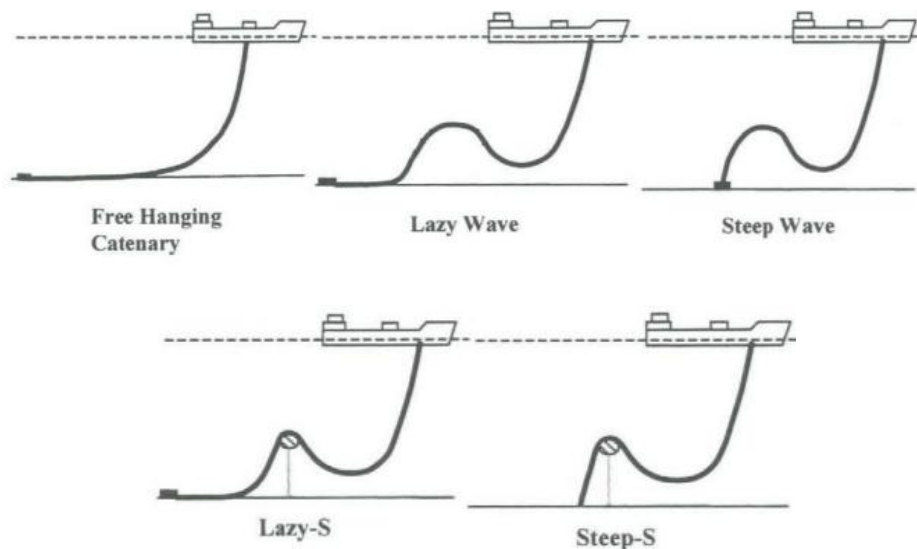


Figure 2-2. Compliant Riser configurations (Bai and Bai, 2005).

Due to their configuration, compliant riser systems are more susceptible to experiencing more significant static and dynamic excursions when compared to top tensioned risers. Because of that, environmental load conditions are one of the concerns when considering compliant configurations. Critical locations on these risers are typically the wave zone,

hog and sag bends, touch-down area at the seafloor, and the terminations to rigid structure (DNV, 2001).

The free-hanging catenary is easy to install, requires minimum subsea infrastructure, and is cost-effective for deep-water development. However, it can be subjected to high bending moments and buckling, especially at the hang-off and touch-down point, due to wave frequency or low frequency of vessel motions. Also, high vessel motions can lead to compression on the riser touch-down point and cause failure at this point (Gemilang, 2015).

An option discussed is the use of titanium on the TDA because of its low modulus of elasticity which implies a higher degree of flexibility, yield stress typically higher than steel, and lower specific weight (DNV, 2001).

### 2.2.3 Hybrid Riser

The hybrid riser is a combination of the TTR and Compliant riser. It is an alternative for more complex environments that require large diameter risers, reduced load on the vessel, flow assurance requirements, and a robust layout for later development phases (Dikdogmus, 2012).

This system is composed of two sections: a lower vertical steel under tension (hybrid tower) and an upper catenary section of flexible pipe (jumper) (Dikdogmus, 2012). These two sections are connected by a buoyancy tank located at the top of the tower section, which is positioned below the main wave zone. The jumper is then connected to the floater. In Figure 2-3, it can be seen how it is arranged.

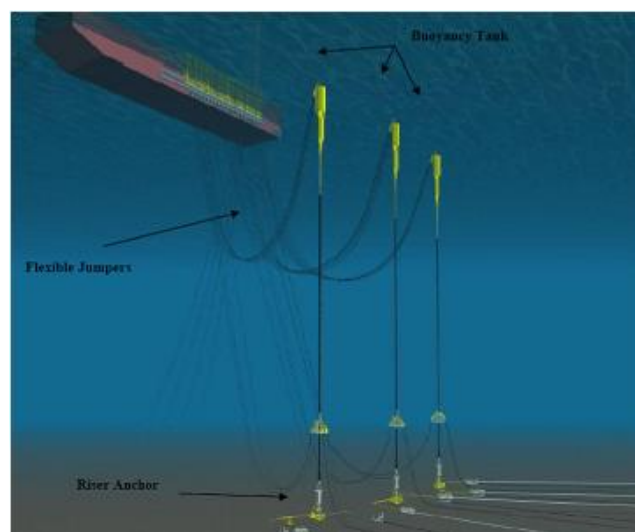


Figure 2-3. Hybrid riser configuration (Bai and Bai, 2010).

As the jumper is a flexible pipe, the floater motions can be absorbed, reducing the dynamic effects on the rest of the riser, and avoiding fatigue issues in the tower section. Because in this configuration, the jumper can isolate the floater's dynamic motion from the vertical riser, this concept is characterized as uncoupled risers (Gemilang, 2015). This characteristic makes this concept suitable to be used in deep and even ultra-deepwater in addition to a harsh environment.

Free-standing hybrid risers can assume two arrangements, single line or bundle. The first is called Single Line Offset Risers (SLORs) and consists of a concentric pipe in pipe vertical steel riser section. The latter consists of some smaller diameter steel pipe strings and umbilicals that are assembled together (Dikdogmus, 2012).

## **2.3 Riser Material**

The material selected for the riser system has to be in accordance with the operation requirement. Factors such as the internal fluid, floater type, floater motions, water depth, environmental conditions, and design pressure and temperature have to be considered for the design. The selected material must be suitable for the entire life of the riser (DNV, 2017). According to the selection, risers are categorized as Flexible or Rigid.

### **2.3.1 Flexible Riser**

According to Bai and Bai (2005), a flexible riser has as its main characteristic low relative bending to axial stiffness, which is achieved through the use of a number of layers consisting of different materials in the pipe wall fabrication. The property of low bending stiffness is due to the ability of the layers to slip past each other when they are under the influence of external and internal loads. Each layer of this type of riser has a specific function that, when combined, can provide strength to the structure and guarantee fluid integrity.

There are two types of flexible pipes: bonded and unbonded flexible pipes. Bonded pipes are defined by different layers of fabric, elastomer, and steel bonded together through a vulcanization process. The steel reinforcement is embedded in rubber, giving them good corrosion resistance. Usually produced on a rigid mandrel, their limited individual length is about 45m, and, therefore, they are used for short sections, e.g., jumpers (Bai and Bai, 2005). On the other hand, unbonded pipes are produced by mandrel-less technology in long continuous lengths and are used for long sections for dynamic applications. An unbonded pipe is presented in Figure 2-4.

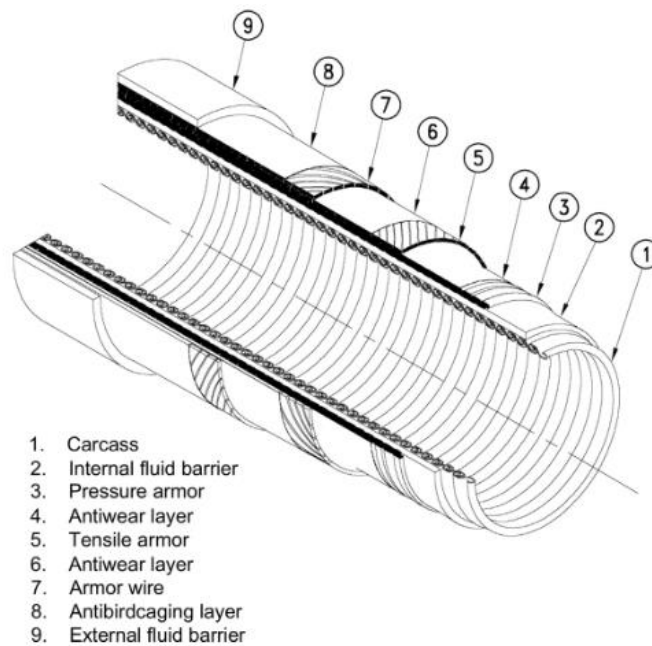


Figure 2-4. Unbonded flexible pipe (Zhang et al., 2003).

### 2.3.1 Rigid riser

The material selected for the riser must be suitable for the intended use during the entire service life (DNV, 2017). Hence, different materials can be used according to the environment and operation of the riser. Steel catenary risers are a well-known type of riser and have been successfully deployed in many fields for years. However, titanium and composite pipes are being suggested for deep-water application due to their advantages over steel in several situations. Benefit as achieving the top tension required is one of the examples of it.

#### 2.3.1.1 Carbon Steel Pipe

Standard API 5L Code is considered for selecting a carbon steel pipe. The specification covers several materials such as Grades A25, X42, X46, X52, X56, X60, X65, X70, and X80. Each of them has different characteristics and properties according to the composite and constituent material. Due to the chemical composition, different yield stress strengths can be encountered, as well as the corrosion tolerance (Gemilang, 2015).

#### 2.3.1.2 Titanium risers

Due to its essential properties, titanium alloy usage can extend the possibilities for metallic risers beyond the limits of steel. It is significantly lighter than steel and has a lower elastic modulus (around half of the steel), implying a higher degree of flexibility (DNV, 2018). In addition, it consists of an increased yield and tensile strength, high fatigue resistance, and great resistance to corrosive fluids (Frazer, 1998). The

combination of corrosive resistance, lightweight, flexibility, and high strength makes titanium preferable to the carbon steel material. However, the low elastic modulus can affect its buckling performance, which can partly compensate for its superior strength. Thus, the wall thickness should be accurately designed to withstand the combined loads (Systems, 2005).

Tapered stress joints at the upper termination of SCRs and at the subsea wellhead of some TTRs are where titanium alloys are routinely used. Nevertheless, considering its improvement in fatigue life and HPHT reservoirs, it has now been considered for the whole riser length or for the TDA. Two grades of titanium are commonly used for catenary risers (Baxter et al., 2007):

- ASTM Grade 29 (nominally Ti-6% Al-4%V-0.1%Ru): the addition of 0.1 wt.% ruthenium (Ru) to the Grade 23 alloy makes it a more corrosion-resistant alloy since its crevice and stress corrosion temperature limits are raised to over 260°C in sweet and sour chloride brines and seawater. Also, it is approved for sour service where NACE standard is required and when it is expected to have temperatures over 75° during riser service.
- ASTM Grade 23 (nominally Ti-6% Al-4%V): for service temperatures below the limits above and where is not required NACE standard for sour service, it represents the most economic alloy choice.

However, due to the high costs associated with titanium risers, they may not be suitable for all projects. Thus, titanium catenary risers are a candidate for conditions like (Bell et al., 2005):

- Shallow water in which fatigue exposure and extreme response are more significant than in deeper water;
- When sour services need a material with higher fatigue capacity than carbon steel, for instance.

In this case, an option that is discussed and more suitable for installation is the implementation of titanium sections along the riser instead of making it entirely of titanium.



## 2.4 Riser components

The riser stability due to external loads can be achieved by using different components in the critical locations to make it cope with the design criteria. Some of the main features will be presented below.

### 2.4.1 Flex joint

A flex joint consists of a laminated metal and elastomer assembly, which is often used on the top region of the SCR as an interface between the upper termination point and the riser (DNV, 2001). According to Bai and Bai (2010), it allows the riser to rotate with a minimum bending moment, reducing bending stress at termination to the floater and the seafloor.

An important property that should be considered in its design is the flex joint stiffness since it will determine the maximum fatigue and stress in the region where it is applied. Temperature variations, rotations, and residual torque after installation are some of the parameters that can affect the stiffness. Also, the high top-tension and tension range for fatigue design shall be considered for deep-water application. An illustration of a flex joint can be seen in Figure 2-5.

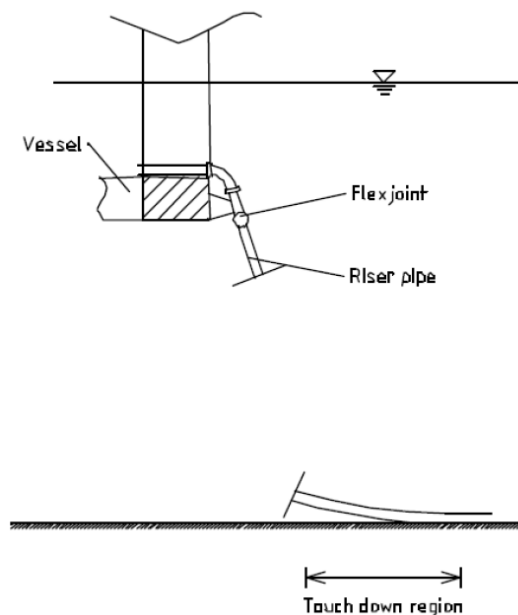


Figure 2-5. Flex-joint (DNV, 2001).

### 2.4.2 Tapered stress joint

A tapered stress joint (TSJ) is used as a member that can accommodate the transition between rigidly fixed or stiffer sections of the production riser and less stiff sections of it

(API, 2006). With its use, excessive bending and fatigue issues between the two different areas may be avoided (Gemilang, 2015).

The design of a TSJ considers a linear variation of stiffness, where the bending stiffness at one end is close to the stiffness of the more rigid section of the riser, and the other end has a lower stiffness than the less stiff member of the riser (API, 2006). This concept can be executed by having a wall thickness variation on the transition member, as shown in Figure 2-6.

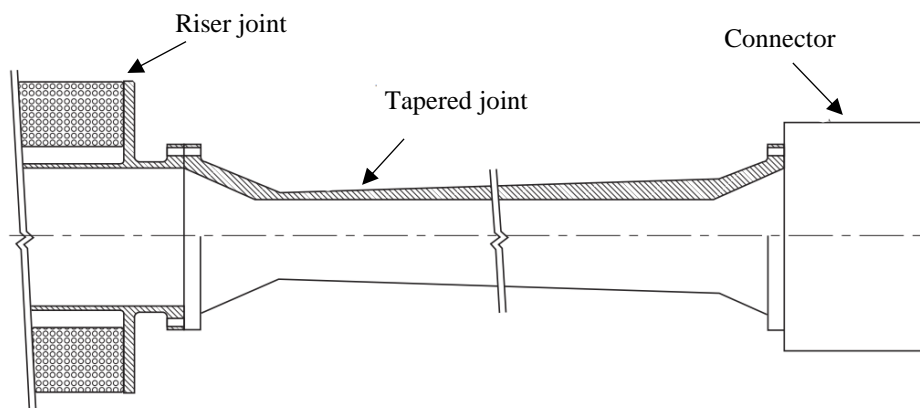


Figure 2-6. Tapered Stress Joint (API, 2006).

### 2.4.3 Bend Stiffener and Bell Mouths

The top part of a flexible riser is a critical area subjected to overbending. Therefore, an alternative to increase the riser stiffness and prevent bending beyond its allowable bend radius is to incorporate a bend stiffener or a bell mouth. For high-motion vessels, the bend stiffener is known to provide a better performance, making it preferable to the bell mouth. It is able to give a moment transition between the riser and its rigid end connection by providing a gradual stiffening to the riser (Bai and Bai, 2014). Figure 2-7 illustrates both devices.

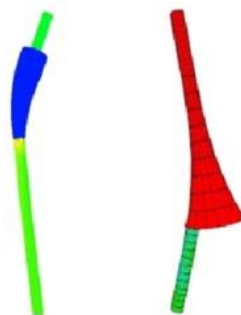


Figure 2-7. Bend stiffener and Bell mouth (Bai and Bai, 2014).

#### 2.4.4 Bend restrictor

Usually located at the bottom and top connections, the bend restrictor is used to provide additional overbending resistance for the critical points of the riser (Bai and Bai, 2014). As the device presented before, they are also designed for flexible pipelines. An illustration of a bend restrictor is in Figure 2-8.

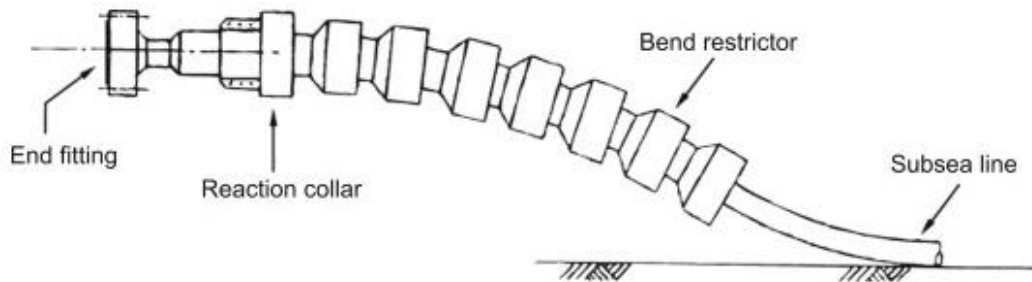


Figure 2-8. Bend restrictor (API, 2002).

#### 2.4.5 Buoyancy modules

The buoyancy modules are structures that are strapped or clamped to the exterior of riser joints, as shown in Figure 2-9. They are made of light weight material, usually foamed polymers, and are intended to decrease the submerged weight of the riser and obtain the desired riser configuration (DNV, 2017).

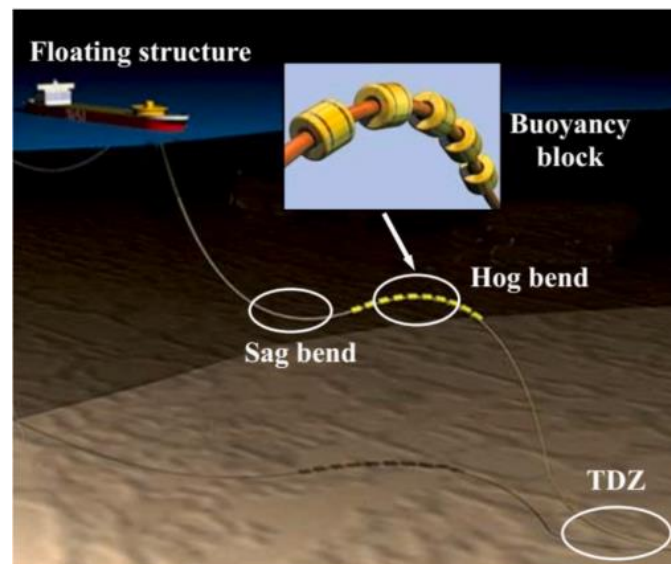


Figure 2-9. Riser with buoyancy modules (Fergestad and Løtveit, 2014).

## 2.5 Riser design loads

Different loads have to be considered when a riser system is designed. According to DNV (2018), the load classification relates the load effect to the various uncertainties and occurrences. Therefore, they are categorized into four groups as below:

- Pressure loads;
- Functional loads;
- Environmental loads;
- Accidental loads.

### 2.5.1 Pressure loads

Pressure loads, P-loads, are defined as the ones strictly related to the combined effect of hydrostatic internal and external pressures. For this, it is considered the following:

- External hydrostatic pressure;
- Internal fluid pressure;
- Hydrostatic static and dynamic contributions;
- Water levels.

### 2.5.2 Functional loads

Functional loads, F-loads, consider the loads that happen due to the system's physical existence and how it is operated and handled during its lifetime. They can be defined as dead, live, and deformation loads that take place during transportation, storage, testing, operation, installation, and general use (Dikdogmus, 2012). It does not consider environmental or accidental loads. DNV (2018) presents the following examples of these loads:

- Weight of internal fluid;
- Weight and buoyancy of riser, tubing, coating, buoyancy modules, contents, and attachments;
- Applied tension for top-tension risers;
- Thermal loads;
- Marine growth;
- Loadings from drilling operations.

Dead loads are described as the ones due to weight in air of principal structures and its fixed/attached parts, and loads originated by the external hydrostatic pressure and

buoyancy when they are based on still water level. On the other hand, live loads include the ones that can change during operations which can be due to the flow, weight, pressure, and temperature of containment (Dikdogmus, 2012).

### 2.5.3 Environmental loads

Environmental loads, E-loads, consider the loads caused by the ocean environment, directly or indirectly. The following loads are taken into account:

- Waves;
- Current;
- Floater motions;
- Earthquake (considered in the riser design for regions seismically active);
- Ice (for areas where ice may develop or drift).

In this work, only the three first ones will be considered.

#### 2.5.3.1 Waves

According to DNV (2018), a major source of dynamic environmental forces on the risers is wind-driven surface waves. This is due to their shape irregularity, length, and height variation and because the riser can be approached from one or more directions simultaneously.

A way to describe the wave conditions is either by a deterministic design or stochastic methods applying wave spectra. The application and assumptions used for adjacent structures drive the selection of appropriate wave theories.

#### 2.5.3.2 Current

Current is a significant contributor to static and dynamic loadings on risers (Dikdogmus, 2012). Actual ocean currents are composed of shear flows, which means that different current velocities can impact the riser along its length. It exposes it to experience in-line and cross-flow vortex-induced vibrations (VIV) since one or more current velocities can reach the natural frequency of the riser (DNV, 2017). Relevant effects of VIV on the riser system are:

- Significant fatigue;
- Higher mean drag coefficient to be applied in global load effect analyses and riser interference analyses;
- Influence on wake-induced oscillations of riser arrays;

- Contribution to the relative collision velocity of two adjacent risers.

### 2.5.3.3 Floater motions

Floater motions cause displacements imposed on the riser due to the vessel's motions. The riser's static and dynamic loading may be caused by floater offset and motions. According to DNV (2018), for the riser design, the following data is required:

- Static offset (horizontal): caused by waves, wind, and current loads;
- Wave frequency motion (horizontal and vertical): first-order wave-induced motions;
- Low-frequency motions: caused by wind gusts and second-order wave forces;
- Set down/pulldown: originated by the combined effect of mooring lines/tether constraints and floater offset.

### 2.5.4 Accidental loads

Accidental loads usually occur due to abnormal operations, incorrect operations, or technical failure. The riser design against these loads can be done directly or indirectly. The first one is done by calculating the effects imposed by the loads on the structure, and the latter by designing the system as tolerable to accidents (DNV, 2018).

## 2.6 Deep-water challenges

Over the last years, offshore developments in water depths of 2000m or more have become more common, especially in areas such as the coast of Brazil and the Gulf of Mexico. Risers are one of the components most affected by the increasing depths. Installations become more complex, weight increases due to the length, and consequently, costs increase. Factors such as the following must be considered to develop a feasible design that can operate in deep waters (Howells and Hatton, 1997).

### 2.6.1 Sizing

Risers shall be designed such that their sizing must be rationalized to minimize the loading applied to the production vessel. For deep waters, the wall thickness must resist collapse from external pressure. However, this can lead to excessive wall thickness that is not feasible to riser design life, in addition to high magnitude loads and weights during extreme environmental conditions. Wall thickness changes with depth may be required, and the adoption of different materials, e.g., titanium.

### **2.6.2 Dynamic response**

Fatigue and fracture resistance are known as issues in deep-water risers. SCRs can handle extreme storm loading with reduced riser top angles which reduces the loads on the vessel. On the other hand, higher stress gradients at the touch-down point may be encountered due to the more severe static curvature, resulting in significant fatigue loading concentration from vessel motions. In addition, VIV is of important consideration for rigid risers in steady current flow since it can increase the riser drag and affect its fatigue life.

### **2.6.3 Riser/vessel interaction**

Vessel drift offsets affect the riser arrangements that are feasible for an area. Vertically tensioned risers or simple SCR can be considered for spars and TLP's with relatively small offsets. With the increase in the offset and dynamic motions, the need to control vessel drift motions makes necessary to consider other alternative riser arrangements such as buoyant wave catenaries or hybrid risers.

### **2.6.4 Material selection**

Riser weight increases significantly at increased water depth; therefore, there is a need to consider alternative materials to be adopted. They shall be able to reduce the weight and maintain strength and collapse resistance.

## Chapter 3. Steel Catenary Riser

Steel catenary risers can assume the three following configurations:

- Conventional SCR;
- Weight Distributed SCR (WDSCR);
- Steel Lazy Wave Riser (SLWR).

With the development of deep-water fields over the years, it has been proven to be an attractive choice. However, the large motion faced by the host platforms has demonstrated to be a big challenge for this type of riser in harsh environments. Characteristics of each one will be presented below.

### 3.1 Conventional SCR

The conventional SCR is a simple free-hanging configuration that, due to its self-weight, assumes the shape of a catenary, being horizontal at the lower end and generally within about  $20^\circ$  of the vertical at the top end (Bai and Bai, 2010). In order to offset the relative rotational movement between the riser and the platform, a flex joint, stress joint, and pull tube can be used. A schematic of a steel catenary riser is presented in Figure 3-1.

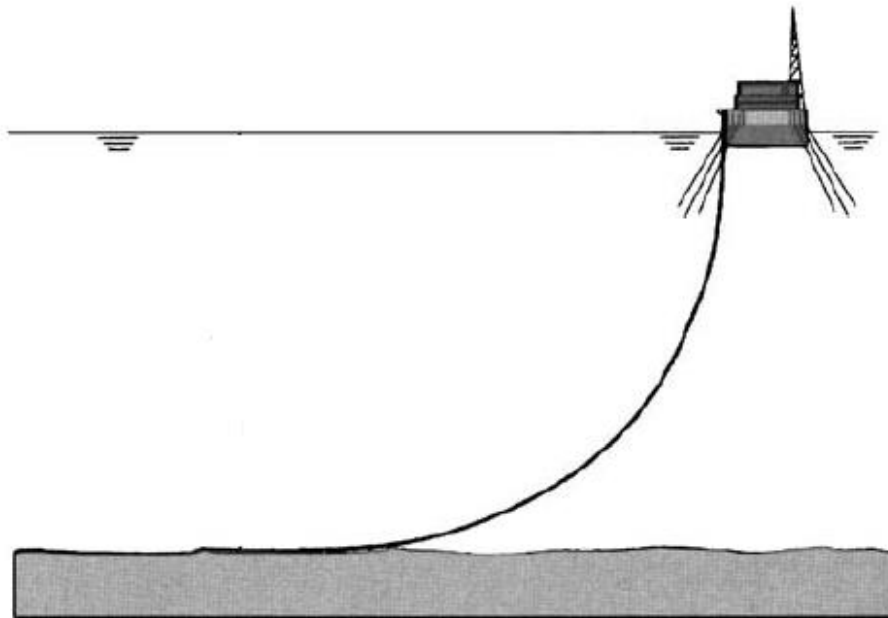


Figure 3-1. SCR schematic (Sen, 2006).

The use of steel lines makes this riser concept a cost-effective alternative since the material is cheap, making it possible to be used in greater depths without a non-suitable increase in cost. Also, the complexity of the riser system is reduced since it does not need



mid-depth buoys, its installation is easier than the other types of risers, and the need for a riser base, stress, or flex joint has been eliminated at the seabed (Dikdogmus, 2012).

This configuration is self-compensated for heave movement, i.e., it does not have a heave compensator. This makes it sensitive to environmental loading since the vessel offset changes the riser's suspended length, impacting the TDP. Significant heave and surge motions from the vessel can result in a continuous lift-off and laid down of the riser, making this area critical to fatigue and buckling issues. Also, this is the zone of maximum fatigue damage for VIV. The following optimizations in this area in order to improve SCR fatigue and strength performance have been discussed (Bhat et al., 2004):

- Increase in SCR departure angle;
- Incorporating draft changes in SCR fatigue analysis;
- Strakes as a swing parameter for vessel motion-induced fatigue (not only for VIV);
- Occasional vessel repositioning to spread fatigue damage;
- Lightening the TDA;
- Titanium in TDA.

In addition to these optimizations, other modifications to the SCR have been studied and applied to make it feasible for harsh environments and deep water. This includes alterations to its weight in different sections and the use of buoyancy modules, as discussed in the following two sections.

### **3.2 Weight distributed SCR (WDSCR)**

This concept is defined by variation in the weight along the suspended riser, which is desirable to have the lightest cross-sections in the TDA and the heaviest at the bottom of the straight section of the riser. Using a weight variation, both fatigue performance and strength criteria of the SCR can be improved. With the application of weight optimization along the riser length, the following results were achieved: a significant improvement of the SCR dynamic behavior, a considerable reduction in the von Mises stresses at TDP, and a reduction in the effect of soil-riser interaction on the fatigue response when a lightweight coated SCR was used (Karunakaran et al., 2005).

The weight variation can be done by: applying different density coatings along the riser length, attaching well-qualified ballast elements to the SCR sections above the TDP to

reduce the stresses around the TDP, and/or by attaching lightweight wrapping at the TDP and on risers on the seabed (Karunakaran et al., 2013). Fabrication and installation of the weight-distributed SCR can be done the same way as the conventional SCR. Figure 3-2 below shows the schematic of this riser.

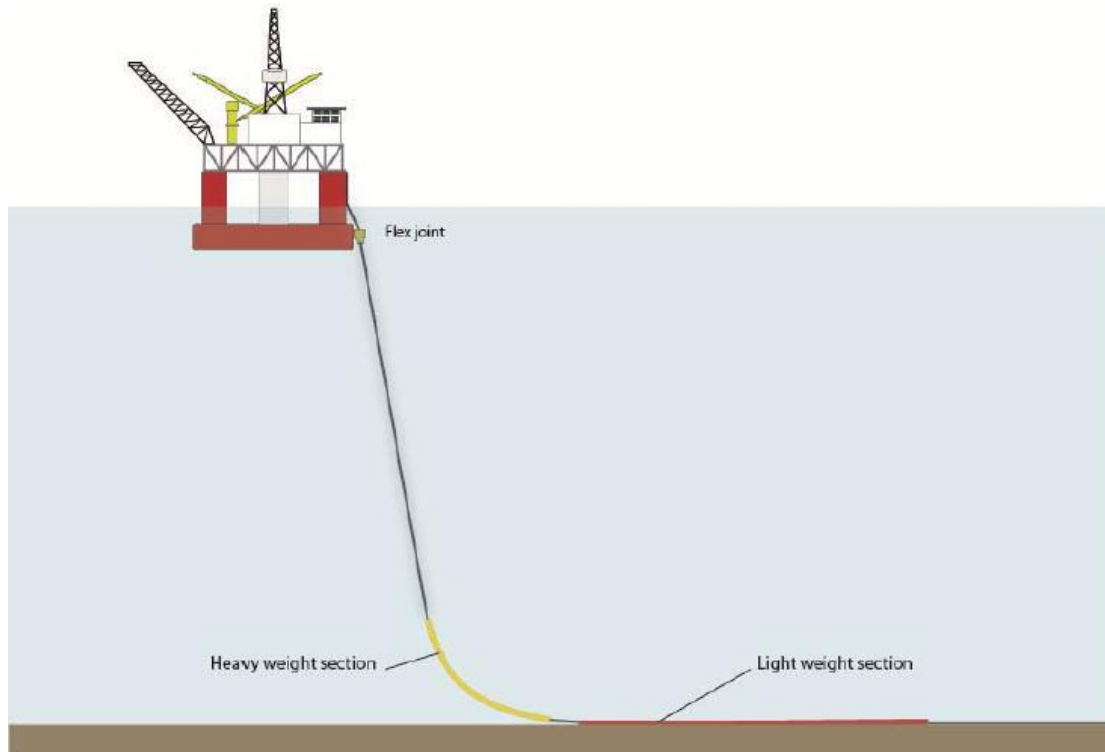


Figure 3-2. Weight distributed SCR for harsh environments (Karunakaran et al., 2013).

According to Karunakaran et al. (2013), the effects of a heavy cross-section at the bottom of the straight section of SCR are:

- Reduction in the dynamics of the straight section, which reduces the dynamic stresses at the TDP;
- Greater hang-off loads and dynamic axial stress closer to the hang-off, in case of deep-water applications;
- Reduced stress variations, which improve the fatigue response.

Furthermore, the lightweight at the seabed effects are:

- Significant improvement of the fatigue performance at TDP due to the increased flexibility of the dynamic riser system;
- Less pronounced pipe-soil interaction.

### 3.3 Steel Lazy Wave Riser (SLWR)

Traditional catenary riser configurations, when combined with a ship-based production system, are very challenging and may not be feasible to be developed in locations with very harsh environmental conditions (Karunakaran et al., 1996). Therefore, as an alternative to absorb the dynamic stresses due to the vessel heave motions, the concept of a steel lazy wave riser was first discussed by Karunakaran et al. (1996), which demonstrated to be very efficient with low stresses.

This concept configuration combines buoyancy modules with a conventional SCR, creating the arch shape of a lazy wave riser. By doing this, an uplift force is created that uncouples the vessel motions from the TDA (Felisita et al., 2015). With that, the sag bend of the SLWR becomes a pseudo touchdown area, which absorbs and reduces the amount of stress that the TDP would experience (Felisita et al., 2017).

Different riser concepts have been investigated and analyzed that the buoyancy modules effectively absorb the heave motion, isolating the dynamic motion of the floater from the TDP motion (Gemilang and Karunakaran, 2017). Thus, larger horizontal or drift offsets of the vessel are allowed with this configuration compared to the conventional SCR without significantly changing the TDP position. By having significantly less movement on the TDP, the riser's strength and fatigue performance is improved (Gemilang, 2015).

In addition, comparing the SLWR configuration and WDSCR, the first has much lower dynamic motion at the TDP, which is beneficial for fatigue.

However, besides the design required to incorporate the right amount of buoyancy especially close to the seabed, the buoyancy modules are costly and not easy to install (Cheng and Cao, 2013). Also, additional bending stress is encountered at the sag and hog bend regions.

Different curvatures for the shape of the "wave" can be discussed according to the environment, type of fluids, and costs in which this riser is situated. A schematic of an SLWR is presented in Figure 3-3.

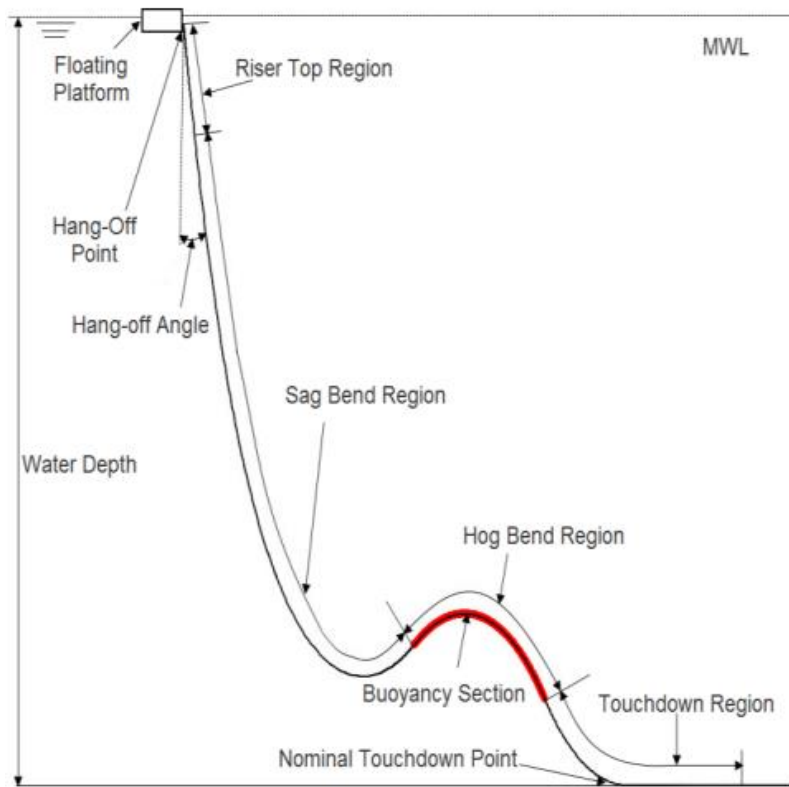


Figure 3-3. SLWR schematic (Lal et al., 2019).

## Chapter 4. Design Codes and Standards

### 4.1 Introduction

During offshore operations, equipment and structures are subjected to different loads, which can be due to usual or accidental events. As part of the system, risers shall be designed to cope with the accepted standards and regulations during their service life. These standards are essential for technical definitions of the offshore structures and installations in a regional, national or international scope. This ensures that the companies are aligned with the specifications applicable to the region where they are operating.

Gemilang (2015) states that minimum requirements for risers must be established to meet construction, installation, commissioning, operation, maintenance, requalification, and abandonment. Hence, the design is assumed to be safe when the resistance is greater than the minimum requirement. For that, uncertainties and inaccuracies are covered by a safety factor applied during the analysis of each stage of an application.

Different authorities and classification societies developed riser design guidelines such as NPD, NS, BS, HSE, CSA, ISO, API, DNV, and ABS (Bai and Bai, 2005). According to API, different types of these guidelines can be found (Orimolade, 2014):

- Specifications: documents that make the communication between purchasers and manufacturers easier;
- Recommended practices: documents based on proven industry practices;
- Standards: a combination of specifications and recommended practices;
- Codes: documents that shall be adopted by regulatory agencies or authorities with jurisdiction;
- Technical reports and bulletins: documents with technical information about a specific topic.

They can follow two design approaches:

- Working Stress Design (WSD) and
- Load Resistance Factored Design (LRFD)

One of the differences between them is that for the WSD, a single safety factor is used. On the other hand, in LRFD, partial safety factors are considered, which means that the uncertainty and inaccuracy from each specific response and resistance of each limit state

are covered. Also, WSD considers the relation between allowable stress to the material's yield stress. LRFD is an approach that considers the relation of allowable loading to the material's ultimate strength (Kavanagh et al., 2003).

In the case of deep-water risers, the most commonly applied guidelines are the following (Kavanagh et al., 2003):

- API-RP-2RD: "Design of Risers for Floating Production Systems (FPSs) and Tension-Leg Platforms (TLPs)", 2013.
- API-RP-1111: "Design, Construction, Operation and Maintenance of Offshore Hydrocarbon Pipelines (Limit State Design)", 2021.
- ASME B31.4: "Pipeline Transportation Systems for Liquids and Slurries, Chapter IX – Offshore Liquid Pipeline Systems", 2019.
- ASME B31.8: "Gas Transmission and Distribution Piping Systems", Chapter VIII – Offshore Gas Transmission, 2020.
- Offshore Standard DNV-ST-F201: "Dynamic Risers", 2018.

These documents are governed by design requirements of failure mode caused by:

- Collapse
- Combined stress
- Longitudinal stress
- Hoop stress
- Propagation buckling

## 4.2 Dynamic Riser Design

The standards for dynamic risers are API-RP-2RD and DNV-ST-F201, in which the first follows the WSD approach while the latter presents WSD and LRFD approaches. The other standards listed are related to pipelines. Usually, risers are designed following the LRFD approach. However, the WSD method shall be considered when using titanium. Hence, this section will be focused on the WSD method of API-RP-2RD and LRFD of DNV-ST-F201.

### 4.2.1 WSD Code – API-RP-2RD

The design guidelines for a riser system used on Floating Production Systems (FPSs) will be addressed in this section through the Working Stress Design (WSD) method. This recommended practice is based on the principles of limiting stresses in risers under

normal, extreme, and accidental conditions (API, 2006). A single safety factor is considered for uncertainties and inaccuracies. The loads and loads effects than can contribute to or cause failure in the riser system during its intended use must be identified and accounted for in the design (API, 2013). For design criteria, design limits on the following will be presented in this section:

- Allowable stress;
- Allowable deflection;
- Collapse;
- Fatigue/service life;

#### 4.2.1.1 Allowable stresses

Section 3.4 on API (2006) describes the allowable stress approach as the one that defines acceptability on the basis that calculated stresses in the riser are below allowable stresses for all applicable conditions. Thus, the riser design should be able to cope with the external and internal loads it will be subjected.

All critical locations in the riser should be considered to calculate the three principal stresses, which are the axial, hoop, and radial directions in a plain pipe. Von Mises yield criterion can be used for combining all principal stress at each critical location and is defined by the following equation.

$$\sigma_e = \frac{1}{\sqrt{2}} \sqrt{(\sigma_1 - \sigma_2)^2 + (\sigma_2 - \sigma_3)^2 + (\sigma_3 - \sigma_1)^2} \quad (4-1)$$

Where:

$\sigma_e$  = Von Mises equivalent stress

$\sigma_1, \sigma_2, \sigma_3$  = Principal stresses

A safe design considers that the Von Mises equivalent stress should be less than the allowable stress of the right-hand side of the following equation.

$$(\sigma_p)_e < C_f \sigma_a \quad (4-2)$$

Where:

$\sigma_a$  =  $C_a \sigma_y$  = basic allowable combined stress

$C_a$  = Allowable stress factor,  $C_a = 2/3$

$\sigma_y$  = Material minimum yield strength

$C_f$  = Design case factor, presented in Table 4-1

Table 4-1. Design matrix for rigid risers (API, 2006).

Design Case	Load Category	Environmental Condition	Pressure	One mooring line broken	Cf
1	Operating	Maximum operating	Design	No	1.0
2	Extreme	Extreme	Design	No	1.2
3	Extreme	Maximum operating	Extreme	No	1.2
4	Extreme	Maximum operating	Design	Yes	1.2
5	Temporary	Temporary	Associated	No	1.2
6	Test	Maximum operating	Test	No	1.35
7	Survival	Survival	Associated	No	1.5
8	Survival	Extreme	Associated	Yes	1.5

#### 4.2.1.2 Allowable deflections

Unlimited riser deflections might cause unacceptably high bending stresses. It is essential to consider that large riser curvature, even having the riser stress and bend radius below the acceptable limit, may result in an overstress on the tubing or in other parts constrained to move with the riser body (API, 2006). Also, a controlled riser deflection may prevent multiple risers from interfering with each other or with parts of the production system, such as tensioners, flex joints, telescopic joints, or other attached items.

#### 4.2.1.3 Collapse pressure

A collapse that occurs when a riser cannot withstand the external hydrostatic pressure is called a collapse pressure. The tubular design should be adequate to guarantee that it can handle the external pressure and not experience a collapse failure at any period during installation or operation. For that, some loads such as tension and bending should have their effects considered when performing the analysis (API, 2006). The criterion used in this method can be observed in Equation (4-3), where the predicted collapse pressure,  $P_c$ , times the design factor,  $D_f$ , should be higher than the net allowable external design pressure,  $P_a$ .

$$P_a \leq D_f P_c \quad (4-3)$$

Where:

$D_f = 0.75$  for seamless or Electric Resistant Welded (ERW) API pipe;



= 0.60 for (DSAW) internally cold expanded API pipe.

#### 4.2.1.4 Collapse propagation

According to API (2006), a pipe designed to meet the above criteria may still experience collapse at a lower pressure due to accidental means. If a collapse initiates, it may travel along the pipe and only stops when the external pressure drops below the propagation pressure. This categorizes what is called a propagating buckle. Pipes with uniform properties along the pipeline are commonly more subjected to this failure.

Means of mitigation can include a change in properties of the pipe or buckle arrestors that can be incorporated along the pipe. With that, in case a propagating buckle happens, this limits the extent of the propagating failure. The design criterion to prevent this failure is given by Equation (4-4), where the predicted propagation pressure differential,  $P_p$ , times the design factor,  $D_p$ , should be more than the design pressure differential,  $P_d$ .

$$P_d \leq D_p P_p \quad (4-4)$$

Where:

$$D_p = 0.72$$

#### 4.2.1.5 Overall Column Buckling

Excessive negative tension, also called compression, may cause an overall column buckling on the riser. This compression has as consequence, excessive curvature and bending moments at critical locations. A way to prevent this buckling is to provide tension at the top end termination of the riser.

#### 4.2.1.6 Fatigue/service life

The time a component stays in service is defined as its service life. However, it must be considered that the component will be affected by fatigue during its service life. Thus, the cumulative fatigue damage ratio calculations are used to predict the design fatigue life.

API (2006) recommends a safety factor of at least 10 times the service life for locations that cannot be inspected or have safety and pollution risks classified as high. The factor should be at least three times the service life for other locations that can be inspected or have low safety and pollution risks. With that, the following criterion should be satisfied.

$$\sum_i SF_i D_i < 1.0 \quad (4-5)$$

Where:

$D_i$  = Fatigue damage ratio for each phase of loading

$SF_i$  = Associated safety factor

#### 4.2.2 LRFD Code – DNV-ST-F201

In order to ensure the structural safety of the riser, this standard used a safety class methodology. Some basic principles shall be considered during the design of the riser system as the below:

- Functional and operation requirements given in the design basis shall be satisfied;
- Design must ensure that unintended events do not turn into an accident to a greater extent than the original event;
- Installation and retrieval must be simple, reliable, and robust for use;
- Inspection, maintenance, replacement, and repair shall be adequately accessed;
- Riser joints and components shall comply with fabrication recognized techniques and practice;
- Effects of corrosion erosion and wear shall be minimized in the design of structural details;
- Design of "fail-safe" riser mechanical components, when possible;
- The design will facilitate monitoring of tension, stresses, angles, vibrations, fatigue cracks, wear, corrosion, etc.

This method aims to keep the failure probability below a specific value. The relevant failure modes for the risers must be identified, and no corresponding limit state must be exceeded. The limit states are categorized as the following (DNV, 2018):

- **Ultimate Limit State (ULS)**

It involves the structural integrity or strength of the structure, which shall be designed to have a very low probability of reaching this state since the consequences are severe.

- **Fatigue Limit State (FLS)**

It involves the fatigue damage resulting from cyclic dynamic loads (currents, waves, slugging) accumulated throughout the riser's life. The riser must be designed such that its life, accounting for fatigue damage from all sources, meets or exceeds the design life.

- **Serviceability Limit State (SLS)**

This state considers the disruption of the use of the structure as intended. It is related to the criteria limiting or governing the riser's functional use.

- **Accidental Limit State (ALS)**

This state involved damage or failure due to unusual, accidental, or unplanned loading conditions.

The general LRFD safety factor, according to DNV (2018), considers several load effects multiplied by their corresponding load effect factors, which are compared to the resistance factor. The expression for this is as presented in Equation (4-6).

$$S_d(S_P; \gamma_F \cdot S_F; \gamma_E \cdot S_E; \gamma_A \cdot S_A) \leq \frac{R_K}{\gamma_{SC} \cdot \gamma_m \cdot \gamma_c} \quad (4-6)$$

Where:

$S_d$  = Sum of design load factor

$S_P$  = Pressure loads

$S_F$  = Load effect from functional loads (vector or scalar)

$S_E$  = Load effect from environmental loads (vector or scalar)

$S_A$  = Load effect from accidental loads (vector or scalar)

$\gamma_F$  = Load effect factor for functional loads (vector or scalar)

$\gamma_E$  = Load effect factor for environmental loads

$\gamma_A$  = Load effect factor for accidental loads

$\gamma_{SC}$  = Resistance factor to take into account for the safety class

$\gamma_m$  = Resistance factor to account for material and resistance uncertainties

$\gamma_c$  = Resistance factor to account for special conditions

$R_K$  = Generalised resistance (vector or scalar)

#### 4.2.2.1 Design loads

Design load effects consider each load effect and its corresponding load effect factor. Equation (4-7) below presents how the calculation for bending moment is.

$$M_d = \gamma_F \cdot M_F + \gamma_E \cdot M_E + \gamma_A \cdot M_A \quad (4-7)$$

Where:

$M_d$  = Bending moment design

$M_F$  = Bending moment from functional loads

$M_E$  = Bending moment from environmental loads

$M_A$  = Bending moment from accidental loads

Design effective tension in case of functional and environmental induced load effects is calculated as Equation (4-8).

$$T_{ed} = \gamma_F \cdot T_{eF} + \gamma_E \cdot T_{eE} + \gamma_A \cdot T_{eA} \quad (4-8)$$

Where:

$T_{ed}$  = Effective tension design

$T_{eF}$  = Effective tension from functional loads

$T_{eE}$  = Effective tension from environmental loads

$T_{eA}$  = Effective tension from accidental loads

And the effective tension is given by Equation (4-9).

$$T_e = T_w - p_i \cdot A_i + p_e \cdot A \quad (4-9)$$

Where:

$T_w$  = True wall tension

$p_i$  = Internal (local) pressure

$p_e$  = External (local) pressure

$A_i$  = Internal cross-sectional area

$A_e$  = External cross-sectional area

#### 4.2.2.2 Ultimate Limit States

The riser shall be designed to be able to remain intact and avoid rupture. This corresponds to maximum resistance to applied loads with  $10^{-2}$  annual exceedance probability. Typical limit states for this category are:

- Bursting
- Hoop buckling (collapse)
- Propagating buckling
- Gross plastic deformation and local buckling
- Gross plastic deformation, local buckling, and hoop buckling
- Unstable fracture and gross plastic deformation

- Liquid tightness
- Global buckling

#### 4.2.2.2.1 Bursting

Bursting is a severe damage that shall be avoided during the operations. Risers must be designed to operate during their lifecycles without bursting. The dominating load is internal overpressure combined with bending (Bai and Bai, 2005). The failure mode is governed by the tensile hoop stress, defined by the local differential pressure of external and internal pressure. Therefore, the top-end of the riser is a critical area since it is where there is maximum internal pressure and minimum external pressure.

According to DNV (2018), pipe members subjected to net internal overpressure must be designed to have the condition in Equation (4-10) satisfied at all cross-sections.

$$(p_{li} - p_e) \leq \frac{p_b(t_l)}{\gamma_m \cdot \gamma_{SC}} \quad (4-10)$$

Where:

$p_{li}$  = Local incidental pressure. It is the maximum expected internal pressure with a low annual exceedance probability.

$p_e$  = External pressure

$p_b$  = Burst resistance

$t_l$  = Pipe wall thickness

$\gamma_m$  = Material resistance factor

$\gamma_{SC}$  = Safety class factor

Local incident pressure,  $p_{li}$ , considers the design pressure,  $p_d$ , and the local internal design pressure,  $p_{ld}$ . Equation (4-11) calculates it.

$$p_{li} = p_{ld} + 0.1 \cdot p_d \quad (4-11)$$

Burst resistance,  $p_b$ , is dependent on the yielding limit and tensile limit of the riser material. So, it is determined by the minimum value of Equation (4-12) and Equation (4-13):

$$p_{b\_yield} = \frac{2}{\sqrt{3}} \frac{2t}{D - t} f_y \quad (4-12)$$

$$p_{b\_tensile} = \frac{2}{\sqrt{3}} \frac{2t}{D-t} \frac{f_u}{1.15} \quad (4-13)$$

Where:

$D$  = Outer diameter of the pipe

$t$  = "dummy" variable to be substituted by  $t_1$  or  $t_2$  where relevant

$f_y$  = Yield strength

$f_u$  = Tensile strength

Two conditions can specify wall thickness for burst and collapse design checks: mill pressure test and system pressure test condition (Equation (4-14)) or operational condition (Equation (4-15)):

$$t_1 = t_{nom} - t_{fab} \quad (4-14)$$

$$t_1 = t_{nom} - t_{fab} - t_{corr} \quad (4-15)$$

Where:

$t_{nom}$  = Nominal (specified) pipe wall thickness

$t_{fab}$  = Fabrication (manufacture) negative tolerance

$t_{corr}$  = Corrosion/wear/erosion allowance

For other limit states related to extreme loading, resistances must consider the Equation (4-16) for wall thickness calculation of installation/retrieval and system pressure test and Equation (4-17) for other cases:

$$t_2 = t_{nom} \quad (4-16)$$

$$t_2 = t_{nom} - t_{corr} \quad (4-17)$$

Risers without allowances and tolerances must consider the minimum required wall thickness as expressed in Equation (4-18):

$$t_1 = \frac{D}{\frac{4}{\sqrt{3}} \cdot \frac{\min\left(f_y; \frac{f_u}{1.15}\right)}{\gamma_m \gamma_{SC} (p_{li} - p_e)} + 1} \quad (4-18)$$

#### 4.2.2.2.2 System Hoop Buckling (Collapse)

Pipe collapse due to overpressure is one of the failure modes. The bottom section of the riser is subjected to maximum external pressure. Therefore, wall thickness shall be

governed by the differential pressure between internal and external pressure. Pipes subjected to external overpressure shall be designed to satisfy the condition given below for Equation (4-19).

$$(p_e - p_{min}) \leq \frac{p_c(t_1)}{\gamma_{SC} \cdot \gamma_m} \quad (4-19)$$

Where:

$p_e$  = External pressure

$p_{min}$  = Minimum internal pressure

$p_c$  = Resistance for external pressure, given by Equation (4-20):

$$(p_c(t) - p_{el}(t)) \cdot (p_c^2(t) - p_p^2(t)) = p_c(t) \cdot p_{el}(t) \cdot p_p(t) \cdot f_0 \cdot \frac{D}{t} \quad (4-20)$$

Where the elastic collapse pressure (instability),  $p_{el}$  is given by Equation (4-21):

$$p_{el}(t) = \frac{2 \cdot E \cdot \left(\frac{t}{D}\right)^3}{1 - \nu^2} \quad (4-21)$$

Moreover, the plastic collapse pressure is given by Equation (4-22):

$$p_p(t) = 2 \frac{t}{D} \cdot f_y \cdot \alpha_{fab} \quad (4-22)$$

Where:

$\alpha_{fab}$  = Fabrication factor

The initial ovality,  $f_0$ , i.e., the initial departure from the circularity of pipe and pipe ends is defined by the following Equation (4-23):

$$f_0 = \frac{D_{max} - D_{min}}{D} \quad (4-23)$$

However, it must not be considered less than 0.005%. It should consider ovalization caused during the construction and installation phase, but not the one due to external pressure or moment as the as-installed position (DNV, 2018).

#### 4.2.2.2.3 Propagating buckling

A local buckle can escalate and lead to successive hoop buckling of neighboring pipe sections, which causes a collapse due to propagating buckling. To ensure that it remains local, the following check defined by Equation (4-24) is required:

$$(p_e - p_{min}) \leq \frac{p_{pr}}{\gamma_c \gamma_m \gamma_{SC}} \quad (4-24)$$

Where  $\gamma_c=0.9$  if the buckle is allowed to travel a short distance and  $\gamma_c=1.0$  shall be considered if no buckle propagation is allowed.

Resistance against buckling propagation is given in the following Equation (4-25):

$$p_{pr} = 35 \cdot f_y \cdot \alpha_{fab} \cdot \left(\frac{t_2}{D}\right)^{25} \quad (4-25)$$

The propagating buckling is dependent on the wall thickness of the pipe. Hence, the design will be more conservative if this criterion has to be met, resulting in a significantly thicker wall thickness compared to other criteria. However, to overcome this and save weight and cost, buckle arrestors are installed at the critical regions instead of using thicker wall thickness uniformly (DNV, 2018).

#### 4.2.2.2.4 Combined load criteria

Equation (4-26) shall be satisfied when designing pipe members subjected to bending moment, effective tension, and net internal overpressure.

$$\{\gamma_{SC} \cdot \gamma_m\} \left\{ \left( \frac{|M_d|}{M_k} \cdot \sqrt{1 - \left(\frac{p_{ld} - p_e}{p_b(t_2)}\right)^2} \right) + \left(\frac{T_{ed}}{T_k}\right)^2 \right\} + \left(\frac{p_{ld} - p_e}{p_b(t_2)}\right)^2 \leq 1 \quad (4-26)$$

Where:

- $M_d$  = Design bending moment
- $T_{ed}$  = Design effective tension
- $p_{ld}$  = Local internal design pressure
- $p_e$  = Local external pressure
- $p_b(t_2)$  = Burst resistance

The plastic bending moment resistance,  $M_k$ , and the plastic axial force resistance are given by Equation (4-27) and Equation (4-28).

$$M_k = f_y \cdot \alpha_c \cdot (D - t_2)^2 \cdot t_2 \quad (4-27)$$

$$T_k = f_y \cdot \alpha_c \cdot \pi \cdot (D - t_2) \cdot t_2 \quad (4-28)$$

Equation (4-29) below shall be satisfied for pipe members subjected to bending moment, effective tension, and net external overpressure.



$$\{\gamma_{SC} \cdot \gamma_m\}^2 \left\{ \left( \frac{|M_d|}{M_k} \right) + \left( \frac{T_{ed}}{T_k} \right)^2 \right\} + \{\gamma_{SC} \cdot \gamma_m\}^2 \left( \frac{p_e - p_{min}}{p_c(t_2)} \right)^2 \leq 1 \quad (4-29)$$

#### 4.2.2.3 Accidental Limit State

Loads caused due to abnormal conditions, incorrect operation, or technical failure are called accidental loads. Accidental loads and load effects are determined by their occurrence frequency and magnitude. These loads or events categorize the accidental limit state.

Design against the accidental loads can be done directly by calculating the effects imposed by the loads on the structure or indirectly by designing the structure tolerable to accidents. They can be categorized into (but not limited to):

- Fires and explosions
- Impact/collisions
- Hook/snag loads
- Failure of support system
- Exceedance of incidental internal overpressure
- Environmental events

A simplified design check can be performed as in Table 4-2.

Table 4-2. Simplified design check for accidental loads (DNV, 2018).

Prob. of occurrence	Safety class low	Safety class normal	Safety class high
$> 10^{-2}$	Accidental loads may be regarded similar to environmental loads and may be evaluated similarly to the ULS design check		
$10^{-2} - 10^{-3}$	To be evaluated on a case-by-case basis		
$10^{-3} - 10^{-4}$	$\gamma_c = 1.0$	$\gamma_c = 1.0$	$\gamma_c = 1.0$
$10^{-4} - 10^{-5}$	*	$\gamma_c = 0.9$	$\gamma_c = 0.9$
$10^{-5} - 10^{-6}$	*		$\gamma_c = 0.8$
$< 10^{-6}$	* Accidental loads or events may be disregarded		

#### 4.2.2.4 Serviceability Limit State

The serviceability limit state is associated with the requirements that ensure a normal operation, which means determining acceptable limitations. Operating limitations and/or design assumptions must be clearly highlighted and implemented in the operating

procedures. Tools like FMEA (Failure Mode and Effects Analysis), HAZOP (Hazard Operability Study), and design reviews can be used to identify SLS.

However, a failure shall not be led by an exceedance of an SLS, and ALS must be defined in association with it. Events caused by exceeding SLS shall be controlled by maintenance and inspection routines and by implementing early warning or fail-safe type systems in the design.

Limitations regarding deflections, displacements, and rotation of the global riser or ovalization of the riser pipe are some of the SLS for the global riser behavior. Examples are presented below:

- Ovalization limit due to bending

Excessive ovalization must be avoided on the risers. Premature local buckling can be prevented by limiting the flattening due to bending together with the out-of-roundness tolerance from the fabrication of the pipe to 3.0% (DNV, 2018). The following equation (4-30) shall be fulfilled.

$$f_o = \frac{D_{max} - D_{min}}{D} \leq 0.03 \quad (4-30)$$

- Riser stroke

A top tensioned riser has a tensioner that pulls it upward on the top part of the riser to limit bending and maintain constant tension. It must continue to pull as the riser and the floater move vertically to each other. Stroke is defined as the travel of the tensioner. Sufficient stroke shall be considered in the design of the riser system to avoid damages to the riser, components, and equipment (DNV, 2018).

#### 4.2.2.4.1 Fatigue Limit State

Fatigue damage is caused by cyclic loadings during the lifetime of the riser. For the fatigue limit state, cyclic loadings with magnitude and number of cycles large enough to cause fatigue damage effects must be considered. Because of that, the design of the riser system shall ensure adequate safety against fatigue during its service life. Sources that cause fatigue damage include:

- Currents (VIV)
- Waves

- Vessel motions
- Slugging

According to DNV (2018), fatigue assessment can be categorized into two methods:

- Methods based on S-N curves

The fatigue criterion, given in Equation (4-31), must be satisfied:

$$D_{fat} \cdot DFF \leq 1.0 \quad (4-31)$$

Where:

$D_{fat}$  = Accumulated fatigue damage

DFF = Design fatigue factor

Table 4-3. Design fatigue factors.

Safety class		
Low	Normal	High
3.0	6.0	10.0

- Methods based on fatigue crack propagation

A fatigue crack propagation originates when an initial defect size grows to a critical size during service life or time to first inspection. Because of that, riser components must be designed and inspected considering a damage tolerant design approach to ensure this does not happen. The condition in Equation (4-32) for the fatigue crack growth life shall be satisfied.

$$\frac{N_{tot}}{N_{cg}} \cdot DFF \leq 1.0 \quad (4-32)$$

Where:

$N_{tot}$  = Total number of applied stress cycles during service or in-service inspection

$N_{cg}$  = Number of stress cycles necessary to increase the defect from the initial to the critical defect size

## Chapter 5. Design Basis and Methodology

### 5.1 Introduction

This chapter presents the design basis and methodology used for determining the optimum SCR with titanium section configuration and its behavior in environmental conditions. The data is also be used for the fatigue analysis on the TDA, which will be presented.

The objective of this study was to investigate the use of a titanium section in the TDA of the SCR in terms of fatigue of the riser. Therefore, a riser configuration was designed and optimized to satisfy the requirements in both strength and fatigue. Data presented in this chapter was used as input in the OrcaFlex software, version 11.1, which was developed by Orcina, and it is able to perform both static and dynamic analysis of risers. A description of the software is presented in Appendix A.

### 5.2 Description

This study will consider parameters of the Brazilian offshore area, specifically the southeast region, as shown in Figure 5-1. The field under consideration is in a remote area with a water depth of 2000 meters, classified as deep-water.



Figure 5-1. Brazilian south and southeast basins (Souza and Sgarbi, 2019).

A spread moored FPSO is the concept selected. This type of platform is one of the main concepts used in that region, considering the environmental conditions and the location

of the field, which is in a remote area with no nearby structures. This vessel's Response Amplitude Operator (RAO) will consider typical data for this type of vessel in this region. Different scenarios and their analysis will be performed in the software OrcaFlex. A general concept of the SCR layout is presented in Figure 5-2 below.

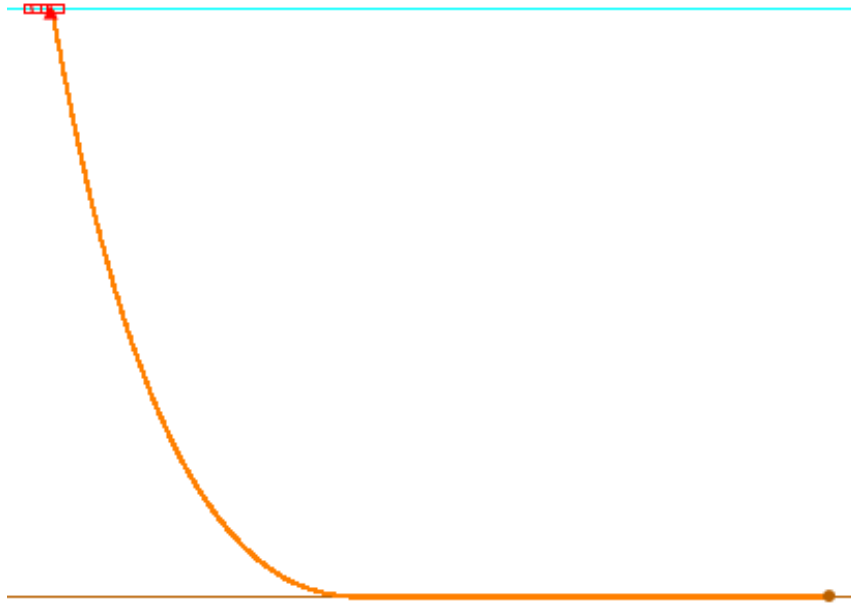


Figure 5-2. SCR configuration.

### 5.3 Design standards

The standard API (2006) is utilized to design the SCR and SCR with titanium section. However, other design criteria are established in accordance with the following standards:

- Submarine Pipeline Systems – DNV-OS-F10, 2017
- Fatigue Design of Offshore Steel Structures – DNV-RP-C203, 2016
- Riser Fatigue – DNV-RP-F204, 2019
- Specification for Line Pipe – API SPECIFICATION 5L, 2018

### 5.4 Design data

#### 5.4.1 FPSO data

The local coordinate system of the vessel is defined in OrcaFlex as:

- Origin: amidship of the FPSO
- X-axis: longitudinal axis positive to FPSO bow (vessel heading) and surge direction
- Y-axis: transversal axis and sway direction

- Z-axis: vertical axis and heave direction

Dimensions of the FPSO are presented in Table 5-1:

Table 5-1. FPSO dimensions.

Parameter	Value	Unit
Length	320	m
Width	60	m
Height	28	m

## 5.4.2 FPSO motions

According to DNV (2019), to correctly analyze the global riser load effect, the following floater motions shall be considered:

- Wave frequency motions (WF);
- Low-frequency motions (LF);
- FPSO static offsets.

### 5.4.2.1 Wave frequency motions (WF)

These are the FPSO first-order motions described by RAOs, which result from the hydrodynamic analysis of the floater. They are caused by wave actions and are represented in terms of amplitude and phase angle as a function of several discrete wave frequencies and directions (DNV, 2019). The WF regime is between the period range of 3-25 seconds.

The FPSO harmonic functions in six degrees of freedom (surge, sway, heave, roll, pitch, yaw) defined the RAO data used in this work. The vessel's center of gravity is the origin of the RAO.

### 5.4.2.2 Low-frequency motions (LF)

Second-order wave frequencies and wind loading cause this motion. It is categorized by frequencies below wave frequencies at, or near, surge, sway, and yaw natural periods for the floater. The LF motions have periods that typically range from 30 to 300 seconds (DNV, 2018)

### 5.4.2.3 FPSO static offsets

The floater offset considers the motions caused by the wind, waves, and current. As a result, the platform can be encountered in three positions: mean (nominal), near, or far.

Near position refers to when the FPSO displaces toward the riser connection point at the seabed. On the other hand, the far position is when the FPSO displaces away from the riser connection point at the seabed. Figure 5-3 below represents the three configurations for the SCR.

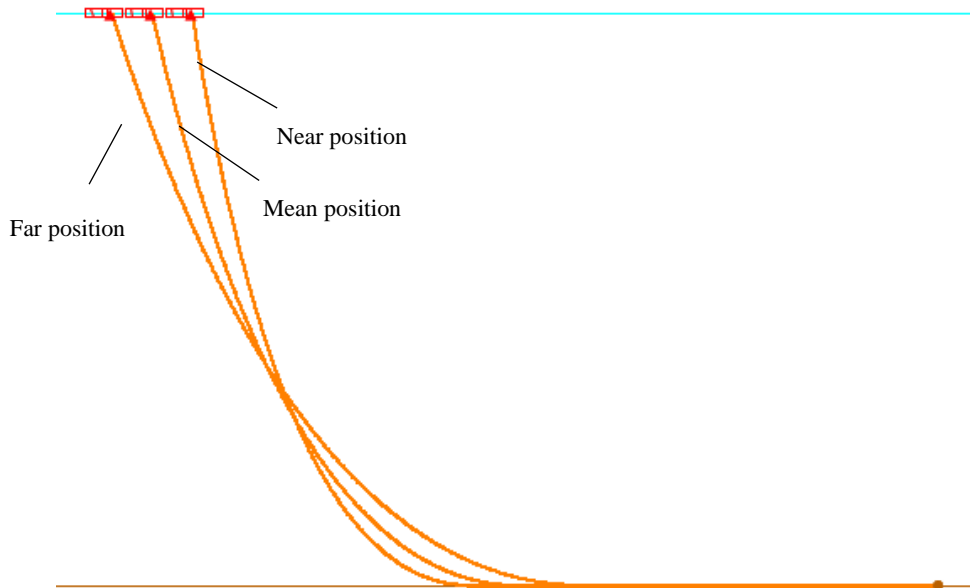


Figure 5-3. SCR near, mean, and far position.

### 5.4.3 Environmental data

The water depth considered in this study is 2,000 meters, which is an average depth of the area being studied. A constant seawater density of 1025 kg/m<sup>3</sup> and temperature of 10° is assumed.

A combination of a 100-year wave with 10-year current drives the ULS design. As the objective of this work is to analyze an alternative proposal of SCR in order to have a better fatigue response in a harsh environment, an extreme sea state is modeled using the JONSWAP (Joint North Sea Wave Project) spectrum.

JONSWAP spectrum is an extension of PM (Pierson Moskowitz) spectrum, which includes fetch limited seas and is described by Equation (5-1).

$$S_J(\omega) = A_\gamma S_{PM}(\omega) \gamma^{\exp(-0.5(\frac{\omega-\omega_p}{\sigma\omega_p})^2)} \quad (5-1)$$

Where:

$S_{PM}(\omega)$  = Pierson-Moskowitz spectrum

$\gamma$  = non-dimensional peak shape parameter

$\sigma$  = spectral width parameter

$$\sigma = \sigma_a \text{ for } \omega \leq \omega_p$$

$$\sigma = \sigma_b \text{ for } \omega > \omega_p$$

$A_\gamma = 1 - 0.287 \ln(\gamma)$  is a normalizing factor

This model is expected to be reasonable for the condition in Equation (5-2).

$$3.6 < \frac{T_p}{\sqrt{H_s}} < 5 \quad (5-2)$$

The projected wave was chosen considering the highest vertical velocity on the top of the riser. For that, a metocean conditions report with a return period of 100 years was used.

Assuming an FPSO heading of  $195^\circ$ , the most common in Brazil's Santos and Campos Basin, the maximum vertical velocities based on a 3-hour sea state are presented in Figure 5-4 below.

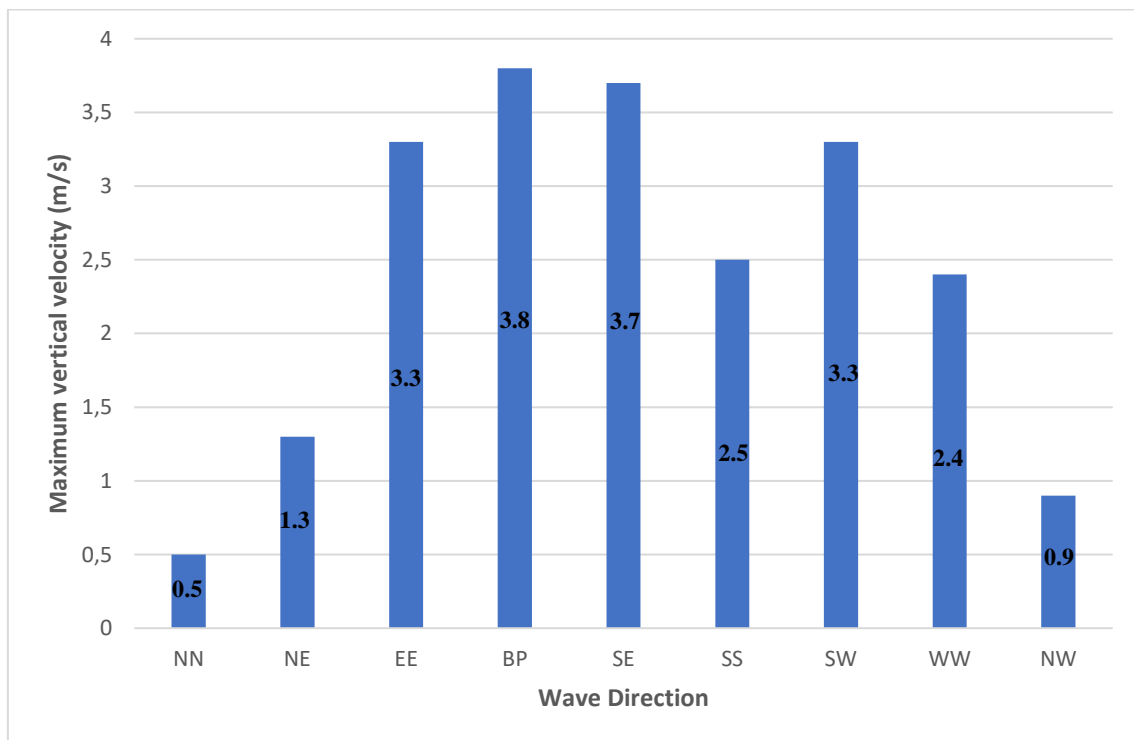


Figure 5-4. Distribution of maximum vertical velocity versus wave direction.

The figure above presents the cardinal directions of the wave incidence on the FPSO. Direction BP (Beam portside) represents the wave incidence at  $90^\circ$  of the FPSO. In this direction, it is where it is observed the highest vertical velocity of 3.8 m/s. According to Gemilang (2015), the highest tensions on the TDP occur after a maximum vertical



velocity. For that reason, the significant wave height ( $H_s$ ) and the wave period ( $T_p$ ) of this wave were selected for the study. The respective values can be observed in Table 5-2.

Table 5-2. Project wave.

$H_s$ (m)	$T_p$ (s)	$\gamma$
6.0	14.5	1.721664

The hang-off position of the SCR is presented in Table 5-3, which is demonstrated in Figure 5-5 with the respective vessel orientation.

Table 5-3. SCR hang-off position.

$x$	$y$	$z$
30	0	6.22

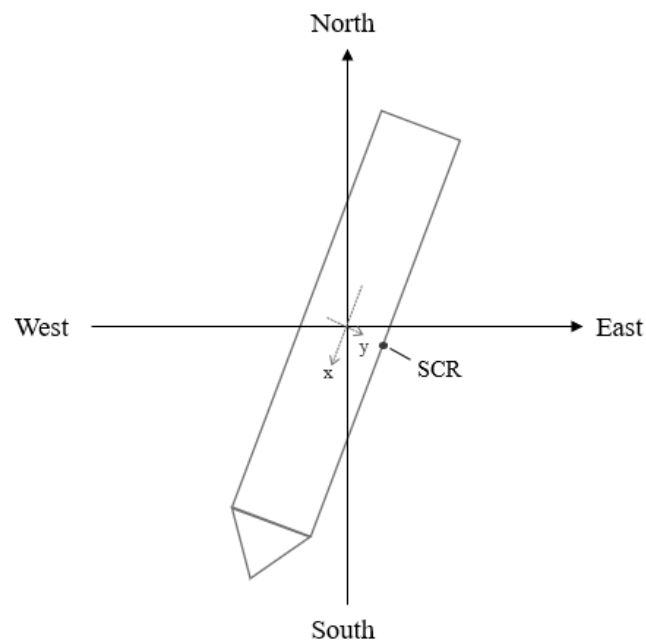


Figure 5-5. Vessel orientation.

#### 5.4.4 Operational and accidental design conditions

Operational and accidental design conditions are being considered for the strength analysis of the riser. The operational condition is when intact mooring is considered. For that condition, the ULS offset of 7% of the water depth is considered for the near and far positions of the FPSO.

An accidental condition, in ALS, considers a failure of one mooring line. Therefore, for this condition, an offset of 8% of the water depth is considered for the near and far position of the FPSO.

A summary of the offsets in each condition is presented in Table 5-4.

Table 5-4. FPSO offsets.

<b>Mooring condition</b>	<b>FPSO offset (% of water depth)</b>	<b>FPSO offset (m)</b>
Intact	7%	140
Accidental	8%	160

#### 5.4.5 Riser properties

The SCR selected for this study is a production riser with a top angle of 10° when located in its mean position. Its main properties are presented in Table 5-5.

Table 5-5. Riser properties.

<b>Riser parameter</b>	
Internal diameter (in/mm)	10/254
Steel grade	X65
Steel density (kg/m <sup>3</sup> )	7,850
Specified minimum yield strength (SMYS) (MPa)	448.2
Specified minimum tensile strength (SMTS) (MPa)	530.9
Elastic Modulus (MPa)	207,000
Poisson ratio	0.3
<b>Coating</b>	
External coating thickness (mm)	40
Coating density (kg/m <sup>3</sup> )	690

##### 5.4.5.1 Titanium section

The titanium section taken into account is located on the TDA of the riser. Since the fatigue analysis carried on in this work will be performed on the TDP, it has to be defined so that it covers the TDA in the mean, near, and far offset positions. Hence, a section of 610-meter length was considered. Later in this thesis work, a sensitivity analysis will be performed to check if this can be optimized.

The properties considered for this material are presented in Table 5-6. Figure 5-6 represents the three configurations of SCR with this section.

Table 5-6. Titanium properties.

<b>Titanium section</b>	
Internal diameter (in/mm)	10/254
Titanium density (kg/m <sup>3</sup> )	4,420
Specified minimum yield strength (SMYS) (MPa)	758
Specified minimum tensile strength (SMTS) (MPa)	826
Elastic Modulus (MPa)	113,000
Poisson ratio	0.33

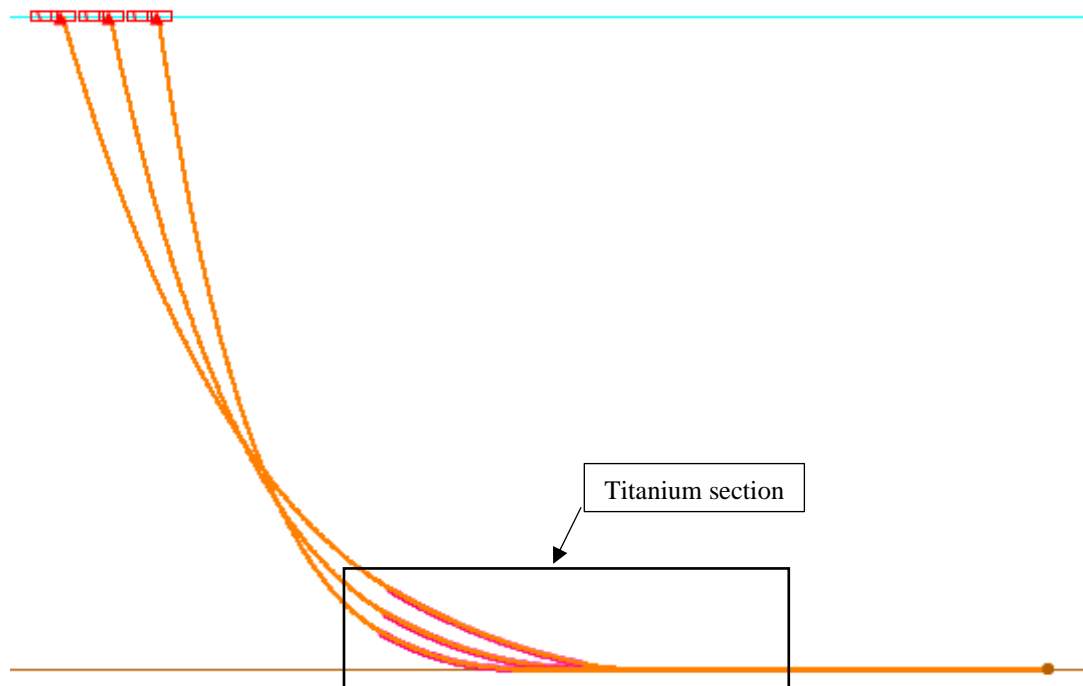


Figure 5-6. SCR with titanium section.

#### 5.4.5.2 Internal fluid

The internal fluid considered for the design basis is a production fluid with a density of 575 kg/m<sup>3</sup>. Its internal design pressure is 500 bar on the top of the riser.

#### 5.4.6 Design life

A design life of 25 years is considered for the production riser. The safety class will be regarded as high, and a safety factor of 10 will be applied for the wave-induced fatigue. Hence, the minimum fatigue life for the SCR and SCR with titanium section is 250 years.

### 5.4.7 Hydrodynamic data and Marine Growth

Slender structures can have their hydrodynamic loading expressed by the Morison equation regarding the relative fluid-structure velocities and accelerations. The Morison formulation can mainly cause nonlinearities in the response characteristics of these structures. The hydrodynamic coefficients, drag, inertia, and added mass, which are part of the equation, depend on the Reynolds number, Keulegan Carpenter number (KC), roughness ratio, reduced velocity, and the relative current number.

However, DNV (2018) states that a natural choice for circular bare pipes is to use an inertia coefficient equal to 2 and a drag coefficient between 0.1 and 1.0. A conservative approach was applied to this study which kept the values constant over the entire depth. The marine growth effects may result in an increase in hydrodynamic load during the service life. In this study, these effects are considered covered by the hydrodynamic coefficients presented in Table 5-7.

Table 5-7. Hydrodynamic coefficients.

Parameter	Value
Normal drag coefficient	1.2
Axial drag coefficient	0.008
Normal added mass coefficient	1.0
Axial added mass coefficient	0.0

### 5.4.8 Riser-soil interaction

Soil interaction between the riser and the seabed is a factor that must be taken into account when considering the fatigue response of the riser. During a loading cycle, the most severe degradation happens when the riser pipe is separated from the soil (Cluckey et al., 2007). A trench can be formed during the separation, making the degradation greater if the pipe riser moves back to it.

Therefore, to a better fatigue performance estimation, the soil properties of the place where the riser pipe is encountered must be considered. The parameters used in this study are presented in Table 5-8.

Table 5-8. Soil properties.

Parameter	Value
Lateral and axial (shear) soil stiffness	200 kN/m/m <sup>2</sup>
Normal (vertical) soil stiffness	1500 kN/m/m <sup>2</sup>
Axial friction coefficient	0.3
Lateral (normal) friction coefficient	0.5

## 5.5 Wall thickness

The riser's wall thickness must be selected to handle internal overpressure, external hydrostatic pressure, and combined loading. The minimum wall thickness can be obtained by a derivation from the fundamental hoop stress, which is a stress generated to resist the bursting effect because of the pressure applied. It is represented by Equation (5-3).

$$t = \frac{P_i D_i - P_o D_o}{2\sigma_n} \quad (5-3)$$

Where:

$P_i$  = Internal pressure

$P_o$  = External pressure

$D_i$  = Internal diameter

$D_o$  = External diameter

$\sigma_n$  = Normal stress, represented by Equation (5-4).

$$\sigma_n = f_1 \cdot \sigma_y \quad (5-4)$$

$f_1$  = Design factor, which can be assumed to be 0.72

$\sigma_y$  = Yield stress

Considering that on the top of the riser, external pressure is equal to the atmospheric pressure, there is no pressure difference and  $P_o$  is zero. Substituting Equation (5-4) on Equation (5-3), wall thickness can be calculated by Equation (5-5).

$$t = \frac{P_i D_i}{2f_1 \sigma_y} \quad (5-5)$$

The necessary parameters for the calculation of steel and titanium are in Table 5-5 and Table 5-6, which resulted in a minimum wall thickness of 19.7 mm and 11.6 mm, respectively.

## 5.6 Design cases

The extreme response analysis considers the load cases defined by the environmental loads (waves and current). A worst-case scenario must be captured in the strength analysis. Once the vessel is moored, wind and current are the environmental loads that most affect its displacement. Thus, waves are considered in one direction only and do not change according to the offsets. On the other hand, the current flow is considered to be in the same direction as the vessel offsets. As identified in section 5.4.3, the critical wave that gives the highest downward velocity is the one that incidents at 90° on the vessel. In OrcaFlex, due to the software settings, this corresponds to a wave direction of 165°.

In this study, lateral load cases are not considered critical for the riser dimensioning and therefore are not considered. The load cases for both statics and dynamics analysis can be seen in the matrix presented in Table 5-9.

Table 5-9. Load case matrix.

Load case	Stage/Limit Stage	Load Type	Environmental Wave Direction	Offset	In-plane distance (x)
1	Static	Functional	-	Mean	0 m
2	Dynamic – ULS	Functional + Environmental	165°	Near	140 m
3	Dynamic – ULS	Functional + Environmental	165°	Far	- 140 m
4	Dynamic – ALS	Functional + Environmental	165°	Near	160 m
5	Dynamic – ALS	Functional + Environmental	165°	Far	- 160 m

## 5.7 Extreme response methodology

The extreme response aims to verify the integrity of the SCR and SCR with titanium section from the FPSO when exposed to extreme sea-state conditions. A nonlinear time-domain analysis results in a nonlinear action effect and is used to calculate the extreme response (Gemilang, 2015). As described in section 5.4.3, the JONSWAP spectrum generates the irregular waves used to model the sea-state realization. Thus, the sea-state realization comprises random wave trains, defined by a user-defined seed number of wave components, significant wave height ( $H_s$ ), and peak period ( $T_p$ ). For every user-defined seed, a different sea-state realization is generated, which has distinct effects on the

structure's response. Therefore, a sufficiently long-accumulated duration of critical weather conditions should capture the extremes' natural variability (NORSOK, 2007). For short-term sea-states, the statistical confidence can be achieved by 3-hour storm simulations with different random seeds.

A percentile response of 90% for each load case is recommended by NORSOK (2007). This will typically require 20 realizations or more of the 3-hour sea state, i.e., 20 random seed simulations have to be considered. Each simulation results in a 3-hour maximum response, denoted by “X”, which will give an output of 20 maximum independent responses. For instance, the 90% percentile is then achieved by an extreme value distribution, as Gumbel. This method captures different responses according to sea-state realizations, ensuring adequate statistical confidence.

The percentile response is applied to the downward velocity at the hang-off point since in the global strength analysis, this is the parameter that dominates the critical reactions of the riser as stress and buckling (Gemilang, 2015). In this work, however, the Company provided the downward velocity, which was obtained by an average of the results of the seeds. The methodology used was different due to other confidential requirements and, therefore, will not be presented.

## 5.8 Acceptance criteria

As acceptance criteria, the strength performance of the risers analyzed in this study shall fulfill the combined loading criteria for:

- Effective tension, bending moment, and pressure.

According to API (2013), which is the standard utilized in this work, a safe design requires to have its Von Mises stress taking into account a design factor,  $F_d$ , as expressed in Equation (5-6). In case this criterion is not satisfied, the design is considered to be unsafe, and a new one needs to be carried out.

$$\sigma_e \leq F_d \cdot \sigma_y \quad (5-6)$$

Where:

$$\begin{aligned} \sigma_e &= \text{Von Mises equivalent} \\ F_d &= 0.8 \text{ for ULS} \\ &= 1.0 \text{ for ALS} \end{aligned}$$

$\sigma_y$  = yield strength

Hence, the maximum allowable stresses for the ULS and ALS design of steel and titanium are demonstrated in Table 5-10.

Table 5-10. Maximum allowable stresses.

<b>Material</b>	<b>Maximum allowable stress (MPa)</b>	
	<b>ULS</b>	<b>ALS</b>
Steel	360	606
Titanium	448	758

### **Compression**

It is undesired to have excessive compression (minimum negative tension), which means that compression shall be avoided or minimized.

### **Fatigue Life for Wave Induced Fatigue Analysis**

For wave-induced fatigue analysis, an acceptable fatigue life shall be at least 250 years.



## Chapter 6. Extreme Response Analysis

### 6.1 Introduction

The extreme response analysis for the SCR and SCR with titanium section in the TDA will be presented in this chapter. Both configurations will be considered in order to have a comparison of how the titanium section impacts the results. Thus, statics and dynamics analysis were performed for those concepts. According to Gemilang (2015), static analysis determines the system equilibrium configuration when subjected to functional loads such as self-weight, hydrostatic effect, buoyancy, and top tension. From that, the results obtained are used for the dynamic simulation, as its initial configuration.

The dynamic analysis considers several excitation forces, such as current, direct wave, and wave frequency (WF) floater motions. The simulation, in this case, is performed considering specified periods, in which the starting position is the one resulted in the static analysis.

The following procedures will be presented in this chapter, as well as the results obtained in every case:

- Definition of the SCR concept;
- Definition of the SCR with titanium, including how long the titanium section must be in order to be in contact with the TDP in the near and far position;
- Static analysis, which determines the optimum static configuration for these concepts;
- Dynamic analysis, which is performed in the extreme sea-states;
- Stress check.

### 6.2 Static analysis

An optimum static design for the SCR and SCR with titanium section in the nominal, near, and far offset positions and their static analysis will be presented in this section. All data utilized is presented in Chapter 5 above. The riser is considered to have a coating on the steel and titanium sections, and since the work aims to explore the use of a titanium section in the TDA, analysis with no coating is not in the scope. The study and results presented in this section and the next ones referring to the SCR with titanium section will use the terminology of SCRT.

The different offsets of the vessel will be considered to analyze how the static response changes when it has an offset of 140 meters. If the displacement occurs to be in-plane towards the TDP, it categorizes the near offset position. However, if the displacement occurs to be in-plane away from the TDP, it refers to the far offset position.

Environmental loads are not considered in this analysis, which only considers functional ones. Hence, for the strength analyses, results such as the static effective tension and static bending moment are the ones of great importance to be investigated. Von mises stress is considered to analyze the allowable stresses that shall not be exceeded. With that, the design will be driven by the acceptance criteria presented in section 5.8.

The SCR and SCRT hang-off locations were explained and shown in section 5.4.3. The top angle relative to vertical was defined as  $10^\circ$  for the mean position, which consequently will change for the near and far offset positions. For SCRT, the riser was initially designed to have a 610-meter length titanium section in the TDP for all offset positions and a steel section of 2040-meter before and 1360-meter length after the titanium. With that, the total length of the riser is 4,010 meters, which is also the length of the SCR.

The minimum wall thickness for steel and titanium was calculated in section 5.5. However, it is assumed to be 25,4 mm for both materials in the base design for study purposes. A coating thickness of 40 mm and density of  $690 \text{ kg/m}^3$  is considered for steel. Since titanium is significantly lighter than steel, 40 mm of a coating with a density of  $2,200 \text{ kg/m}^3$  is considered. These parameters are taken into account since steel and titanium must have the same inner and outer diameter, as well as similar weight per unit length. This makes the transition between the two materials smoother and avoids bending moment peaks on the connection.

The results obtained by the static equilibrium of the SCR and SCRT, given by the static analysis, are presented in Table 6-1 and Table 6-2.

Table 6-1. Static results - SCR.

SCR	Offset Position		
	Far	Mean	Near
<b>Hang-off angle (<math>^\circ</math>)</b>	14	10	7.5
<b>Effective top tension (kN)</b>	2,954	2,708	2,533
<b>Max. Bending moment (kN.m)</b>	71	107	168
<b>Max Von Mises stresses (MPa)</b>	312	307	304

Table 6-2. Static Results - SCRT.

SCRT	Offset Position		
	Far	Mean	Near
<b>Hang-off angle (°)</b>	13	10	7
<b>Effective top tension (kN)</b>	2,933	2,686	2,515
<b>Max. Bending moment (kN.m)</b>	43	65	104
<b>Max Von Mises stresses (MPa)</b>	312	307	304

### **Discussion of Static Analysis Results:**

The results of the response at the mean, near, and far offset positions when subjected to functional loads lead to the following discussion.

- Different offset positions affect the configuration of the riser and, consequently, its hang-off angle. This is the expected response, and since the offsets are 7% of the water depth, the variation between the near and far positions compared to the mean one is very similar for both SCR and SCRT.
- Effective tension increases from the near to the far position. As the effective tension is a function of the riser suspended length and the three configurations have the same length, the expected result is to have a higher value the further the vessel moves away from the anchor point. Also, the maximum value occurs at the hang-off point since this is where the whole submerged weight is supported.
- The bending moment results, differently from the effective tension, decreases with the in-plane distance of the TDP. This is due to how the riser bends when approaching the seabed. In the near offset position, the riser has a small sag-bend curvature in the TDA compared to the mean and far offset positions. This curvature increases with the increase in the suspended length, resulting in a smoother approach of the riser to the seabed. Hence, the far offset position will have a significantly lower bending moment than the near offset position in the statics analysis.

It is important to keep in mind that the SCRT is being analyzed with titanium on the TDA, which, due to different properties, can lead to lower bending moment values if compared to a conventional SCR.

- The maximum stresses for SCR and SCRT are the same, indicating that the titanium sections on the statics analysis do not impact this parameter. The values in Table 6-1 and

Table 6-2 correspond to the hang-off point and are below the allowable limit, which is 360 MPa for the steel section and 606 MPa for the titanium section.

- Considering the stress, the maximum SCR and SCRT values do not have a relevant variation for any offset positions. This indicates that none of them is significantly more critical to the extreme response in the design than the others on the statics analysis.

### 6.3 Dynamic Analysis

The dynamic responses of the risers took into consideration the dynamic analysis for the ULS and ALS configurations. The first considers an intact position with an offset of 140 meters, and the latter considers a damaged condition which offset is 160 meters. The extreme response of the 3-hour sea state was based on a time-domain analysis. A seed number corresponding to the higher downward velocity for the hang-off point, 3.8 m/s, was provided and used for the simulation. With that, it is possible to identify the worst response interval. Thus, a simplified and shorter analysis method can be implemented where the simulation duration considers five periods before and two periods after the point where the worst response happens. This means that the simulation could be reduced to 120 seconds in this study.

Stress results are the most interesting since they indicate the risers' capability to cope with the floater motions. However, effective tension, bending moment, and compression will also be discussed. As for the static analysis, the dynamic responses of the SCR will be presented in order to have a comparison of how the titanium section can affect the results.

#### 6.3.1 Dynamic analysis of conventional SCR

The results of the dynamic response of the conventional SCR are summarized in Table 6-3 for ULS and ALS design.

Table 6-3. Dynamic response for SCR.

SCR	ULS		ALS	
	Near	Far	Near	Far
<b>Max Effective tension (kN)</b>	3652	5283	3616	5388
<b>Max Compression (kN)</b>	616	1043	590	1089
<b>Max Bending moment (kN.m)</b>	1229	976	1228	1231
<b>Max Von Mises stress (MPa)</b>	891	717	890	886

- According to Table 6-3, the effective tension increases from the near to the far position. This is expected and, therefore, reasonable. Also, compared to the static analysis, the most significant increase is observed for the far offset position due to the suspended riser's length under environmental loads.
- The bending moment is the same for the near offset position in ULS and ALS. For the far offset position in ULS, it had a significant decrease compared to the near. However, for the ALS, it increased slightly. This difference in results when compared to the static position is due to the effect of the environmental conditions. The 20-meter difference in the vessel displacement between the far offset position in ULS and ALS increases the riser suspended length, making it more exposed to experience the vessel motions.

For both conditions, the maximum values occur when the vessel experiences the highest downward velocity, as presented in Figure 6-1. The point where the riser has its peak in the bending moment is depicted in Figure 6-2 by the black dot, where it can be seen that it diverges and explains the maximum values.

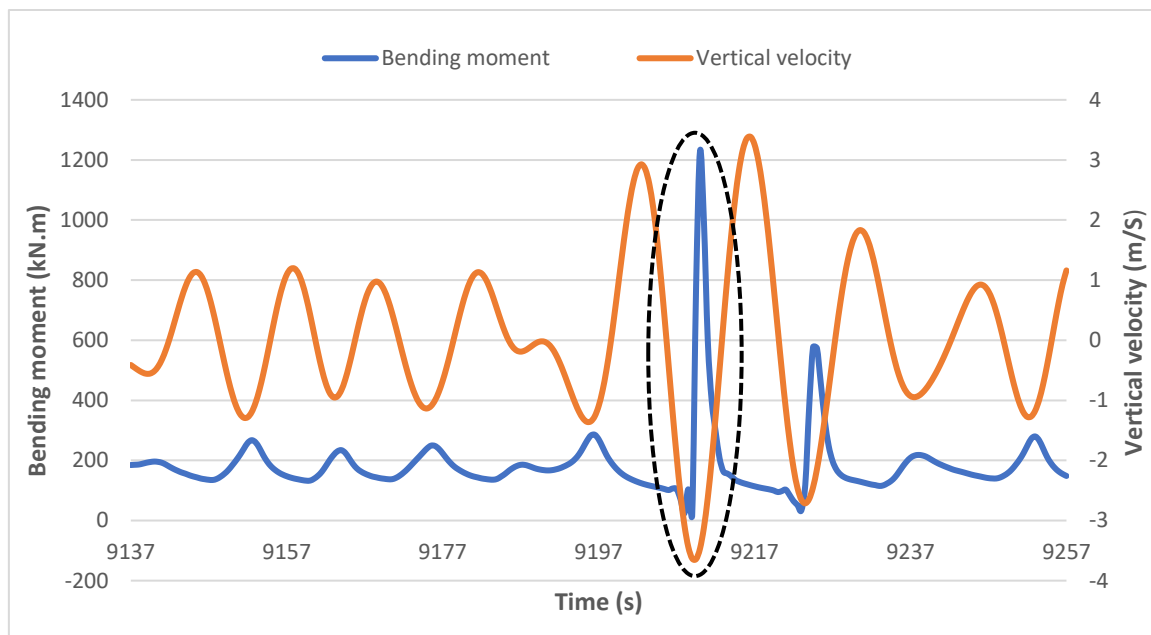


Figure 6-1. Time history: Bending moment - SCR Near - ULS.

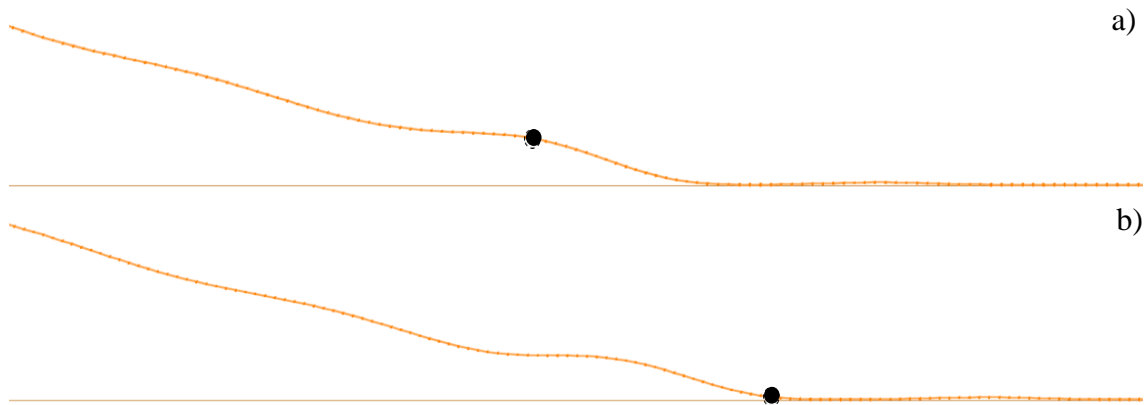


Figure 6-2. Point of the maximum bending moment for the far offset position in a) ULS and b) ALS.

- The maximum Von mises stress is on the TDP when the vessel is under the most extreme loads, as shown in Figure 6-3. Considering the time history plot for the bending moment, it can be observed that it induces the maximum stress values. For both offset positions, in ULS and ALS, the values are much above the allowable design criteria, 360 and 448 MPa, respectively. This indicates that this riser does not cope with the downward velocity it is exposed to and, therefore, is unsuitable.

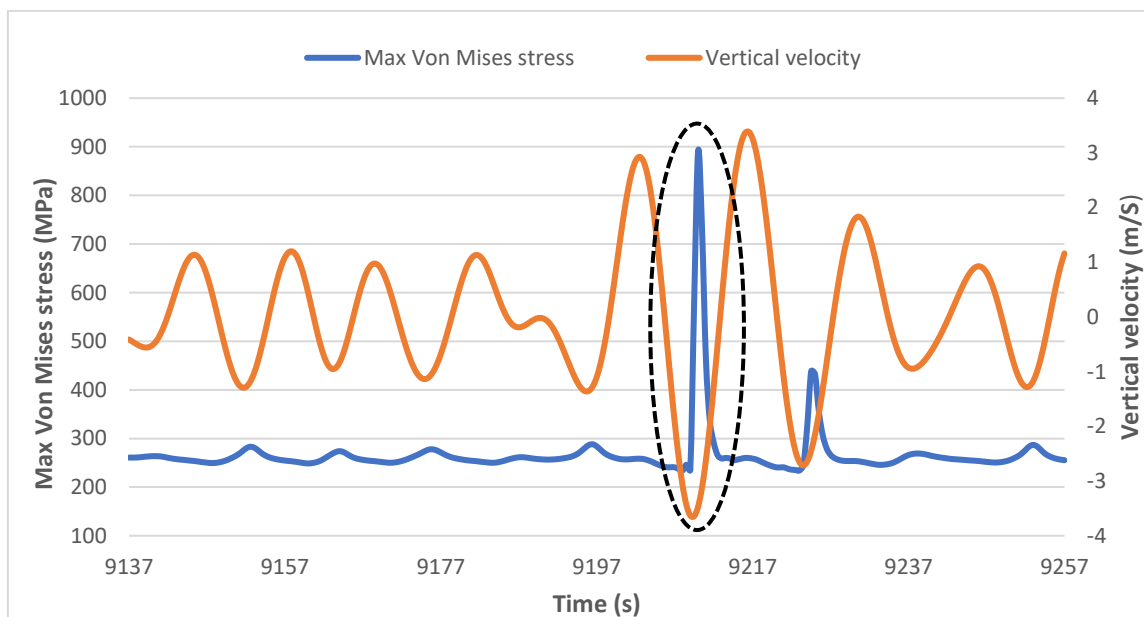


Figure 6-3. Time history: Max Von Mises stress - SCR Near - ULS.

- It can be seen in the graph above that on the points where the downward velocity increases, the maximum Von Mises stress also increases. Thus, the peak of Von Mises stress occurs at the same point as the maximum downward velocity.

### 6.3.2 Dynamic analysis of SCRT

Similar to the SCR, the dynamic results after implementing the titanium section are summarized in Table 6-4 for ULS and ALS design. In this case, the maximum Von Mises stress on the steel after the titanium length was also analyzed to check how this part was affected.

Table 6-4. Dynamic response of SCRT.

SCRT	ULS		ALS	
	Near	Far	Near	Far
<b>Max Effective tension (kN)</b>	3703	5310	3587	5395
<b>Max Compression (kN)</b>	548	912	529	845
<b>Max Bending moment (kN.m)</b>	785	779	801	797
<b>Max Von Mises stress on the titanium section (MPa)</b>	592	587	602	600
<b>Max Von Mises stress on steel after titanium section (MPa)</b>	237	280	236	297

- Like the SCR, the effective tension was significantly higher for the far offset position. For ULS and ALS, the maximum value is similar to the values encountered for the SCR in both offset positions. As the effective tension is related to the suspended length and steel and titanium have a similar weight per unit length, this result is expected.
- The compression levels changed slightly for the near position and had a more considerable change for the far position. However, compression is unwanted because it can cause the riser to buckle. In this case, it may be explained by the light weight of the riser. So, it is a parameter to be improved by applying other techniques.
- Unlike the SCR, the bending moment between the near and far offset positions does not substantially differ due to titanium's different properties. However, as for the SCR, the maximum value occurs at the higher downward velocity, as shown in Figure 6-4.

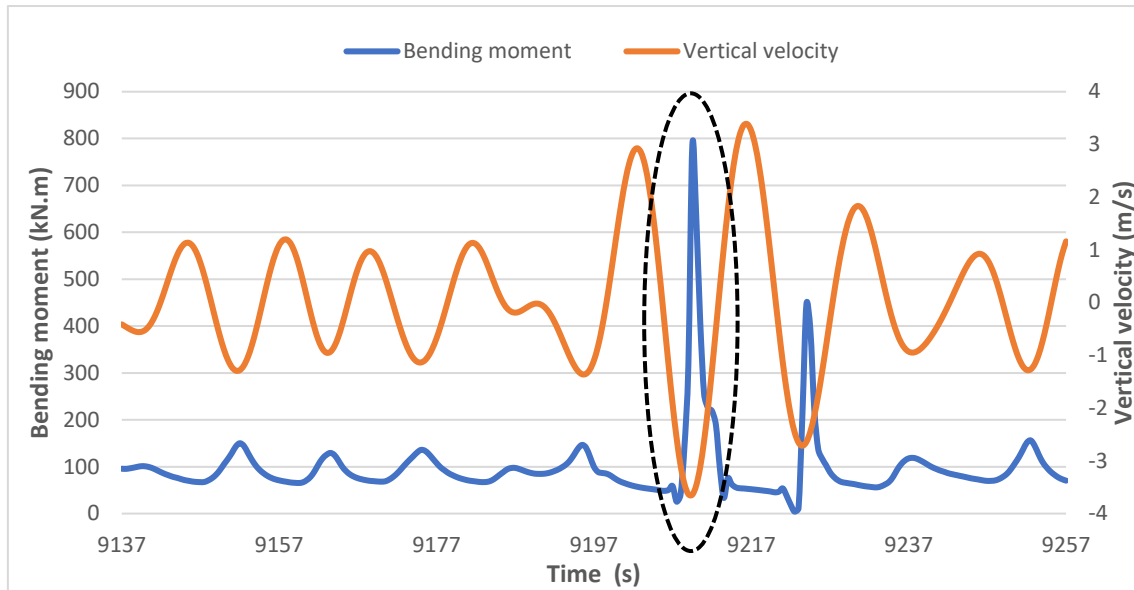


Figure 6-4. Time history: Bending moment - SCRT Near - ULS.

- A significant improvement in the maximum stress experienced by the riser can be noted. In all cases, the maximum values were below the allowable criteria for both materials. This means that applying the titanium section on the TDA can improve the resistance of the riser against the loads, making it feasible for a downward velocity of 3.8 m/s. The graph in Figure 6-5 below shows that, similar to the SCR, the higher stress is experienced at the same point as the maximum downward velocity.

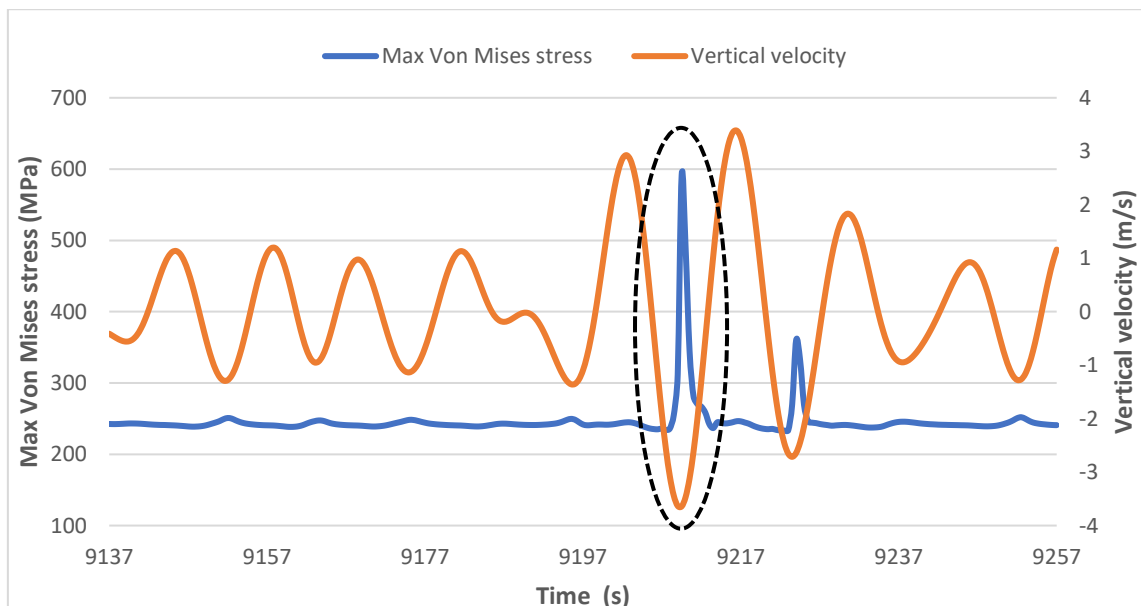


Figure 6-5. Time history: Max Von Mises stress - SCRT Near - ULS.

In summary, the responses of the SCR and SCRT are as follows:



- The maximum downward velocity induces the maximum value of bending moment, which generates the maximum Von Mises stress experienced. This indicates that the maximum downward velocity at the hang-off point is a crucial parameter that drives the riser integrity.
- The SCR is very sensitive to the floater motions, as could be observed by the difference between the effective tension, bending moment, and maximum Von Mises stress on the static and dynamic analyses. Gemilang (2015) performed a study about the feasibility of SCR, and his results demonstrated that the SCR with coating is not able to cope with a downward velocity of 2.33 or higher. Considering this, it is expected that the SCR in this study would not be able to cope with the downward velocity of 3.8 m/s.
- Although the static results of the SCRT are not substantially different from the SCR, the dynamic response presented in Table 6-4 demonstrates that the implementation of a titanium section on the TDA improves the response of the riser. Due to its high yield strength compared to steel, it can cope with the stresses experienced, making the configuration of a catenary riser feasible in an environment with the conditions considered in this study.

## Chapter 7. Fatigue Analysis

A riser is considered to be a slender structure that, when in deep-water and harsh environment, is subjected to oscillatory motions due to the waves and current. This makes the riser to be continuously lifted off and laid down during its service life as a response to the vessel's heave motion. How much the riser can cope with these motions will determine its fatigue life. According to DNV (2018), for the fatigue damage, three different contributions should be addressed:

- Wave-induced stress cycles;
- Low-frequency stress cycles;
- Vortex-induced vibrations (VIV) stress cycles;

Due to the vessel motions and soil-riser interaction, the critical region subjected to fatigue damage on a catenary riser is at the welded joints near the TDP. Welded joints generally have weld toe/root discontinuities, which behave as pre-existing cracks. Therefore, their fatigue life can be attributed to the time these cracks propagate to an extent where they are no longer repairable (DNV, 2016).

In order to analyze the fatigue performance of the SCRT compared to the conventional SCR, a calculation of their fatigue life will be performed on OrcaFlex, as well as the previous simulations.

### 7.1 Fatigue design conditions

#### 7.1.1 Riser structural modeling

As presented in the previous chapter, the basic configuration of the SCR and SCRT that will be considered for the analysis are presented below.

#### SCR

- Inner diameter: 10"/25.4 cm
- Wall thickness: 25.4 mm
- Coating thickness: 40 mm
- Carbon steel density: 7,850 kg/m<sup>3</sup>
- Coating density: 690 kg/m<sup>3</sup>
- Riser length: 4,010 m

**SCRT**

- Inner diameter: 10"/25.4 cm
- Wall thickness: 25.4 mm
- Coating thickness: 40 mm
- Carbon steel density: 7,850 kg/m<sup>3</sup>
- Titanium density: 4,420 kg/m<sup>3</sup>
- Coating density steel: 690 kg/m<sup>3</sup>
- Coating density titanium: 2,200 kg/m<sup>3</sup>
- Titanium section length: 610 m
- Riser length: 4,010 m

Apart from that and the other parameters presented in Chapter 5, the only different parameter considered is the drag coefficient,  $C_d$ , now assumed to be 0.7. The reason behind this change is that the previous value of 1.2, if considered for the fatigue analysis, can result in a too damped configuration.

**7.1.2 S-N curve**

The calculation will follow the S-N curve methodology approach, which expresses the number of stress cycles to failure,  $N$ , for a given constant stress range,  $S$ . For steel, considering DNV (2016), the following equations express it.

$$\log(N) = \log(\bar{a}) - m \log(S) \quad (7-1)$$

$$S = S_o \cdot SCF \cdot \left( \frac{t_3}{t_{ref}} \right)^k \quad (7-2)$$

Where:

$N$  = Number of stress cycles to failure

$S$  = Stress range

$\bar{a}, m$  = Empirical constant

$S_o$  = Nominal stress range

$SCF$  = Stress concentration factor

$\left( \frac{t_3}{t_{ref}} \right)^k$  = Thickness correction factor, applicable to  $t_3 > t_{ref}$

$t_3$  = Pipe wall thickness

$t_{ref}$  = Reference wall thickness = 25 mm

$k$  = Thickness exponent

According to DNV (2016), the S-N data result from the fatigue testing of small specimens in test laboratories, and the redistribution of stresses during crack growth for these specimens is not possible. Different curves are given by the recommended practice. In this study, curves D with cathodic protection and F1 in air will be considered for steel's outer and inner diameter, respectively. The F1-curve is expected to give a lower fatigue life when compared to the D-curve. The parameters used for each one are presented in Table 7-1 and Table 7-2, and both curves can be seen in Figure 7-1 and Figure 7-2.

Table 7-1. D-curve in seawater with cathodic protection.

S-N curve	N ≤ 10 <sup>6</sup> Cycles		N > 10 <sup>6</sup> Cycles	Fatigue limit at 10 <sup>7</sup> cycles (MPa)	Thickness exponent k
	$m_1$	$\log \bar{a}_1$	$\log \bar{a}_2$ $m_2 = 5.0$		
D	3.0	11.764	15.606	52.63	0.2

Table 7-2. F1-curve in air.

S-N curve	N ≤ 10 <sup>7</sup> Cycles		N > 10 <sup>7</sup> Cycles	Fatigue limit at 10 <sup>7</sup> cycles (MPa)	Thickness exponent k
	$m_1$	$\log \bar{a}_1$	$\log \bar{a}_2$ $m_2 = 5.0$		
F1	3.0	11.699	14.832	36.84	0.25

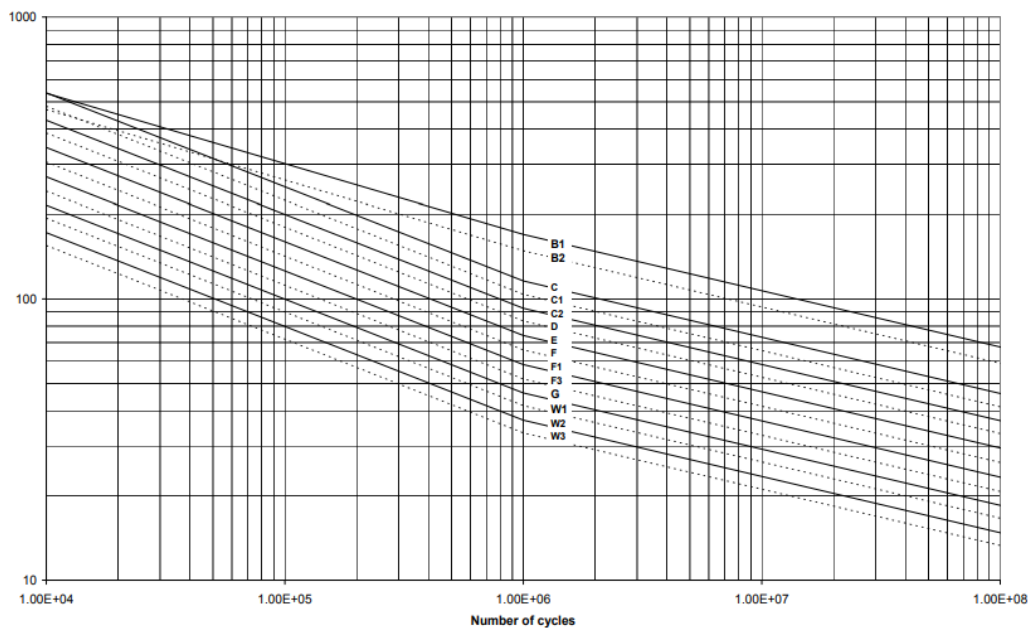


Figure 7-1. S-N curves in seawater with cathodic protection (DNV, 2016).

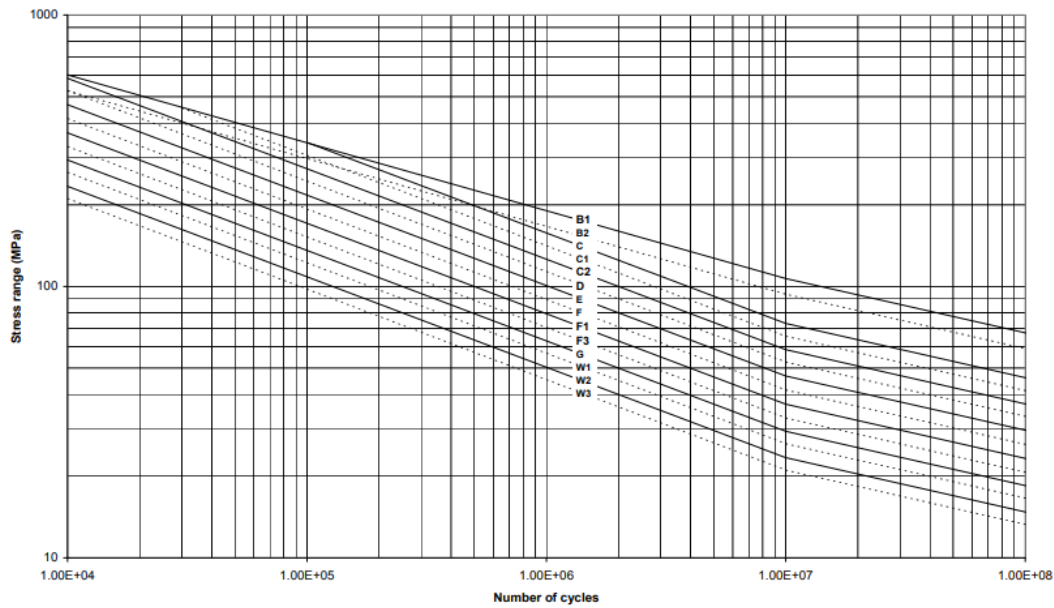


Figure 7-2. S-N curves in air (DNV, 2016).

For the welds on titanium riser components, the process consists of an automatic GTAW (Gas-Shielded Tungsten Arc Welding) followed by a post-weld stress relief anneal treatment (Systems, 2005). The welding can be made in two positions, 1G and 5G, with the following fatigue design equation.

$$N(\Delta S)^m = C \quad (7-3)$$

Where:

$N$  = Number of stress cycles to failure

$\Delta S$  = Stress range ( $S_{max} - S_{min}$ )

$m$  and  $C$  = Constants, given in Table 7-3

Table 7-3. Parameters for 5G and 1G curves (Systems, 2005).

GTA Welding position	$\Delta S$ Units	$m$	$C$
5G	ksi	5	$6.16 \times 10^{12}$
	MPa	5	$9.6 \times 10^{16}$
1G	ksi	6	$6.33 \times 10^{14}$
	MPa	6	$6.8 \times 10^{19}$

These curves are valid for seawater, air, and sweet brine environments. Although base metals have superior fatigue properties than the welds, Systems (2005) has proved that the weld properties also give adequate fatigue lives for the base metal. In this study, 1G-curve will be considered to analyze the fatigue life of the titanium. Those curves'

properties are better than those for steel, as seen in Figure 7-3. With that, the titanium is expected to have lower damage and higher fatigue life.

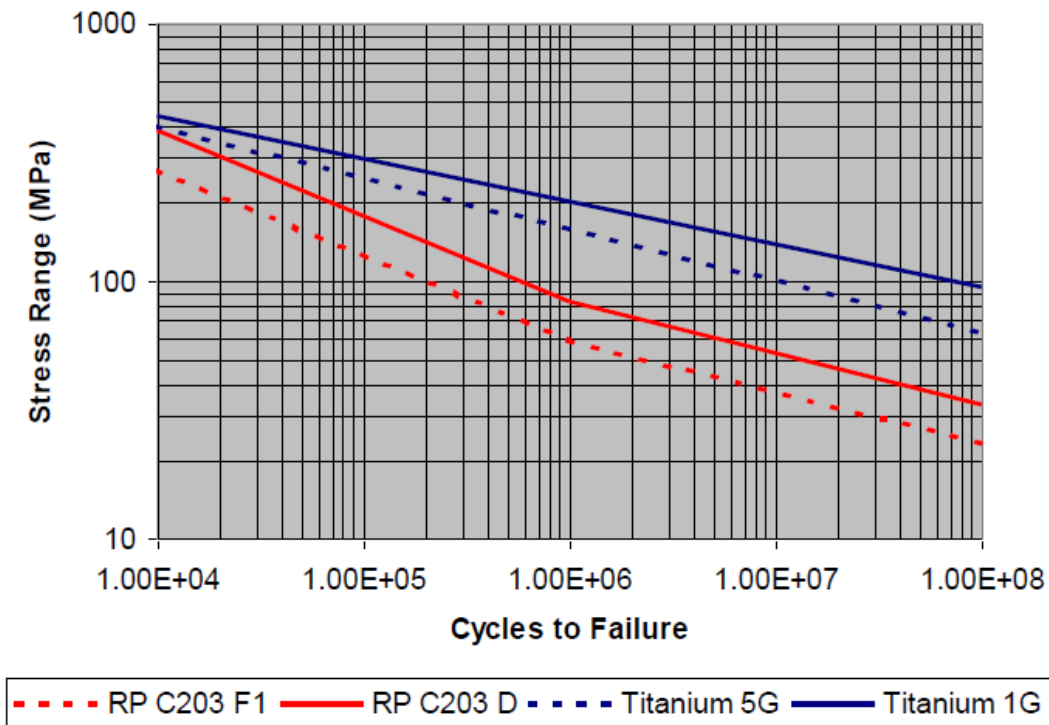


Figure 7-3. 5G and 1G curves (Systems, 2005).

### 7.1.3 Stress concentration factor

This factor is used to account for possible stress amplification due to an imperfect geometry of two adjacent joints. There are two ways of calculating it: detailed finite element analyses or closed-form expressions for the actual structural detail (DNV, 2018). The closed-form expression in Equation (7-4) applies to welded riser joints.

$$SCF = 1 + \frac{3e}{t_3} \exp\left(-\left(\frac{D}{t_3}\right)^{-0.5}\right) \quad (7-4)$$

Where:

$e$  = Representative eccentricity due to geometrical imperfections

$t_3$  = Wall thickness of the pipe

$D$  = Outer diameter of the pipe

By taking this expression into account, an SCF of 1.2 is used for both curves of steel (D and F1) and titanium (1G).

### 7.1.4 Wave-induced fatigue damage

The vessel motion is the main factor contributing to the wave-induced fatigue response. Thus, the hang-off point and the vessel design are of great importance in how the riser will be affected. A total of 9 wave directions, which are the ones considered to have the most effect on the motion, will be used in this study. Since a set of different  $H_s$  and  $T_p$  were accounted for each wave direction, a total of 123 load cases for the wave-induced fatigue calculation were generated and used.

The information used is confidential and, therefore, will not be presented. However, the procedure as described in DNV (2018) is considered for the short-term sea-state definition in each case and is as follows.

- The scatter diagram representing the sea environment at the study location is subdivided into a number of representative blocks.
- For each block, it is selected a single sea-state that represents all the other sea-states of the block. Figure 7-4 below gives an example of what this division and selection look like.

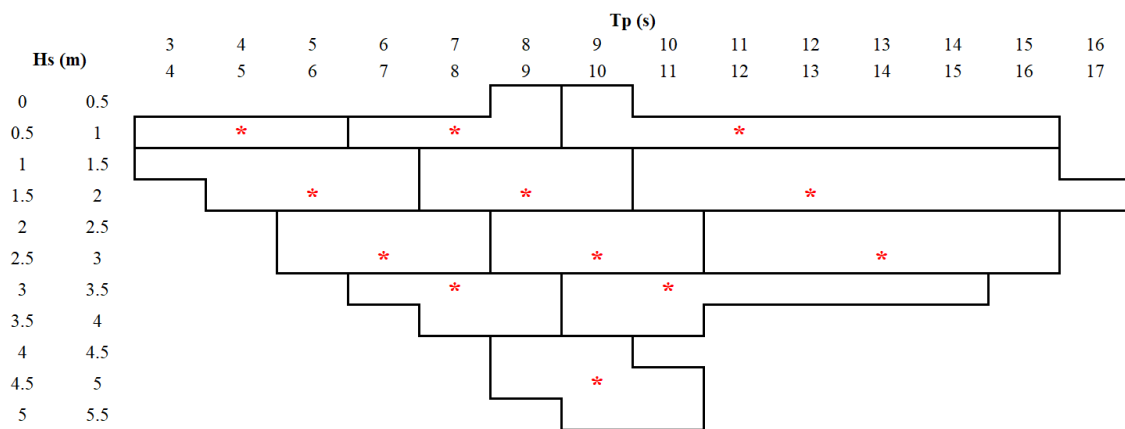


Figure 7-4. Example of a block sub-division on a scatter diagram.

- By having the selected short-term sea-state of each block, it is then used to lump the probabilities of occurrence for all sea-states within the block. The lumped probability of occurrence is defined as the percentage of all the occurrences in each block over the total number of occurrences.
- Then, a fatigue computation for each representative sea-state for all the blocks is performed.

The simulation time for this study was set as 2,700 seconds to capture the fatigue damage. For that, 8 equally spaced points around the circumference along the arc length of the riser are used for the calculation.

- The fatigue damage accumulation is calculated in each block.

The fatigue life is calculated under the assumption of linear cumulative damage (Palmgren-Miner rule), as shown in equation (7-5) below.

$$D = \sum_{i=1}^k \frac{n_i}{N_i} \quad (7-5)$$

Where:

$D$  = Accumulated fatigue damage

$k$  = Number of stress blocks

$n_i$  = Number of stress cycles on stress block  $i$

$N_i$  = Number of cycles to failure at constant stress range (S)

- The fatigue damage accumulation from all sea-states is weighted with the corresponding lumped probability of occurrence, based on the following expression.

$$D_L = \sum_{i=1}^{N_s} D_i P_i \quad (7-6)$$

Where:

$D_L$  = Long-term fatigue damage

$N_s$  = Number of discrete sea-states in the wave scatter diagram

$D_i$  = Short-term fatigue damage

$P_i$  = Sea-state probability

- Thus, the total fatigue damage in a given direction is obtained from the summation of the weighted fatigue damage over all the representative sea-state blocks.



## 7.2 Fatigue analysis results

### 7.2.1 Conventional SCR

A conventional SCR has as critical locations for the fatigue performance the TDP and below the flex joint. In this study, a flex joint was not designed on the riser, which is considered pinned. As the work's objective is to analyze a titanium section's effect on the TDP, the fatigue life will only account for this area. The fatigue life for the S-N curves used is presented in Table 7-4, and the total fatigue damage along the riser length is illustrated in Figure 7-5.

The minimum fatigue life at the TDP is much lower than the minimum acceptable fatigue life of 250 years. The high Von Mises stress discussed in the previous chapter indicated that this riser configuration could not cope with the downward velocity considered in this study. Therefore, the calculated fatigue life concludes that the SCR does not satisfy the fatigue performance's minimum criteria, making it not feasible for this location with the given environmental conditions.

Table 7-4. Fatigue life of SCR at the critical location.

SCR location	D-curve	F1-curve
TDP	4 years	3.5 years

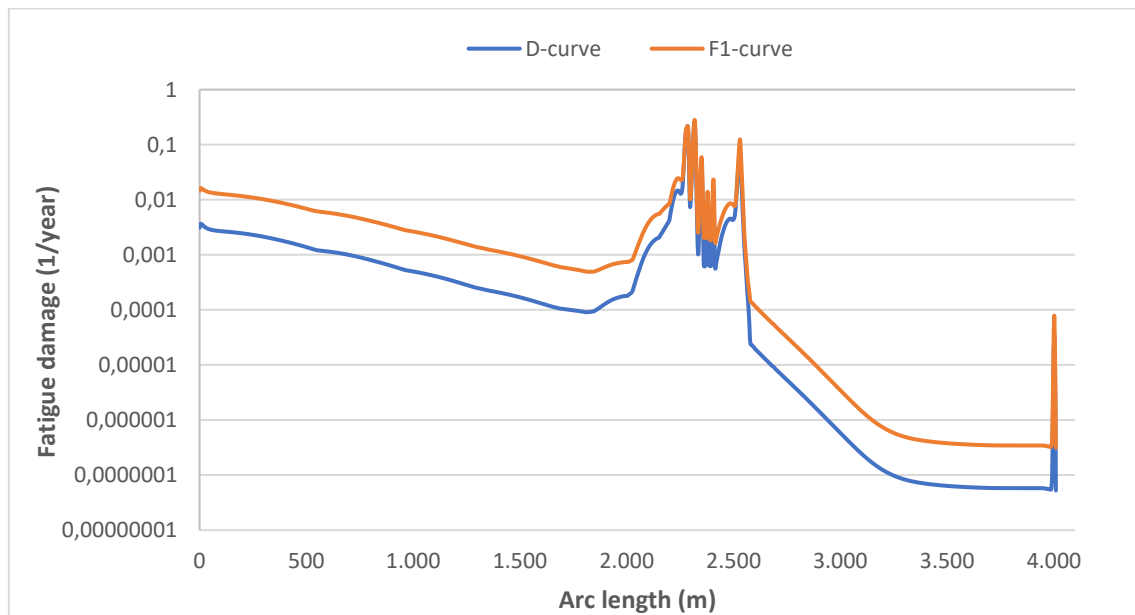


Figure 7-5. Total fatigue damage of SCR.

### 7.2.2 SCRT

Like the SCR, the SCRT has as critical location the TDP for the fatigue performance. However, implementing a titanium section on the TDP is expected to increase the fatigue life of this riser configuration since it was observed that the conventional SCR is not feasible. The fatigue life for the TDP is presented in Table 7-5, and the total damage along the riser length can be seen in Figure 7-6.

It can be seen that there is a significant improvement in the fatigue performance on the TDP when a titanium section is implemented in that region. Due to the material's properties, it can handle the cyclic stresses at the TDA making this configuration feasible to be applied under the environmental conditions of this study. On the inner and outer sections of the riser, the fatigue life is much above the minimum criteria of fatigue performance. Therefore, this region is no more of significant concern regarding wave-induced fatigue failure.

Table 7-5. Fatigue life of SCRT at critical location.

SCRT location	1G-curve (inner)	1G-curve (outer)
TDP	58,234 years	20,231 years

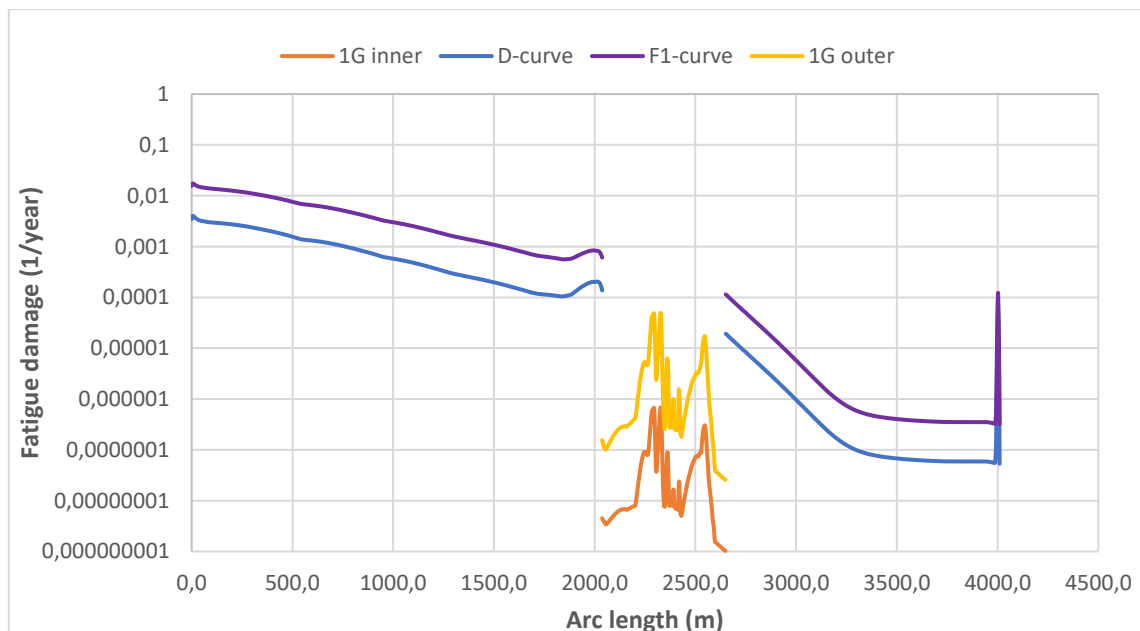


Figure 7-6. Total fatigue damage of SCRT.

## Chapter 8. Sensitivity Analysis

### 8.1 Introduction

The configuration of an SCR with a titanium section has critical parameters that can affect its costs, installation, and feasibility. Considering this, a sensitivity analysis was carried out about the section length, wall and coating thicknesses, and the hang-off angle. The purpose is to check if a better configuration can be found and analyze the behavior of the SCRT when changes are made.

The base case is described in Chapter 5 and Chapter 6. A sensitivity analysis was already carried out to define a configuration that worked, and the reason behind the chosen parameters is presented in the previous chapters. In this chapter, a more refined analysis will be considered to find a range that can be used for further optimization.

The worst responses to the cases will be summarized in the sub-sections below. The same combination of 100-year wave and 10-year current is considered for the analysis.

### 8.2 Titanium length sensitivity study

The preliminary testing for the dynamic configuration showed that the length of titanium is an important parameter to be considered, especially for the far position. When the vessel and the riser are subjected to the worst-case scenario of the extreme loads, it was observed that the titanium section must be touching the seabed. This led to an initial configuration of 610 m of titanium section. However, a parametric study will be demonstrated to define the minimum length that can be used in this case. The analysis considered 5 cases, which are presented in Table 8-1.

All cases considered the following configuration parameters:

- Hang-off angle: 10°
- Steel length before titanium: 2,040 meters
- Steel and titanium wall thickness: 25 mm
- Steel and titanium coating thickness: 40 mm
- Steel coating density: 690 kg/m<sup>3</sup>
- Titanium coating density: 2,200 kg/m<sup>3</sup>

Table 8-1. Cases for titanium length sensitivity study.

<b>Titanium section length</b>				
450 m	500 m	550 m	575 m	600 m

For the dynamic analysis, near and far offset positions were considered for both ULS and ALS design.

### 8.2.1 Dynamic analysis (ULS) – Titanium length sensitivity

The dynamic behavior at the TDP was analyzed since this is the area of most interest to the proposed riser. Results for the ULS are summarized in Table 8-2 and Table 8-3, and a brief discussion is presented afterward.

Table 8-2. Titanium length sensitivity in near offset position.

<b>Near offset position</b>					
<b>Titanium length (m)</b>	450	500	550	575	600
<b>Max Effective tension (kN)</b>	3,708	3,706	3,705	3,704	3,704
<b>Max Compression (kN)</b>	548	548	548	548	548
<b>Max Bending moment (kN.m)</b>	785	785	785	785	785
<b>Max Von Mises stress on the titanium section (MPa)</b>	592	592	592	592	592
<b>Max Von Mises stress on steel after titanium section (MPa)</b>	237	237	237	237	237

Table 8-3. Titanium length sensitivity in far offset position.

<b>Far offset position</b>					
<b>Titanium length (m)</b>	450	500	550	575	600
<b>Max Effective tension (kN)</b>	5,330	5,218	5,348	5,278	5,297
<b>Max Compression (kN)</b>	948	845	784	819	889
<b>Max Bending moment (kN.m)</b>	804	912	832	818	802
<b>Max Von Mises stress on the titanium section (MPa)</b>	592	672	615	613	604
<b>Max Von Mises stress on steel after titanium section (MPa)</b>	553	549	331	289	272

- The results for all parameters did not change for the near offset position in any of the cases. This can be explained because the increase of the titanium section was in its end, which in this offset position was already laying down on the seabed. Since the weight per meter of steel and titanium are almost the same, those small changes were insufficient to change the results. Von Mises stress is lower than the maximum allowed on the titanium section (606 MPa) and on the steel section after titanium (360 MPa), which means that those changes in the length are not critical for the near offset position.
- High levels of compression can be observed for near and far offset positions. This can indicate that the riser is too light, considering the water depth where it is located and the other parameters that are taken into account. For near position, changes in the length do not impact it. However, an increase in the length causes the compression to vary slightly for the far position.

Its peak happens on the titanium section, just before the TDP, when it experiences the most extreme load effects. Since titanium has much higher strength than steel, even with higher compression for the 600-meter length than for some others, it did not cause the riser to fail. This is indicative that this parameter does not drive alone its failure, but it has to be taken into account and improvements be made.

- The higher stress on the titanium occurs at the same point as the highest bending moment. With that, it can be observed that there is a direct relation between them and an increase in the bending moment causes the Von Mises stress to increase and vice-versa.
- The bending moment varies for the different cases due to the length close to or on the seabed. Since titanium and steel have a similar weight per meter length but it is not exactly the same, the titanium section has slightly more buoyancy. With that, the 450-meter section has its maximum value right before the transition between the materials. In the case of the 500-meter section, the connection of the two materials is just after the TDP.

This makes it experience the transition of moments between the materials on the region of free span and, thus, the highest value of bending moment of the cases. With the increase in the length, the titanium section lays on the seabed, making the transition of moments smoother since it does not happen on the free span, as seen in Figure 8-1.

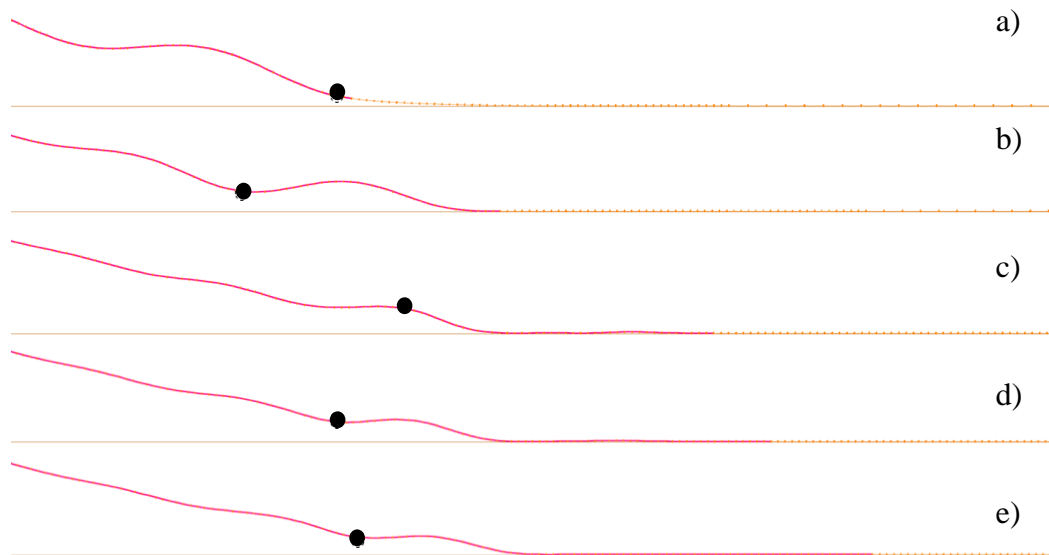


Figure 8-1. Location of the highest bending moment for far offset position when the length of titanium section is: a) 400 m, b) 500 m, c) 550 m, d) 575 m, and e) 600 m.

- The highest value of Von mises stresses for the titanium section was found on the 500-meter section. This can be explained by the short length of titanium that touches the seabed in a static position. When loads of the dynamics analysis start to affect the movement of the riser, it hits the seabed exactly on the transition of the materials, resulting in much higher stresses on that point when compared to the other lengths that either do not touch the seabed (450 m) or that have more contact.
- In addition, for the 550 and 575-meter lengths, the maximum Von Mises for the titanium section reaches values above the limit. Moreover, for the 450 and 500-meter lengths, the stress limit for the steel is also exceeded. In any section, exceeding the stress limit would cause the riser to fail, as can be seen in Figure 8-2 and Figure 8-3. The red line on both figures indicates the maximum allowable stress for each one.

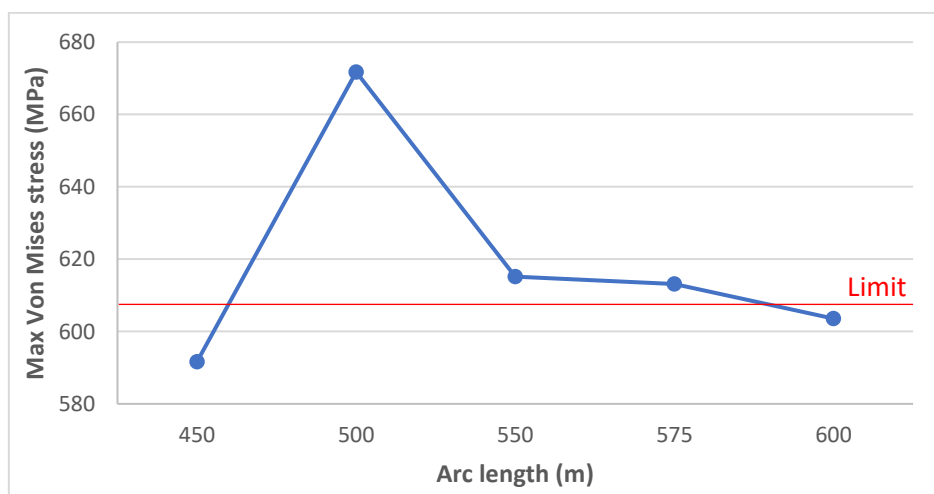


Figure 8-2. Maximum Von Mises stress for the titanium section.

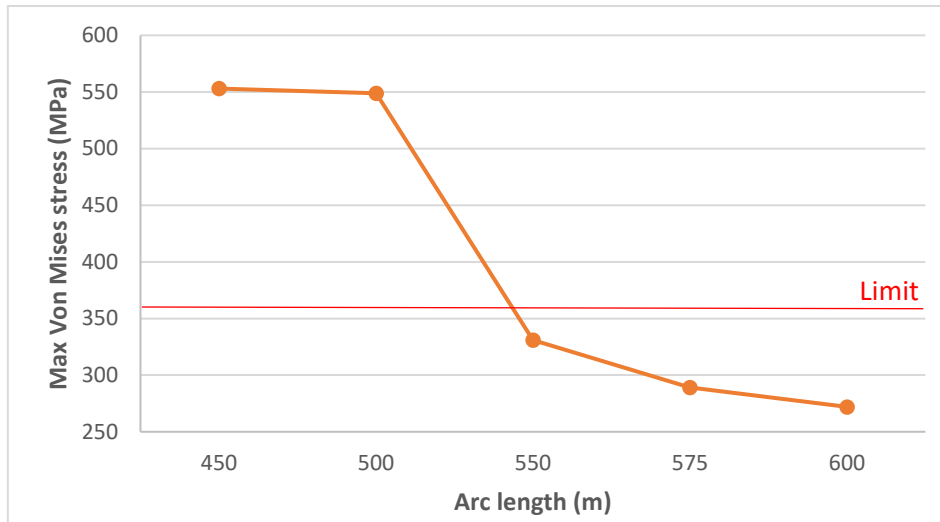


Figure 8-3. Maximum Von Mises stress for the steel section after titanium.

- The 450-m section does not touch the seabed in the static analysis, as can be seen in Figure 8-4. But, although the maximum stress on the titanium section is below the allowed, it was observed that for the steel section after it until the TDP, the stress is above the limit. Taking this into account, it was observed that it is essential that the titanium section touches the seabed when it is under the influence of extreme loads.

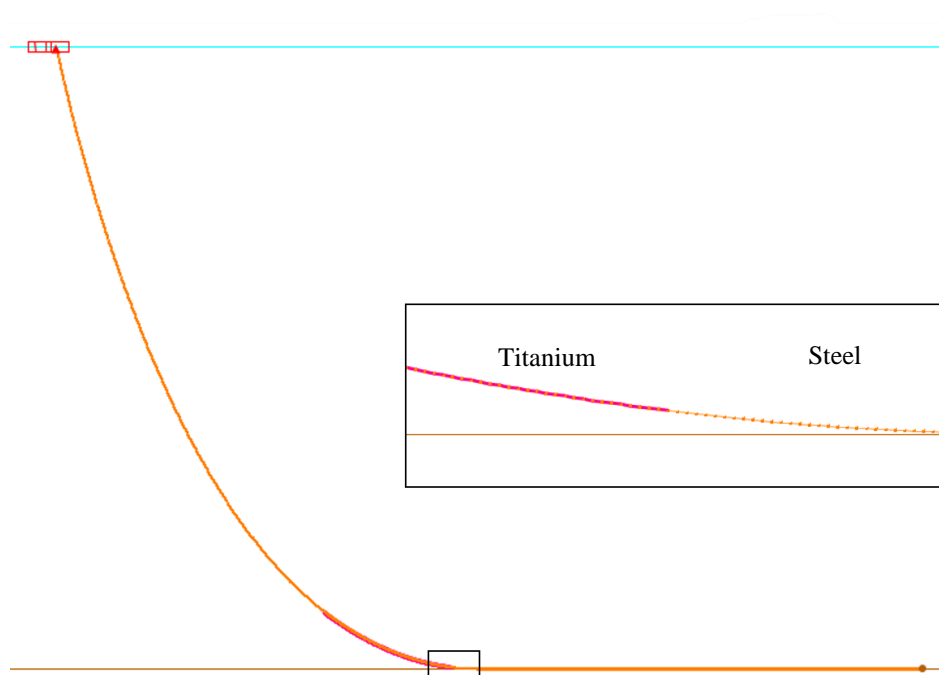


Figure 8-4. SCRT with 450-meter length titanium section.

In summary, results showed that shorter lengths than 600-meter were not feasible for this configuration since they do not cope with the allowable stresses. Thus, the minimum

length of the titanium section for the ULS case was found to be 600 meters. Results for the ALS condition will be presented below to analyze whether it meets the requirements.

### 8.2.2 Dynamic analysis (ALS) – Titanium length sensitivity

It can be observed in Table 8-4 that, for ALS conditions, both near and far offset positions cope with the allowable stresses. The maximum Von Mises stress, in this case, is considered to be the yield strength of the material, which means that even with a higher value than in the ULS for the far offset, it still meets the requirement of the titanium. The other parameters presented did not have significant changes compared to the ULS case.

Table 8-4. 600-meter length titanium section for ALS condition.

	<b>Near</b>	<b>Far</b>
<b>Max Effective tension (kN)</b>	3,587	5,424
<b>Max Compression (kN)</b>	529	828
<b>Max Bending moment (kN.m)</b>	801	844
<b>Max Von Mises stress on the titanium section (MPa)</b>	602	628
<b>Max Von Mises stress on steel after titanium section (MPa)</b>	236	289

### 8.3 Wall and coating thicknesses sensitivity

The wall and coating thicknesses are parameters that affect the weight of the riser, its costs, resistance to loads, feasibility of installation, among other factors. As said in section 6.2, the sections of steel and titanium must have a similar weight per unit length to have a smoother transition between them. Considering this, a parametric study was performed as an attempt to find a different configuration of wall thickness and coating thickness for both steel and titanium that can cope with the ULS and ALS conditions.

For the case of titanium, due to its properties and costs, the objective was to test thinner wall thickness than the initial case. Also, considering the compression level found in the length sensitivity, a 300-meter length of steel with a heavier coating was applied after the titanium section to increase the weight of the riser and try to reduce the compression. It is important to say that, although it has a heavier weight than the titanium section, it is laying on the seabed and, therefore, is not influenced by the loads as the sections on the free span. The main parameters for the study are:



- Hang-off angle: 10°
- Steel length before titanium: 2,040 meters
- Titanium length: 600 meters
- Steel length after titanium with heavier coating: 300 meters
- Length of last section of steel with normal coating: 1,140 meters

The wall thickness, coating thickness, and density for each section are presented in Table 8-5 and Table 8-6.

Table 8-5. Parameters for steel section.

Case	Steel section before titanium				Steel section after titanium			
	WT (mm)	WT Coating (mm)	Coating density (g/cm <sup>3</sup> )	Weight/unit length (ton/m)	WT (mm)	WT Coating (mm)	Coating density (g/cm <sup>3</sup> )	Weight/unit length (ton/m)
1	25	40	0.69	0.205	25	40	2.2	0.270
2	20	40	0.69	0.164	12	48	2.2	0.187
3	23	59	0.69	0.203	12	70	2.2	0.247
4	27	58	0.69	0.233	15	70	2.2	0.271
5	22	48	0.69	0.186	20	50	2.2	0.254

Table 8-6. Parameters for titanium section.

Titanium section				
Case	WT (mm)	WT Coating (mm)	Coating density (g/cm <sup>3</sup> )	Weight/unit length (ton/m)
1	25	40	2.2	0.194
2	12	48	2.2	0.153
3	12	70	2.2	0.213
4	15	70	2.2	0.227
5	20	50	2.2	0.195

### 8.3.1 Dynamic analysis (ULS) - Wall and coating thicknesses sensitivity

Results for this analysis are summarized in Table 8-7 and are discussed afterward.

Table 8-7. Wall thickness and coating thickness sensitivity in near offset position.

<b>Near offset position</b>					
<b>Case</b>	1	2	3	4	5
<b>Max Effective tension (kN)</b>	3,712	2,840	3,283	4,108	3,163
<b>Max Compression (kN)</b>	547	414	442	496	500
<b>Max Bending moment (kN.m)</b>	787	358	394	522	638
<b>Max Von Mises stress on the titanium section (MPa)</b>	593	681	747	733	640
<b>Max Von Mises stress on steel after titanium section (MPa)</b>	238	440	441	365	286

- It can be observed that the maximum effective tension is directly related to the weight of the sections. The lighter the riser, less effective tension is experienced on the top, which is the expected result.
- The compression levels were demonstrated to be also related to the weight of the riser. The biggest drop was with the lightest riser, in case 2. However, it was not such a significant drop, and considering the results of the length sensitivity analysis, it is most likely that it would increase for the far offset position.
- For the bending moment, since its peak happens on the titanium, it is directly related to the wall thickness. Thus, case 1 experiences the highest value of bending moment.
- The maximum Von Mises stress for titanium in the cases 2 to 5, in which the titanium wall thickness was thinner than the base case, reached non-allowable values, as can be seen in Figure 8-5. For cases 2 to 4, the stress on the steel section after titanium also was not within the allowable, as shown in Figure 8-6. Even though the weight per unit length on cases 3 and 5 were not significantly different from the base case, the results demonstrated that the wall thickness is an important parameter when defining an optimum configuration.

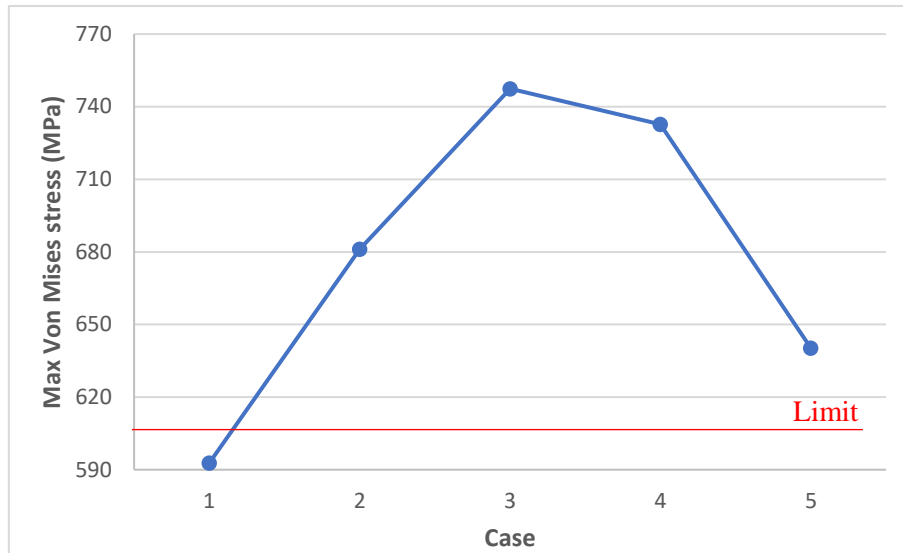


Figure 8-5. Maximum Von Mises stress for titanium section.

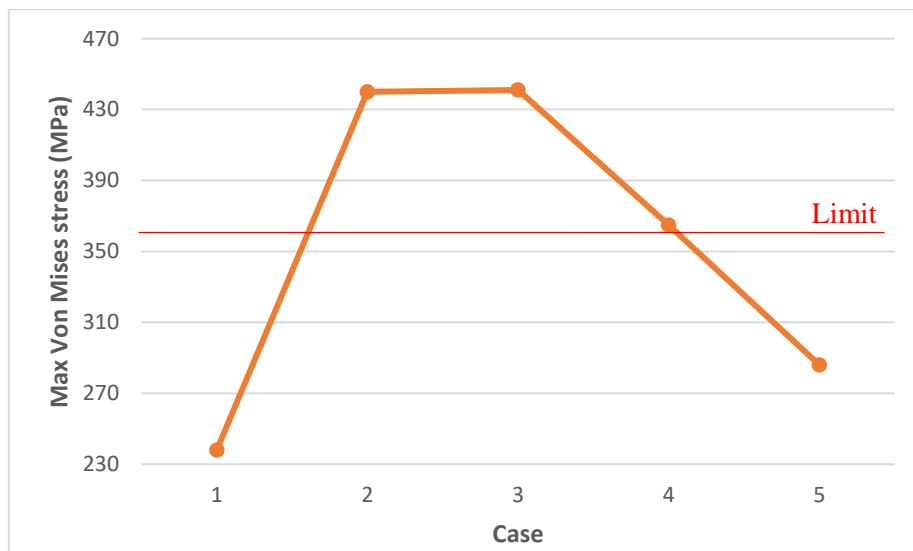


Figure 8-6. Maximum Von Mises stress for steel section after titanium.

In summary, considering the near offset position, only the configuration of case 1 would be suitable. However, when in the far offset position, the results are not within the acceptable criteria anymore, as presented in Table 8-8. Therefore, the heavier section of steel after the titanium does not optimize the riser. It is valid to keep in mind that even if the results were good, other analyses, including costs and installation, would have to be performed.

Table 8-8. Wall thickness and coating thickness sensitivity in far offset position.

<b>Far offset position</b>	
<b>Case</b>	<b>1</b>
<b>Max Effective tension (kN)</b>	5345
<b>Max Compression (kN)</b>	806
<b>Max Bending moment (kN.m)</b>	889
<b>Max Von Mises stress on the titanium section (MPa)</b>	661
<b>Max Von Mises stress on steel after titanium section (MPa)</b>	285

#### 8.4 Hang-off angle sensitivity

Considering that: the compression of the base case is considered to be high; the previous sensitivity analysis did not result in a considerable decrease; the lower compression in all cases was identified in the near position, this section will present how the SCRT is affected by the difference on the hang-off angle on the mean position. For this, the best configuration selected in the previous sensitivity analysis will be considered.

The parametric study will consider the following configuration and the hang-off angles in Table 8-9.

- Titanium length: 600 meters
- Steel and titanium wall thickness: 25 mm
- Steel and titanium coating thickness: 40 mm
- Steel coating density: 690 kg/m<sup>3</sup>
- Titanium coating density: 2,200 kg/m<sup>3</sup>

Table 8-9. Cases for hang-off angle sensitivity study.

<b>Hang-off angle - Mean offset position</b>			
8°	9°	10°	11°

##### 8.4.1 Dynamic analysis (ULS) – Hang-off angle sensitivity

The results obtained with the analysis are presented in Table 8-10 and Table 8-11 and discussed below.

Table 8-10. Hang-off angle sensitivity in near offset position.

<b>Near Offset position</b>				
<b>Hang-off angle</b>	8°	9°	10°	11°
<b>Max Effective tension (kN)</b>	3506	3564	3751	3908
<b>Max Compression (kN)</b>	450	518	556	591
<b>Max Bending moment (kN.m)</b>	867	799	782	804
<b>Max Von Mises stress on the titanium section (MPa)</b>	642	600	590	602
<b>Max Von Mises stress on steel after titanium section (MPa)</b>	234	236	237	238
<b>Declination (°)</b>	5,89	6,69	7,49	8,30

Table 8-11. Hang-off angle sensitivity in far offset position.

<b>Far Offset position</b>				
<b>Hang-off angle</b>	8°	9°	10°	11°
<b>Max Effective tension (kN)</b>	4939	5116	5311	5687
<b>Max Compression (kN)</b>	817	895	858	917
<b>Max Bending moment (kN.m)</b>	679	811	803	901
<b>Max Von Mises stress on the titanium section (MPa)</b>	517	601	605	662
<b>Max Von Mises stress on steel after titanium section (MPa)</b>	258	261	269	419
<b>Declination (°)</b>	9,48	10,73	11,98	13,23

- For both offset positions, it can be observed that the effective tension increases with the increase in the hang-off angle, which is due to the longer suspended length.
- The maximum compression had the most significant drop for the case of 8°. However, the decrease in the maximum values is not considered as relevant as expected. This means that the hang-off angles are not sufficient to cause a significant impact on the compression results.
- The bending moment in the near offset position experienced a decrease in its value with the increase of the hang-off angle for the 8, 9, and 10°. However, for the case with 11°, it resulted in a higher value. This can be explained by the greater free span exposed to the loads. Figure 8-7 below presents how the riser is affected when the hang-off changes for the near offset position. It can be seen that the last case experiences the highest bending moment at a different point than the other cases.

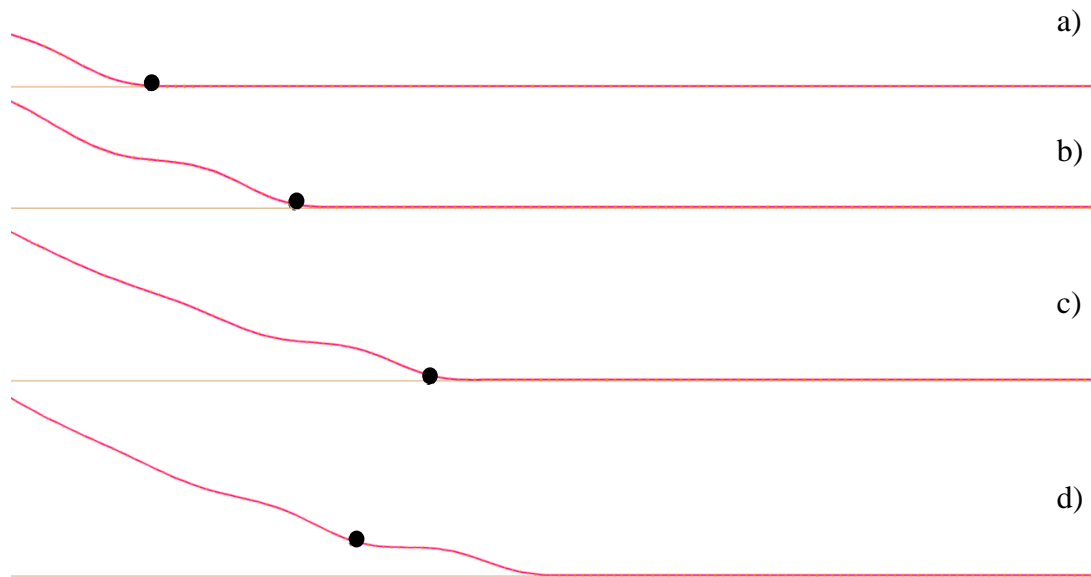


Figure 8-7. Highest bending moment for near offset position with a hang-off angle of a) 8°, b) 9°, c) 10°, and d) 11°.

- For the far offset position, even though the approach of the riser to the seabed is smoother the greater the angle is, it does not have descending values. As for the last case of the near offset position, it can be explained by the increase in the free span that higher angles cause on the riser. As shown in Figure 8-8, the location of the highest bending moment is different for all of them, which is due to their response to the environmental loads.

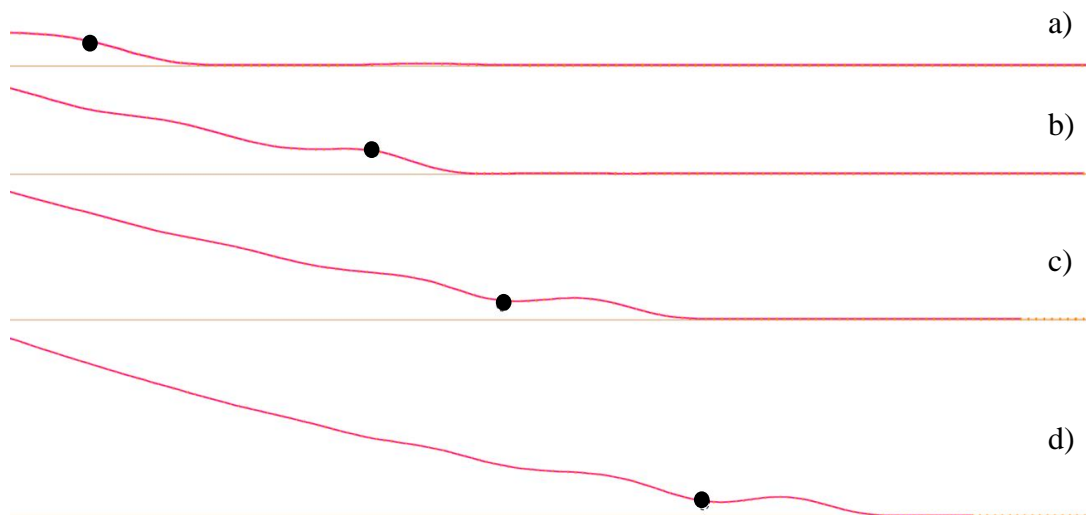


Figure 8-8. Highest bending moment for the far offset position with a hang-off angle of a) 8°, b) 9°, c) 10°, and d) 11°.

- As for the other sensitivity studies in this chapter, the maximum Von Mises stresses in these cases are related to the bending moment. For the steel, the stresses are within the limit for all cases in both offset positions except for the hang-off angle of 11° on the far

position. On the other hand, only the hang-off angles of 8° and 9° are below the allowable criteria for the titanium. Figure 8-9 and Figure 8-10 demonstrate the stresses in all cases.

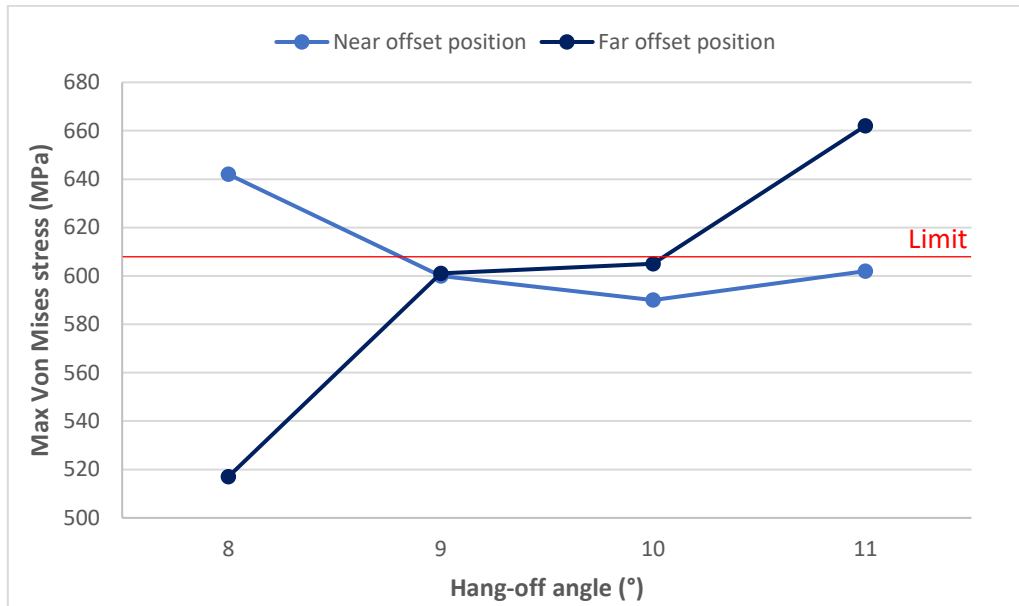


Figure 8-9. Maximum Von Mises stress for titanium section in near offset position - ULS.

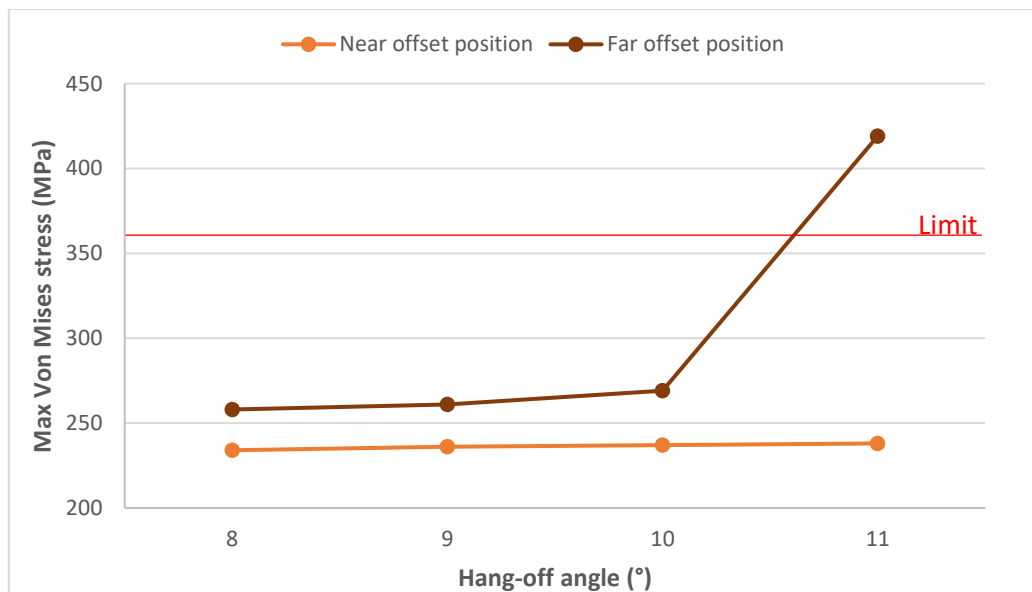


Figure 8-10. Maximum Von Mises stress for steel section after titanium in far offset position - ULS.

In summary, the riser can cope with the cases where the hang-off angle is 9 and 10° on the mean offset position. The compression had its best improvement with a lower hang-off angle of 8°. However, for this case the stress results are not within the allowable criteria.

#### 8.4.2 Dynamic analysis (ALS) – Hang-off angle sensitivity

Considering that the hang-off angles of 9 and 10° were demonstrated to be suitable for ULS conditions, the ALS was tested to check whether they could cope. The results are shown in Table 8-12. It can be seen that even with slightly higher stress for steel and titanium, they still meet the requirements, which consider the yield strength of the material.

Table 8-12. Hang-off angles for ALS conditions.

Offset position	9°		10°	
	Near	Far	Near	Far
<b>Max Effective tension (kN)</b>	3555	5287	3626	5512
<b>Max Compression (kN)</b>	497	908	537	823
<b>Max Bending moment (kN.m)</b>	811	785	791	775
<b>Max Von Mises stress on the titanium section (MPa)</b>	606	592	595	587
<b>Max Von Mises stress on steel after titanium section (MPa)</b>	235	266	236	342
<b>Declination (°)</b>	6,30	11,35	7,49	12,64

The results presented above indicate that when a 600-meter section of titanium is considered in the design, it is suitable to be installed with a hang-off angle of 9 and 10°.



## Chapter 9. Conclusion and Recommendations

### 9.1 Conclusion

This study presents an SCR with a titanium section on the TDA that can cope with the platform host's large motion in a deepwater and harsh environment. A conventional SCR was also evaluated to check how the titanium section can affect the concept results.

The analyses consider the southeast Brazilian offshore location, in which a spread moored FPSO is considered. The metocean data of this location is used for the simulations carried out regarding the strength analysis, fatigue performance, and sensitivity study.

Several tests and evaluations were performed to find a suitable configuration for SCR and SCRT that could withstand the given conditions and result in satisfactory static responses. With that, the riser concepts were exposed to the extreme conditions in which their responses were analyzed.

#### **Extreme response analysis**

Among the types of risers, the SCR is the most attractive choice for deep and ultra-deepwater applications due to its simplicity and low cost. However, the harsh environment induces large motions on the host platform, and since the SCR is a coupled system, it experiences the motions the vessel is subjected. Considering that, an important component is the downward velocity on the hang-off point because it can induce critical responses to the riser and affect its fatigue life. Therefore, the crucial locations on a catenary riser are the hang-off point and the TDP, which must be carefully analyzed when considering this concept.

The sea-state taken into account in this work had 3.8 m/s as maximum downward velocity on the hang-off point. For the SCR case, by analyzing the time story of the downward velocity, it could be observed that the location of the highest value coincides with the peaks in bending moment and Von Mises stress. This means the downward velocity induces the highest values on both. Also, the bending moment along the riser is directly related to the Von Mises stresses. Thus, due to the riser's approach to the seabed, which consequently increases the bending moment, the TDA was the location with the highest values of Von Mises stress. In this case, the maximum stress values encountered for the near and far offset positions in ULS and ALS conditions were much above the allowable

limit. With that, the strength response of the conventional SCR showed that this configuration could not cope with the extreme conditions of the location considered.

Similar to the SCR, the results obtained for the SCRT showed that its extreme responses are also related to the highest downward velocity at the hang-off point. However, the maximum values in the bending moment and Von Mises stress were significantly lower. This can be explained by the higher strength properties of titanium compared to steel. The maximum Von Mises stresses on the titanium section and on the steel section after it were below the materials' allowable limit. With that, it could be demonstrated that implementing a titanium section on the TDA can significantly improve the responses of the catenary riser, making it cope with the environmental conditions of this study.

High compression levels were observed on the TDA for both configurations, which can be explained by the light weight of the riser. Due to the titanium properties, it did not cause the SCRT to fail; however, it is a response that may be improved by applying other techniques.

### **Fatigue performance**

The wave-induced fatigue performance of the SCR and SCRT considered nine wave directions, each with a number of non-linear dynamic analyses. In total, 123 load cases were used for the analysis.

As said before, the critical regions on a catenary riser are the hang-off point and the TDP. Thus, these are the areas of most interest when analyzing fatigue. In this study, a flex joint was not modeled on the riser, which means that the results for the fatigue on the top section of the riser may not reflect reality. Because of this, and since the main objective of this work is to analyze how the titanium section affects the response on the TDA, only the TDP was considered.

The SCR strength results demonstrated it could not cope with a downward velocity of 3.8 m/s, so its fatigue life was expected to be lower than the acceptance limit of 250 years. The analyses proved it by giving a fatigue life of 3.5 years for the F1-curve, which is unsatisfactory.

On the other hand, when implementing the titanium section, the fatigue life on the TDP of the SCRT increased to more than 20,000 years. With that, the use of titanium demonstrated that it could significantly improve the fatigue life of this type of riser,

making it feasible for application in an environment with the harsh conditions of this study.

### **Sensitivity study**

The sensitivity study was carried out considering a variation in the titanium length, wall and coating thicknesses, and hang-off angle, which results are discussed below.

- A minimum length of 600 meters for the titanium section must be considered to have the responses within the allowable limit. Even with a very similar weight per meter for the steel and titanium sections, the transition between the materials affects the response of the riser when exposed to the most extreme loads. Thus, the shorter lengths analyzed are unsuitable for application due to the length of titanium laying on the seabed, which is insufficient to provide a smoother transition between the materials. Therefore, the riser configuration with a 600-meter titanium section was considered for the next sensitivity study.
- By having the previous configuration, different wall and coating thicknesses for the steel and titanium were tested in 5 cases. In addition, an application of a heavier coating on the steel section after the titanium was considered as an attempt to reduce the compression levels. However, four of the five cases reached non-allowable values for stress, and the compression levels did not have expressive changes in any of the cases, meaning that this cannot give enough weight to the riser.

The only case within the allowable limit for the near position demonstrated that it was not feasible for the far offset position due to the heavier coating on the steel section after titanium. So, the response results for all cases were not below the allowable limit. Because of that, the last sensitivity study was performed with the configuration found in the first one.

- The variation on the hang-off angles showed that the riser approaches the seabed in different ways. Therefore, the bending moment is affected, and consequently, the Von Mises stresses. The compression levels did not have significant changes and were still high for all cases. As final result, of the 4 cases analyzed, the hang-off angles of 9 and 10° demonstrated to be suitable for installation when considering a 600-meter titanium section.

### **Summary**

A conventional SCR is not suitable for application in the harsh environment considered in this study. However, implementing a titanium section on its TDA significantly improved its strength analysis, making it within the allowable limits. This was also reflected in the fatigue performance, which showed to be much above the minimum acceptable limit. Thus, it was demonstrated that the SCRT presented was able to make a catenary riser concept feasible for application under those environmental conditions.

## **9.2 Recommendations**

The analyses performed in this study aimed to investigate the feasibility of implementing a titanium section on the TDA of a conventional SCR. Extensive tests and sensitivity analyses were conducted to check how the SCRT is affected when subjected to extreme loads in a harsh environment. The results of the different configurations demonstrated that further work still needs to be done, especially regarding the compression levels. Also, the feasibility of installation and associated costs need to be evaluated. Thus, recommendations are presented below for further studies.

- The investigation of a weight distributed SCR. Since the compression level is related to the weight of the riser and the lighter it is, the more compression is observed; this concept, combined with the implementation of titanium, may reduce this undesirable effect.
- A more extensive analysis of the wall thickness of titanium can be carried out since it can affect the costs and feasibility of installation.
- Detailed installation analyses for the titanium section. This requires information on the welding procedures qualified in this case since it cannot be done offshore. Experience from other projects, such as the titanium catenary riser of the Åsgard B platform in the Norwegian sea, can be considered.

---

## References

- AGGARWAL, R. K., MOURELLE, M. M., KRISTOFFERSEN, S., GODINOT, H., VARGAS, P., ELSE, M., SCHUTZ, R. W., PORTESAN, G., IZQUIERDO, A., QUINTANILLA, H., SCHAMUHN, S. & SCHES, C. 2007. Development and Qualification of Alternate Solutions for Improved Fatigue Performance of Deepwater Steel Catenary Risers. *OMAE 2007*.
- API 2002. Flexible Pipe. *Recommended practice, API-RP-17B*.
- API 2006. Design of Risers for Floating Production Systems (FPSs) and Tension-Leg Platforms (TLPs). *Recommended practice, API-RP-2RD*.
- API 2013. Dynamic Risers for Floating Production Systems. *Standard API-ST-2RD, second edition*.
- BAI, Y. & BAI, Q. 2005. *Subsea Pipelines and Risers*.
- BAI, Y. & BAI, Q. 2010. *Subsea Structural Engineering Handbook*.
- BAI, Y. & BAI, Q. 2014. *Subsea Pipeline Design, Analysis, and Installation*.
- BAXTER, C. F., SCHUTZ, R. W. & CALDWELL, C. S. 2007. Experience and Guidance in the Use of Titanium Components in Steel Catenary Riser Systems. *Offshore Technology Conference*. Houston, Texas.
- BELL, J. M., CHIN, Y. D. & HANRAHAN, S. 2005. State-of-The-Art of Ultra Deepwater Production Technologies. *Offshore Technology Conference*. Houston, Texas.
- BHAT, S., DUTTA, A., WU, J. & SARKAR, I. 2004. Pragmatic Solutions to Touch-Down Fatigue Challenges in Steel Catenary Risers. *Offshore Technology Conference*. Houston, Texas.
- CHENG, J. & CAO, P. 2013. Design of Steel Lazy Wave Riser for Disconnectable FPSO. *Offshore Technology Conference*. Houston, Texas.
- CLUCKEY, E., GHOSH, R., MOKARALA, P. & DIXON, M. 2007. Steel Catenary Riser (SCR) Design Issues at Touch Down Area. *International Offshore and Polar Engineering Conference*. Lisbon, Portugal.
- DIKDOGMUS, H. 2012. *Riser Concepts for Deep Waters*. Master, Norwegian University of Science and Technology.
- DNV 2001. Dynamic Risers. *Offshore Standard, DNV-OS-F201*.
- DNV 2016. Fatigue Design of Offshore Steel Structures. *Recommended Practice, DNV-RP-C203*.

- 
- DNV 2017. Offshore riser systems. *Service Specification, DNV-SE-0476*.
- DNV 2018. Dynamic Risers. *Standard, DNV-ST-F201*.
- DNV 2019. Riser Fatigue. *Recommended Practice, DNV-RP-F204*.
- FELISITA, A., GUDMESTAD, O. T., KARUNAKARAN, D. & MARTINSEN, L. O. 2015. Review of Steel Lazy Wave Riser Concepts for North Sea. *OMAE 2015*.
- FELISITA, A., GUDMESTAD, O. T., KARUNAKARAN, D. & MARTINSEN, L. O. 2017. Review of Steel Lazy Wave Riser Concepts for the North Sea. *Journal of Offshore Mechanics and Arctic Engineering*, Vol. 139.
- FERGESTAD, D. & LØTVEIT, S. A. 2014. *Handbook on Design and Operation of Flexible Pipes.*, NTNU, 4Subsea and SINTEF Ocean, Norway.
- FRAZER, I. 1998. Development of Metallic Riser Systems for Deep Water Applications. *Rio Oil & Gas*. Rio de Janeiro, Brazil.
- GEMILANG, G. M. 2015. *Feasibility Study of Selected Riser Concept in Deep Water and Harsh Environment*. Master, University of Stavanger.
- GEMILANG, G. M. & KARUNAKARAN, D. 2017. Feasibility Study of Selected Riser Concepts in Deep Water and Harsh Environment. *OMAE 2017*. Trondheim, Norway.
- HOWELLS, H. & HATTON, S. A. 1997. Challenges for Ultra-Deep Water Riser Systems. *Floating Production Systems*. London.
- KARUKANARAN, D., LEGRAS, J.-L. & JONES, R. 2013. Fatigue Enhancement of SCRs: Design Applying Weight Distribution and Optimized Fabrication. *Offshore Technology Conference*. Houston, Texas.
- KARUNAKARAN, D., MELING, T. S., KRISTOFFERSEN, S. & LUND, K. M. 2005. Weight-Optimized SCRs For Deepwater Harsh Environments. *Offshore Technology Conference*.
- KARUNAKARAN, D., NORDSVE, N. T. & OLUFSEN, A. 1996. An Efficient Metal Riser Configuration for Ship and Semi Based Production Systems. *International Offshore and Polar Engineering Conference*. Los Angeles, USA.
- KAVANAGH, W. K., LOU, J. & HAYS, P. 2003. Design of Steel Risers in Ultra Deep Water - The Influence of Recent Code Requirements on Wall Thickness Design for 10,000ft Water Depth. *Offshore Technology Conference*. Houston, Texas.
- LAL, M., WANG, F., LU, X. & SEBASTIAN, A. 2019. Strength and Fatigue performance of Steel Lazy Wave Risers with Change in Configuration Parameters. *OMAE 2019*.
-

- MORAIS, J. M. D. 2013. *Petróleo em Águas Profundas*, Ipea.
- NORSOK 2007. N-003: Action and Action Effects. *Norway, Standards Norway*.
- ORCINA. 2022. *Orcaflex Help (version 11.2c)* [Online]. Available: <https://www.orcina.com/webhelp/OrcaFlex/> [Accessed 08.06.2022].
- ORIMOLADE, A. P. 2014. *Steel Lazy Wave Risers from Turret Moored FPSO*. Master, University of Stavanger.
- PADEPOLOUS, P. & THETHI, R. 2012. Top Tensioned Riser (TTR) Engineering Integrator Supply Model.
- RIGZONE. 2021. *How do Risers Work?* [Online]. Available: <https://www.rigzone.com/training/> [Accessed 18.03.2022].
- SEN, T. K. 2006. Probability of Fatigue Failure in Steel Catenary Risers in Deep Water. *Journal of Engineering Mechanics*, 132, 1001-1006.
- SOUZA, L. S. D. & SGARBI, G. N. C. 2019. Bacia de Santos no Brasil: Geologia, Exploração e Produção de Petróleo e Gás Natural. *Boletín de Geologia*.
- SYSTEMS, R. E. 2005. Titanium Design Guidance. *Using Titanium for the Touch Down Zone & Hang-off Steel Catenary Risers*.
- ZHANG, Y., CHEN, B., QIU, L., HILL, T. & CASE, M. 2003. State of the Art Analytical Tools Improve Optimization of Unbonded Flexible Pipes for Deepwater Environments. *Offshore Technology Conference*. Houston, Texas.

## Appendix

### Appendix A - Description of OrcaFlex Software

OrcaFlex was the software used in this thesis and, therefore, a general description of it will be given in this section. All the information presented is based on the manual available. OrcaFlex is a software developed by Orcina for static and dynamic analysis for a wide range of offshore systems such as oil & gas, wet renewables, oceanographic, seismic, defense or aquaculture. It performs its calculations and simulations based on a 3D non-linear time-domain finite element.

It has a robust, intuitive, and user-friendly interface that allows all data to be inputted easily. The program works by building a mathematical computer model of the desired system, consisting of a number of objects representing the parts of the system (vessels, buoys, lines, etc.) (Orcina, 2022).

The initial program window contains the commands as menu, toolbar, status bar, and at least one 3D view. The menu bar comprises the options of open, save and edit a file, create a model, and run calculations and simulations. The toolbar works as a shortcut for the menu options and has the option of the most used commands. Also, it allows starting a statics or dynamics simulation, stopping and replaying it. A status bar can be found below the toolbar, which provides the simulations' status, displaying the current iteration number, time and completion of simulation, error messages, etc. An example of the display screen is shown in Figure A-1. The toolbar options are shown in Table A-1.

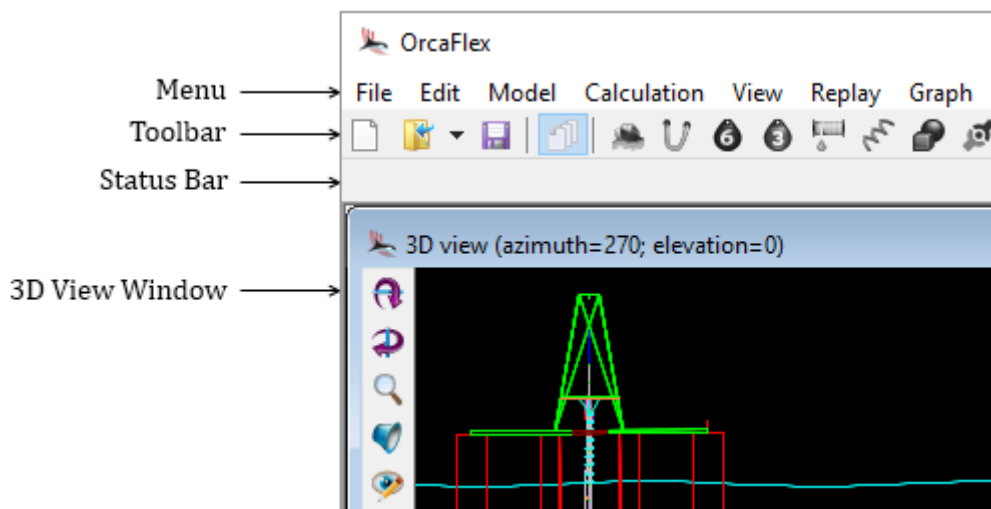



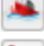














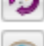






Figure A-1. OrcaFlex main window (Orcina, 2022).



Table A-1. OrcaFlex toolbar (Orcina, 2022).

Button	Action	Equivalent menu item
	Open	File   Open
	Save	File   Save
	Model browser	Model   Model browser
	New vessel	Model   New vessel
	New line	Model   New line
	New 6D buoy	Model   New 6D buoy
	New 3D buoy	Model   New 3D buoy
	New winch	Model   New winch
	New link	Model   New link
	New shape	Model   New shape
	New constraint	Model   New constraint
	New turbine	Model   New turbine
	Calculate statics	Calculation   Statics
	Run dynamic simulation	Calculation   Run dynamic simulation
	Pause dynamic simulation	Calculation   Pause dynamic simulation
	Reset	Calculation   Reset
	Start replay	Replay   Start replay
	Stop replay	Replay   Stop replay
	Step replay forwards	Replay   Step replay forwards
	Edit replay parameters	Replay   Edit replay parameters
	Add new 3D view	Window   Add 3D view
	Examine results	Results   Select results
	Help contents and index	Help   OrcaFlex help

### **Model states**

A mathematical model of the system is built by OrcaFlex, which can be used for the static and dynamic analyses. This model is built up from a series of interconnected objects, e.g., lines, vessels, and buoys (Orcina, 2022).

A flowchart diagram of the steps performed by the program is presented in Figure A-2.

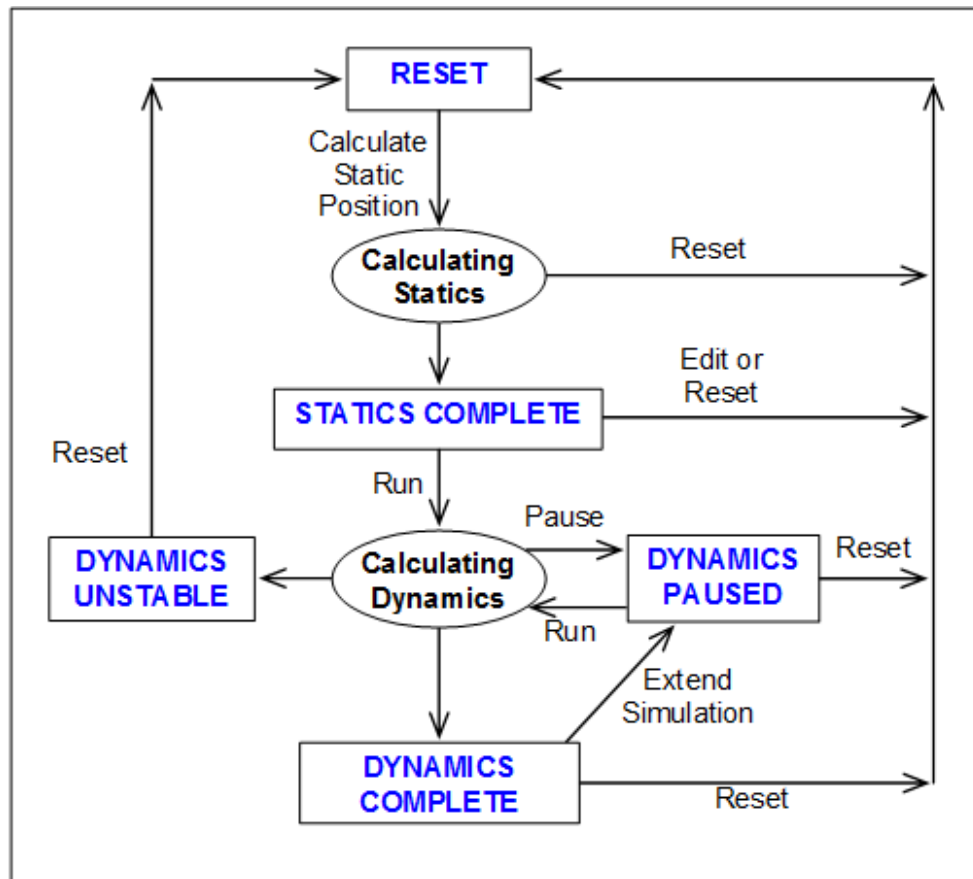


Figure A-2. Model states of OrcaFlex (Orcina, 2022).

### **Coordinate system**

Several frames of reference with their respective reference origin and set of axes directions are used in the program. Thus, the different coordinate systems can be represented. The global one has its reference origin in the global origin, and  $G_x$ ,  $G_y$ , and  $G_z$  denote the global axis directions. Each object generally has its local coordinate system, indicated by  $L_x$ ,  $L_y$ , and  $L_z$ . Also, line end orientations are represented by their own,  $E_{xyz}$ .

They are all right-handed, and positive rotations are clockwise. The global axes and a vessel with its local frame are shown in Figure A-3.

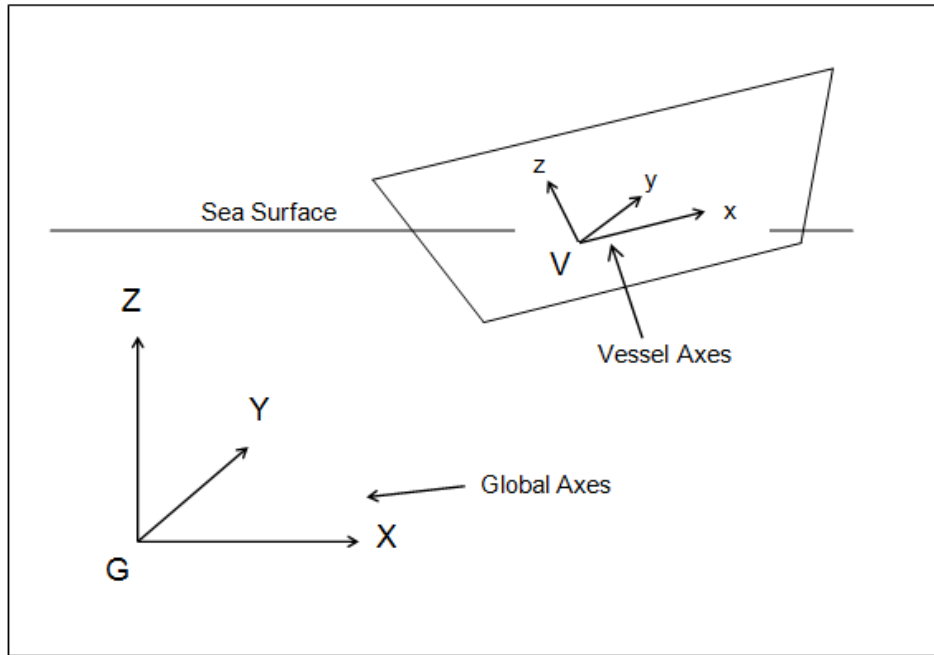


Figure A-3. Coordinate System (Orcina, 2022).

The software has the headings and directions defined in the horizontal plane as the azimuth angle of the direction, measured positive from the  $x$ -axis towards the  $y$ -axis, as presented in Figure A-4.

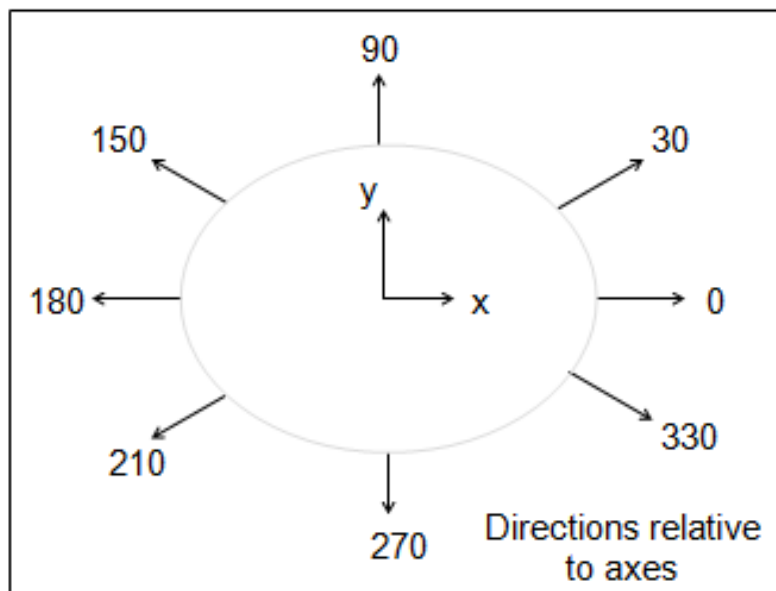


Figure A-4. Headings and directions (Orcina, 2022).

In the case of waves, currents, and wind, directions are specified by the azimuth direction in which they are progressing, relative to global axes.

### Simulation stages

A number of consecutive stages define the simulations' period, and their duration is specified by the data. A built-up stage is usually considered before the main simulation, which is able to smoothly ramp up the wave and vessel motions from zero to their full size. By doing that, a gentle start is provided to the simulation, helping to reduce the transients generated by the transition of the static position to full dynamic motion. This build-up stage is before stage 1 and thus, numbered 0. Its length should usually be set to at least one wave (Orcina, 2022). Figure A-5 demonstrates the time and simulation stages.

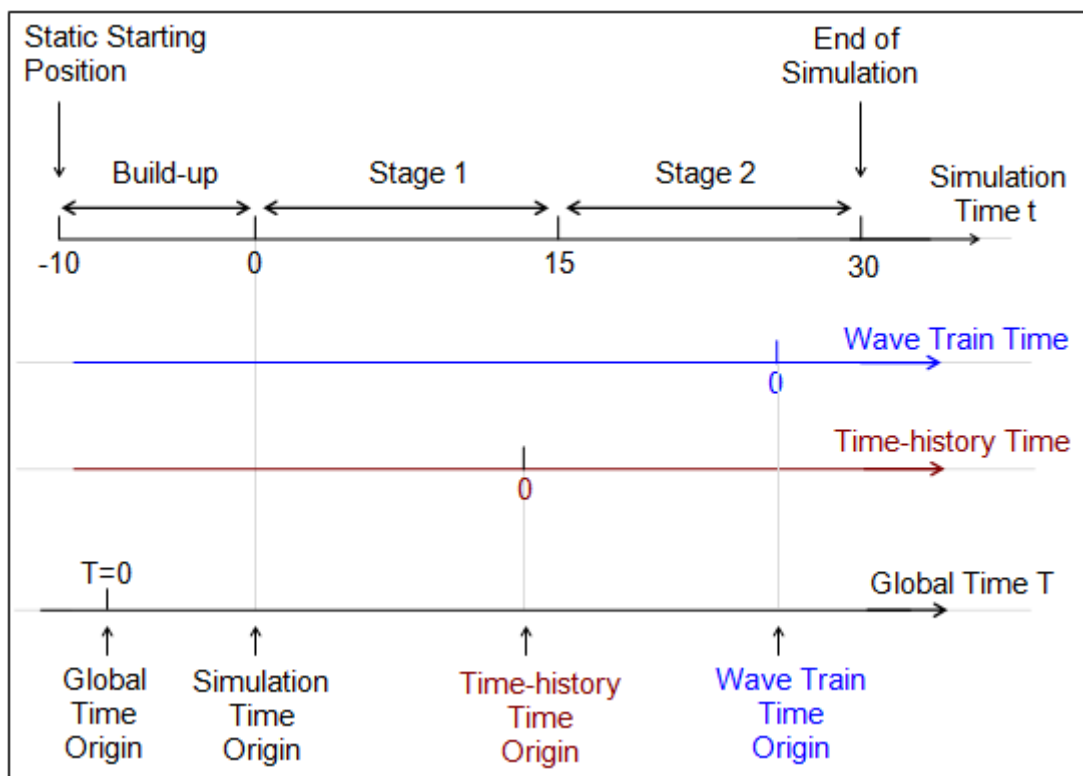


Figure A-5. Time and simulation stages (Orcina, 2022).

### Riser Modeling

A finite element model is used by the software to create a line. This line is then divided by a number of line segments which are modeled by straight massless model segments with a node at each end, as seen in Figure A-6. The properties such as mass, weight, buoyancy, etc., are lumped to the nodes while the segments model the axial and torsional properties.

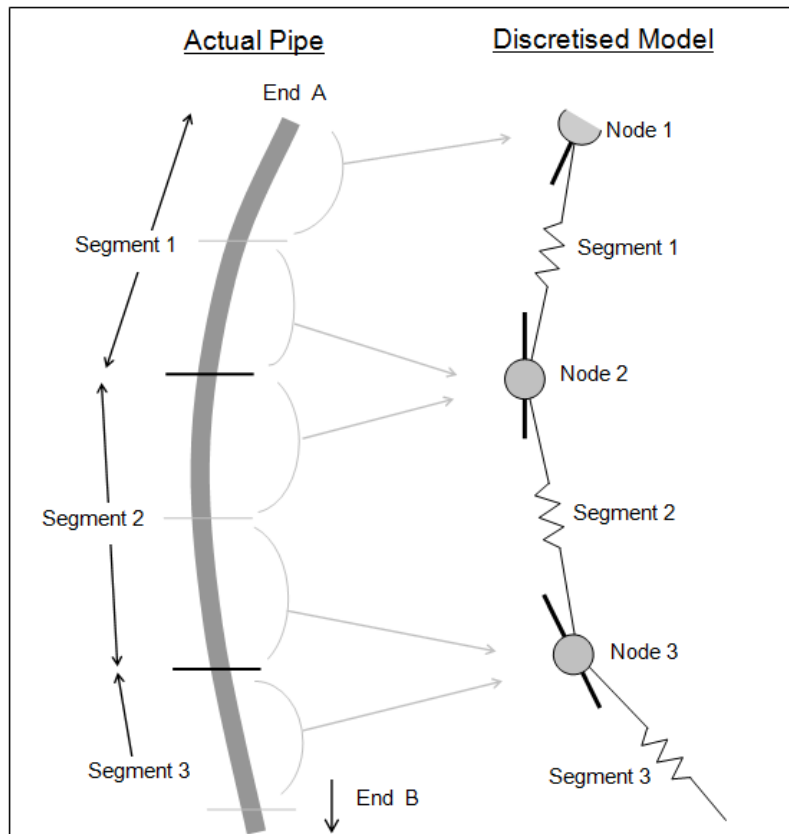


Figure A-6. OrcaFlex line model (Orcina, 2022).